5213773, ja, Downloaded from https://onlinelibrary.wiley.com/doi/10.1002/anie.202214987 by North Carolina State University, Wiley Online Library on [03/02/2023]. See the Terms and Conditions (https://onlinelibrary.wiley.com/terms-and-conditions) on Wiley Online Library for rules of use; OA articles are governed by the applicable Creative Commons License (Commons Library on Indications) on Wiley Online Library for rules of use; OA articles are governed by the applicable Creative Commons License (Commons Library on Indications) on Wiley Online Library on Indications (Commons Library on Indications) on Wiley Online Library on Indications (Commons Library on Indications) on Wiley Online Library on Indications (Commons Library on Indications) on Wiley Online Library on Indications (Commons Library on Indications) on Wiley Online Library on Indications (Commons Library on Indications) on Wiley Online Library on Indications (Commons Library on Indications) on Wiley Online Library on Indications (Commons Library on Indications) on Wiley Online Library on Indications (Commons Library on Indications) on Wiley Online Library on Indications (Commons Library on Indications) on Wiley Online Library on Indications (Commons Library on Indications) on Wiley Online Library on Indications (Commons Library on Indications) on

### **Accepted Article**

**Title:** CRISPR-Cas Biochemistry and CRISPR-Based Molecular Diagnostics

Authors: Zhengyan Weng, Zheng You, Jie Yang, Noor Mohammad, Mengshi Lin, Qingshan Wei, Xue Gao, and Yi Zhang

This manuscript has been accepted after peer review and appears as an Accepted Article online prior to editing, proofing, and formal publication of the final Version of Record (VoR). The VoR will be published online in Early View as soon as possible and may be different to this Accepted Article as a result of editing. Readers should obtain the VoR from the journal website shown below when it is published to ensure accuracy of information. The authors are responsible for the content of this Accepted Article.

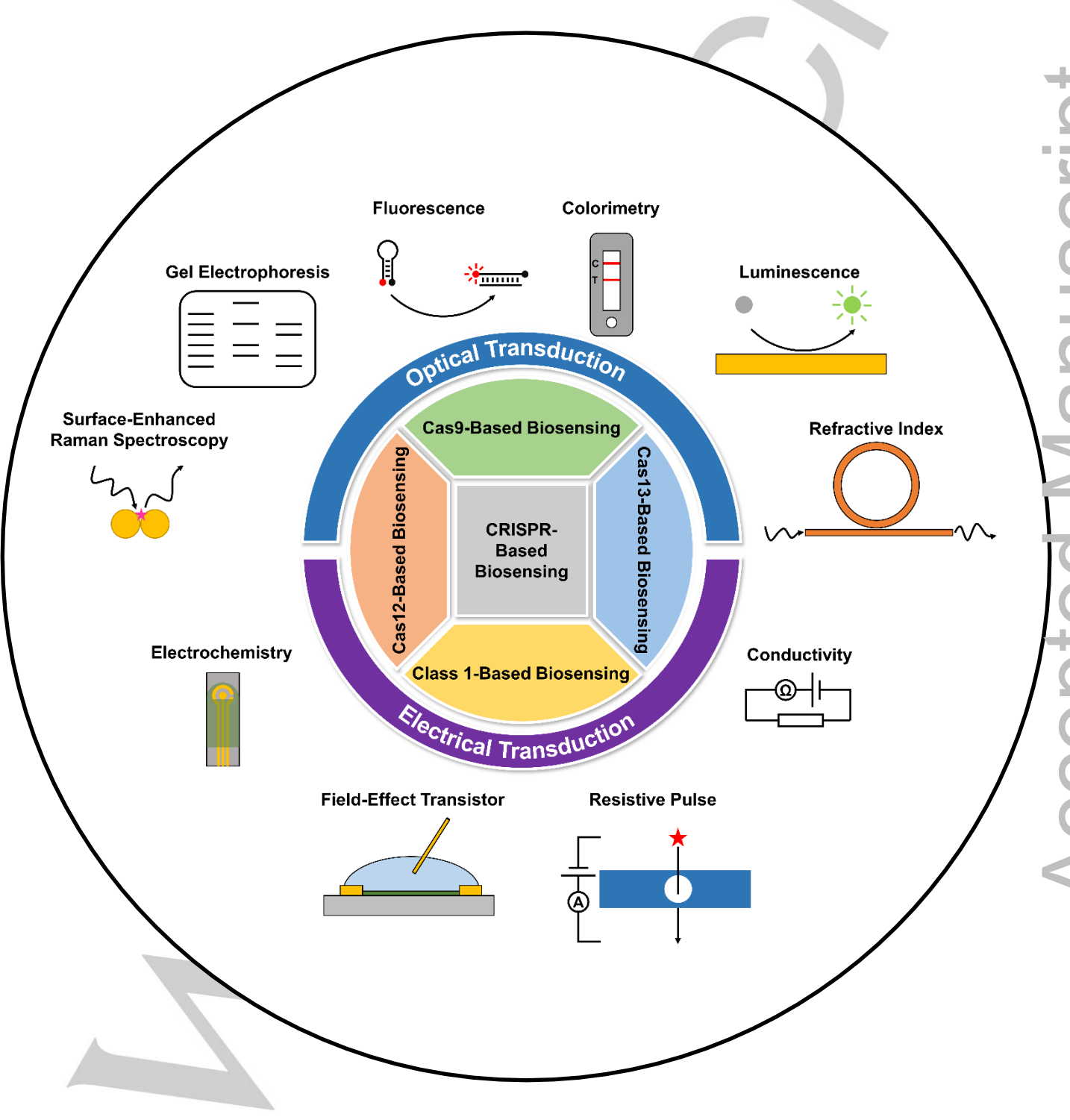
To be cited as: Angew. Chem. Int. Ed. 2023, e202214987

Link to VoR: https://doi.org/10.1002/anie.202214987

### **REVIEW**

# CRISPR-Cas Biochemistry and CRISPR-Based Molecular Diagnostics

Zhengyan Weng, $^{\dagger [a,b]}$  Zheng You, $^{\dagger [c]}$  Jie Yang, $^{[c]}$  Noor Mohammad, $^{[d]}$  Mengshi Lin, $^{[e]}$  Qingshan Wei, $^{[d]}$  Xue Gao, $^{\star [c,f,g]}$  Yi Zhang $^{\star [a,b]}$ 



### REVIEW

[a,b] Z. Weng, Prof. Y. Zhang

Department of Biomedical Engineering, University of Connecticut, Storrs, CT 06269, USA. Institute of Materials Science, University of Connecticut, Storrs, CT 06269, USA.

E-mail: yi.5.zhang@uconn.edu (Prof. Y. Zhang)

[c] Z. You, J. Yang, Prof. X. Gao

Department of Chemical and Biomolecular Engineering, Rice University, Houston, TX 77005, USA. E-mail: xue.gao@rice.edu (Prof. X. Gao)

[d] N. Mohammad, Prof. Q. Wei

Department of Chemical and Biomolecular Engineering, North Carolina State University, Raleigh, NC 27695, USA.

[e]

Food Science Program, Division of Food, Nutrition & Exercise Sciences, University of Missouri, Columbia, MO 65211, USA.

[f,g] Prof. X. Gao

Department of Bioengineering, Rice University, Houston, TX 77005, USA. Department of Chemistry, Rice University, Houston, TX 77005, USA.

Supporting information for this article is given via a link at the end of the document.

Abstract: Polymerase chain reaction (PCR)-based nucleic acid testing has played a critical role in disease diagnostics, pathogen surveillance, and many more. However, this method requires a long turnaround time, expensive equipment, and trained personnel, limiting its widespread availability and diagnostic capacity. On the other hand, the clustered regularly interspaced short palindromic repeats (CRISPR) technology has recently demonstrated capability for nucleic acid detection with high sensitivity and specificity. CRISPR-mediated biosensing holds great promise for revolutionizing nucleic acid testing procedures and developing point-of-care diagnostics. This review focuses on recent developments in both fundamental CRISPR biochemistry and CRISPR-based nucleic acid detection techniques. Four ongoing research hotspots in molecular diagnostics-target preamplification-free detection, microRNA (miRNA) testing, nonnucleic-acid detection, and SARS-CoV-2 detection-are also covered.

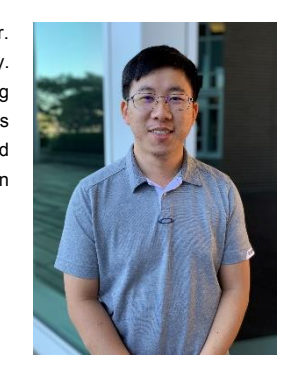
### 1. Introduction

Molecular diagnostics, in particular, nucleic acid testing, is critical in a wide range of fields relevant to the quality of human life, including the fundamental understanding of physiological processes,[1] pathogen detection,[2] and disease prognosis and diagnosis.[3] Nucleic acid detection relies on the identification of nucleic acid sequence, thereby providing superior sensitivity and specificity over other types of tests such as serological testing.[4] Over the past few decades, quantitative polymerase chain reaction (qPCR) has remained the gold-standard technique for nucleic acid testing. [5] However, qPCR is still limited by: 1) expensive instruments and reagents for nucleic acid amplification (NAA) through thermocycling and quantification of amplicons via fluorescence intensity; [6] 2) the need for specialized personnel for nucleic acid extraction, qPCR assay preparation, and data analysis;[7] and 3) long processing time from sampling to delivery

Zhengyan Weng is a Ph.D. student in Dr. Yi Zhang's group at the University of Connecticut, Storrs. He received his B.S. in Chemical and Biomolecular Engineering from the Georgia Institute of Technology in 2015 and M.S.E. in Chemical and Biomolecular Engineering in 2018 from the University of Pennsylvania. Currently, he is working on developing CRISPR-based biosensors for disease diagnostics.



Zheng You is a third year Ph.D. student in Dr. Xue (Sherry) Gao's group at Rice University. He received his B.S. in Chemical Engineering from University of Houston in 2020. His research interest is focused on developing and engineering CRISPR-Cas systems for both in vitro and in vivo applications.



Yi Zhang is an Assistant Professor in the Department of Biomedical Engineering and the Institute of Materials Science at the University of Connecticut, Storrs. He received his Ph.D. degree in Chemical Engineering from the Georgia Institute of Technology in 2016, where he was awarded 2015 Waldemar T. Ziegler Award for Best Research Paper in Chemical Engineering and Exemplary Academic Achievement Award (2013). He did his postdoc training in Prof. John A. Rogers group at Northwestern University. He was awarded 2019 BMES Career Development Award and 2023 NSF CAREER Award. For more



professor in 2017. She earned her Ph.D. in Chemical and Biomolecular Engineering from UCLA in 2013 and was a postdoc at Harvard University from 2013 to 2017. Dr. Gao received the 2020 NIH Maximizing Investigators' Research Award, the 2022 NSF CAREER AWARD, and the 2022 Outstanding Young Faculty at Rice School of Engineering.



### **REVIEW**

of results.<sup>[7b]</sup> Researchers have made efforts to address the above drawbacks, for example, by developing isothermal amplification techniques such as loop-mediated isothermal amplification (LAMP)<sup>[8]</sup> and recombinase polymerase amplification (RPA),<sup>[9]</sup> and by incorporating nucleic acid complementarity into point-of-care (POC) diagnostic platforms such as electrochemical and optical biosensors.<sup>[10]</sup> However, these attempts still suffer from the necessary sequence amplification step or compromised detection sensitivity in comparison to qPCR.

Recent discoveries of the clustered regularly interspaced short palindromic repeats (CRISPR)-Cas (CRISPR-associated) have opened a new path for the manipulation and analysis of nucleic acids,[11] and the engineering of CRISPR-Cas systems has expanded their applications beyond genome editing[12] and gene therapies.<sup>[13]</sup> Leveraging the single-nucleotide target specificity of the CRISPR-Cas systems as a result of base pair complementarity between guide RNA (gRNA) and target nucleic acid sequence,[12a, 14] scientists have developed a variety of CRISPR-mediated biosensing platforms for ultrasensitive and highly specific nucleic acid detection. [15] Because the CRISPR-Cas system operates at body temperature  $^{[15]}$  or even room temperature[16] unlike traditional PCR, it offers a more POCfocused design approach.[17] The emergence of amplification-free assay eliminates the need for PCR primers,  $^{[16b,\ 16c,\ 18]}$  and smartphone imaging with a mobile application lowers the requirements for data collection and analysis.[18-19] CRISPR reagents can also be lyophilized for streamlined field applications. [20] As a result, CRISPR has simplified reaction conditions, which in turn reduces the cost associated with equipment, reagents, and labor and speeds up the turnaround time.

Due to the increasing interest in CRISPR-driven molecular diagnostics, this review focuses on the fundamental biochemistry of CRISPR-Cas systems, more specifically, Cas9, Cas12, and Cas13 systems, and the state-of-the-art CRISPR-Cas biosensing technologies. Four special applications, including target amplification-free detection, miRNA detection, non-nucleic-acid

detection, and SARS-CoV-2 detection, are also discussed to highlight current trends. A brief overview of CRISPR-mediated detection platforms is summarized in Table S1. In addition, this review also presents the future perspectives for CRISPR-Cas bioengineering and CRISPR-based biosensing to discuss prospective research directions in this field.

### 2. Overview of CRISPR-Cas Biochemistry

### 2.1. CRISPR-Associated Protein 9 (Cas9) System

CRISPR-Cas system interferes with invading nucleic acids, providing sequence-specific adaptive immunity in prokaryotes against bacteriophage infections (Figure 1),<sup>[21]</sup> and has become one of the most powerful and programmable tools in molecular biology and at the interface of engineering. Current studies have two major focuses on CRISPR-Cas9: the fundamental biological mechanism and the repurposing of Cas9 as a genetic manipulation tool. For a broad overview of its history, engineering, and immunization functions, we refer the readers to some well-summarized review articles.<sup>[22]</sup>

### 2.1.1. Mechanism of CRISPR-Cas9

The most researched *Streptococcus pyogenes* Cas9 (SpCas9) is an RNA-guided DNA nuclease, targeting double-stranded DNA (dsDNA) (Figure 2A).<sup>[11c]</sup> Two strands of the dsDNA are defined respectively as the complementary strand (target strand) and the non-complementary strand base pairs with the spacer region of the CRISPR RNA (crRNA). The non-complementary strand, also called the protospacer, contains a ~20-nt sequence same as the spacer region, albeit with a T-U difference. At the 3' downstream of the protospacer is an "NGG" sequence, termed protospacer adjacent motif (PAM).<sup>[23]</sup> Applying the CRISPR-Cas9 system for gene editing or other purposes requires the presence of three

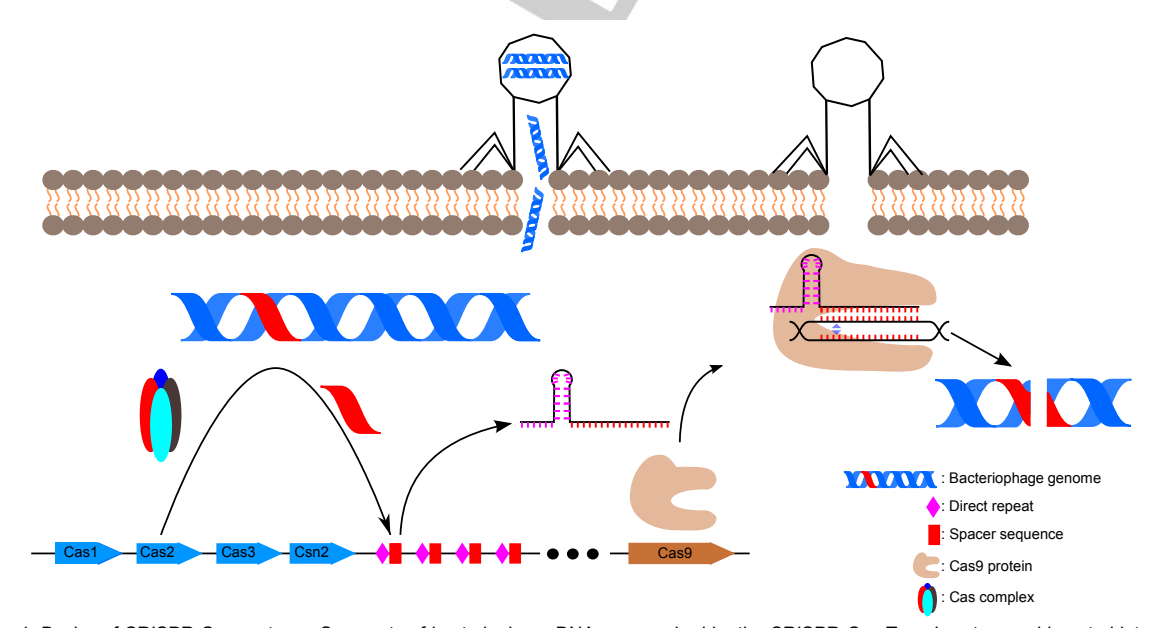


Figure 1. Basics of CRISPR-Cas systems. Segments of bacteriophage DNA are acquired by the CRISPR-Cas Type I system and inserted into the CRISPR array as spacers. When future phase infection occurs, the spacer sequences are transcribed into pre-crRNA and processed into mature crRNA. The mature crRNA combines with the CRISPR-Cas complex or effector to cleave bacteriophage DNA and resist phage infection. Reproduced with permission from reference.<sup>[21]</sup> Copyright 2022 Springer Nature.

### **REVIEW**

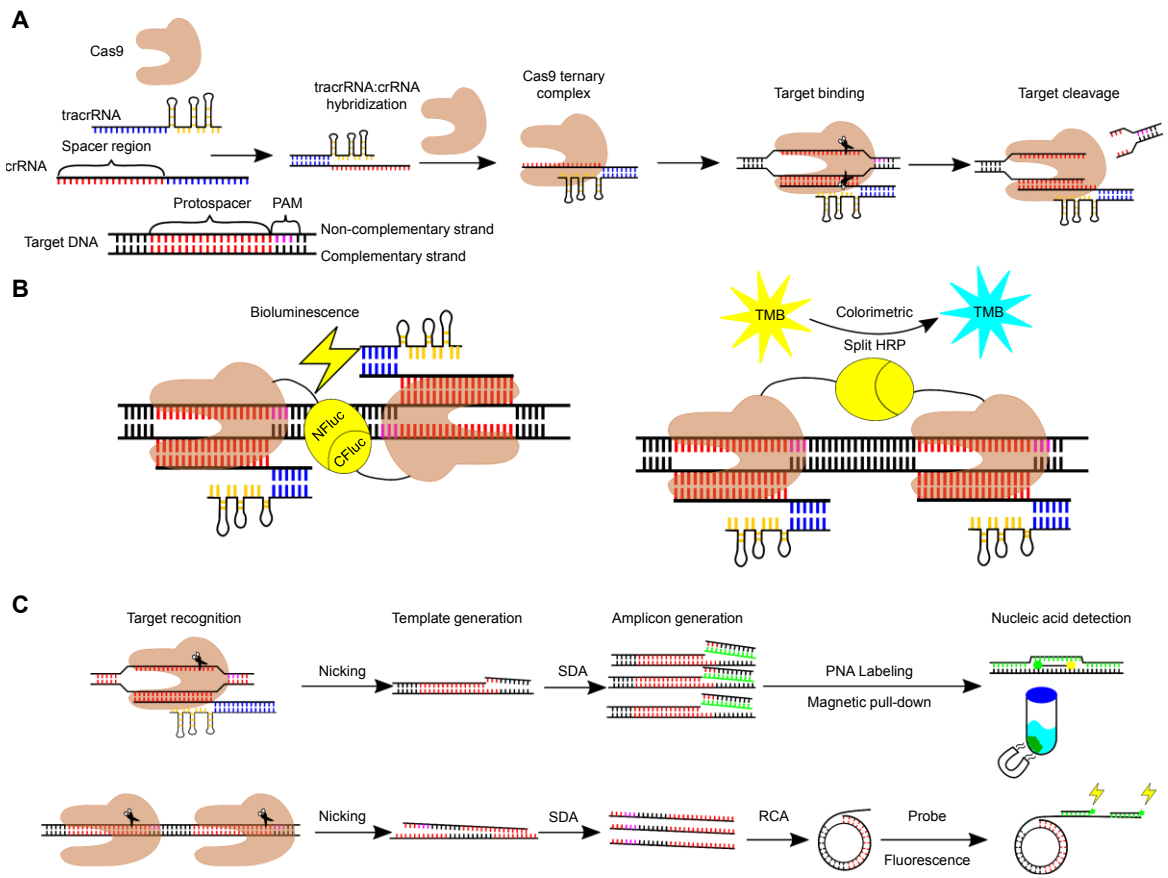


Figure 2. Mechanisms of CRISPR-Cas9 cleavage and Cas9-based detection. (A) Cas9-mediated DNA cleavage requires the Cas9 effector, tracrRNA, crRNA, and the target DNA. (B) Cas9-based detection employing the binding capability of dCas9. Left: dCas9-based luciferase bioluminescent detection. NFluc: N-terminal of the firefly luciferase enzyme. CFluc: C-terminal of the firefly luciferase enzyme. Reproduced with permission from reference. [24] Copyright 2016 American Chemical Society. Right: dCas9-based TMB colorimetric reaction. TMB: 3,3'-5,5'-tetramethylbenzidine. HRP: Horseradish peroxidase. Reproduced with permission from reference. [25] Copyright 2018 American Chemical Society. (C) Cas9-based detection employing the nicking capability of nCas9. Top: CRISPR-Cas9-triggered nicking endonuclease-mediated strand displacement amplification (CRISDA). SDA: Strand displacement amplification. PNA: Peptide nucleic acid. Reproduced with permission from reference. [26] Copyright 2018 The Authors, published by Springer Nature. Bottom: nCas9-based SDA-RCA detection. RCA: Rolling circular amplification. Reproduced with permission from reference. [27] Copyright 2020 American Chemical Society.

components, a crRNA with the 5' spacer region, a trans-activating crRNA (tracrRNA), and a Cas9 protein as the effector. [11c] These three components form a Cas9-crRNA-tracrRNA ternary ribonucleoprotein (RNP) complex, binding to the target dsDNA via complementarity between the ~20-nt spacer region in the crRNA and the target site on the complementary strand and opening the double helix to form an R-Loop, which is a three-stranded RNA-DNA hybrid structure. Two domains of Cas9, RuvC and HNH, perform the nuclease activity to cut the PAM-containing noncomplementary strand and the complementary strand, respectively, leaving a blunt-end double-strand break (DSB) at 3bp upstream of the NGG PAM. Also, linking the crRNA and tracrRNA with a stem-loop structure results in a single-guide RNA (sgRNA), which can function as efficiently as the dual-RNA guide and greatly simplify the CRISPR-Cas9 system for various applications.[11c]

### 2.1.2. Engineering of Cas9 for Versatile Applications

Diverse strategies have been adopted to engineer and optimize the CRISPR-Cas9 systems for genetic and epigenetic modifications. SpCas9 has two independent active sites, and a mutation of the SpCas9 catalytic residues, such as D10A and H840A, inactivates either the RuvC or the HNH domain, generating nickase Cas9 (nCas9). [28] A double mutation results in

catalytically dead Cas9 (dCas9).<sup>[29]</sup> Fusing Cas9/nCas9/dCas9 to different functional proteins such as deaminases,<sup>[30]</sup> reverse transcriptases,<sup>[31]</sup> and transcription factors<sup>[32]</sup> creates target-specific base editors, prime editors, and transcriptional activators or repressors, respectively.

Besides genome editing, Cas9 has been engineered for nucleic acid detection. For in vitro applications, wild-type Cas9 can be combined with NAA methods such as rolling circular amplification (RCA) to generate readout signals. [27a, 33] Both nCas9 and dCas9 have also been successfully utilized in nucleic acid detection based on their specific properties. [24-26, 34] Additionally, the fusion of a tripartite transcriptional activator, VP64-p65-Rta (VPR), to dCas9 promotes the expression of targeted genes and facilitates in vivo cellular imaging for the detection of certain genes or gene products. [35] The following section will discuss in vitro Cas9-mediated nucleic acid detection in detail.

### 2.1.3. Strategies for Cas9-Based Biosensing

As the first highly researched and engineered CRISPR-Cas system, Cas9 is well known for recognizing and cleaving dsDNA.[11a, 11c, 23, 36] In addition, CRISPR-Cas9 can be activated to cleave single-stranded DNA (ssDNA) or RNA (ssRNA) in the presence of short PAM-presenting DNA oligonucleotides

### REVIEW

Table 1. Most Common CRISPR Class 2 Systems in Nucleic Acid Detection

| Туре              | Strain Origin                                        | PAM/PFS                 | Spacer<br>Length         | Need<br>tracrRNA? | Cis-<br>Substrate | Trans-<br>Substrate | Crystal<br>Structure | Example    |
|-------------------|------------------------------------------------------|-------------------------|--------------------------|-------------------|-------------------|---------------------|----------------------|------------|
| Cas9              | Streptococcus<br>pyogenes <sup>[11c]</sup>           | 3'-NGG                  | 20nt                     | Yes               | dsDNA             |                     | [37]                 | [26]       |
|                   | Lachnospiraceae<br>bacterium ND2006 <sup>[14b]</sup> | 5'-TTTV                 | 20nt                     | No                | dsDNA/<br>ssDNA   | ssDNA               | [38]                 | [15b]      |
| Cas12a            | Acidaminococcus sp.<br>BV3L6 <sup>[14b]</sup>        | 5'-TTTV                 | 20nt                     | No                | dsDNA/<br>ssDNA   | ssDNA               | [39]                 | [15b]      |
|                   | Francisella novicida<br>U112 <sup>[14b]</sup>        | 5'-TTTV                 | 20nt                     | No                | dsDNA/<br>ssDNA   | ssDNA               | [40]                 | [15b]      |
| Cas12b            | Alicyclobacillus<br>acidoterrestris <sup>[41]</sup>  | 5'-TTN                  | 20nt                     | Yes               | dsDNA/<br>ssDNA   | ssDNA               | [41]                 | [15b]      |
| 083125            | Alicyclobacillus<br>acidiphilus <sup>[42]</sup>      | 5'-TTN                  | 20nt                     | Yes               | dsDNA/<br>ssDNA   | ssDNA               |                      | [43]       |
| Cas12c            | Cas12c1 <sup>[44]</sup>                              | 5'-TG                   | 17-18nt <sup>[45]</sup>  | Yes               | dsDNA/<br>ssDNA   | ssDNA               | [46]                 | [45]       |
| Cas12e<br>(CasX)  | Deltaproteobacteria <sup>[47]</sup>                  | 5'-TTCN                 | 20nt                     | Yes               | dsDNA/<br>ssDNA   | ssDNA               |                      |            |
| Cas12f<br>(Cas14) | Cas12f1 <sup>[48]</sup>                              | None                    | 20nt                     | Yes               | ssDNA             | ssDNA               | [49]                 | [48, 50]   |
| Cas12g            | Cas12g1 <sup>[44]</sup>                              | None                    | 24nt                     | Yes               | ssRNA             | ssRNA/<br>ssDNA     | [51]                 |            |
| Cas12i            | Cas12i1 <sup>[44]</sup>                              | 5'-TTN                  | 28-30nt                  | No                | dsDNA/<br>ssDNA   | ssDNA               | [52]                 |            |
| Cas 121           | Cas12i2 <sup>[44]</sup>                              | 5'-TTN                  | 28-30nt                  | No                | dsDNA/<br>ssDNA   | ssDNA               | [53]                 |            |
| Cas12j<br>(CasΦ)  | СаsФ <sup>[54]</sup>                                 | 5'- T rich<br>or 5'-TBN | 20nt                     | No                | dsDNA/<br>ssDNA   | ssDNA               | [55]                 |            |
|                   | Leptotrichia buccalis <sup>[15a]</sup>               | None <sup>[56]</sup>    | 20-28nt                  | No                | ssRNA             | ssRNA               | [57]                 | [58]       |
|                   | Leptotrichia shahii <sup>[14a]</sup>                 | 3'-Not-G                | 21-28nt                  | No                | ssRNA             | ssRNA               | [59]                 |            |
| Cas13a            | Leptotrichia wadei <sup>[15a]</sup>                  | None or<br>3'-Not-G     | 21-28nt <sup>[12c]</sup> | No                | ssRNA             | ssRNA               |                      | [15a, 16c] |
|                   | Lachnospiraceae<br>bacterium NK4A179                 |                         | 24nt                     | No                | ssRNA             | ssRNA               | [60]                 |            |
|                   | Prevotella buccae <sup>[61]</sup>                    | 3'-Not-C                | 30nt <sup>[62]</sup>     | No                | ssRNA             | ssRNA               | [61]                 |            |
| Cas13b            | Prevotella sp.<br>MA2016 <sup>[15a]</sup>            |                         | 30nt                     | No                | ssRNA             | ssRNA               |                      | [15a]      |
|                   | Capnocytophaga<br>canimorsus Cc5 <sup>[15a]</sup>    |                         | 28nt                     | No                | ssRNA             | ssRNA               |                      | [15a]      |
|                   | Eubacterium siraeum <sup>[63]</sup>                  | None                    | 22-30nt                  | No                | ssRNA             | ssRNA               | [64]                 |            |
| Cas13d            | Ruminococcus<br>flavefaciens <sup>[65]</sup>         | None                    | 22-30nt                  | No                | ssRNA             | ssRNA               |                      | [65]       |

(PAMmers) that hybridize with the targets.<sup>[66]</sup> Such target-specific cleavage by CRISPR-Cas9 has been directly engineered into biosensing, by initiating subsequent biorecognition events such as gene translation<sup>[67]</sup> and sequence amplification<sup>[68]</sup> upon the generation of post-cleavage products. The DNA binding capability of dCas9 without DSB has also been repurposed for nucleic acid detection by generating signals via follow-up reactions upon dimerization of fused functional domains (Figure 2B)<sup>[34]</sup> or directly probing the binding events.<sup>[24-25]</sup> The nicking capability of nCas9

offers a different option to detect nucleic acid targets by strand amplification. For example, CRISPR-Cas9-triggered nicking endonuclease-mediated strand displacement amplification (CRISDA) unwinds target dsDNAs by creating a pair of nicks at specific sites on the two strands, thus triggering linear strand displacement amplification (SDA) (Figure 2C, Top). These amplified strands undergo additional exponential SDA mediated by a common nicking endonuclease, Nb.BbvCl, and the final amplicons are quantitatively determined by peptide nucleic acid

### REVIEW

(PNA) invasion-mediated fluorescence measurements. Alternatively, a pair of nCas9s nicking on the same strand can result in the generation of ssDNA fragments, and these fragments are then amplified by SDA and RCA into extended oligos with repeated target sequences (Figure 2C, Bottom). [27a] Fluorescent probes, originally quenched by a UiO66 metal-organic framework (MOF), hybridize with the amplicons and start to emit fluorescence signals.

Cas9 is widely engineered for applications in nucleic acid detection, but the reagents and process are often complex because the binding, cleavage, and nicking-induced unwinding activities cannot be easily converted into readable outputs by Cas9 protein alone. As demonstrated below, Cas12 and Cas13 proteins can produce signals much more readily through a special mechanism called collateral cleavage. [15] It greatly simplifies the reaction setup and allows for more focus on the development of sensitive and portable detection platform. As a result, recent CRISPR-based nucleic acid detection research is largely based on Cas12 and Cas13 systems.

### 2.2. CRISPR-Associated Protein 12 (Cas12) System

### 2.2.1. Domain, crRNA and Target Structure

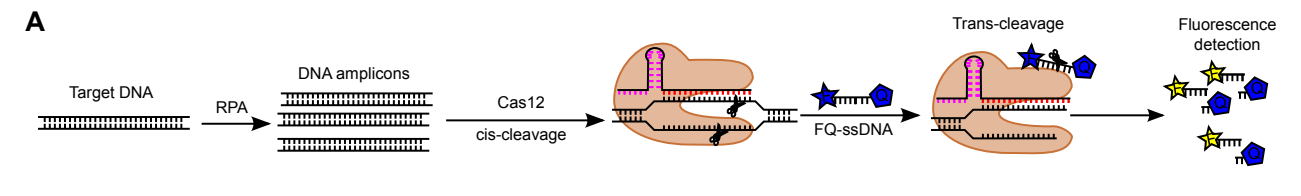
Cas12 effectors also create DSB in DNA, but they differ from Cas9 in several aspects. First, Cas12 nucleases use a single RuvC domain for targeted DNA cutting, and they generate staggered DSBs with a 5' overhang. [14b] Second, some Cas12 orthologs, such as Cas12a, require only a crRNA, but a tracrRNA is still required by other subtype effectors, such as Cas12b.[41] Third, not only dsDNA, but also ssDNA with complementarity to the crRNA spacer region can activate the nuclease activity of Cas12, and PAM sequences are not required for ssDNA targets. [15b] Lastly and most importantly for nucleic acid detection. after target binding, Cas12 can indiscriminately cleave adjacent ssDNAs in a sequence-independent manner in vitro.[15b] This trans-cleavage activity, also known as collateral activity, is predicted to be conserved within the Cas12 family due to their similarities in structures, though with different efficiencies. By far, the trans-cleavage has been experimentally proved in Cas12a, b, -c, -e (previously known as CasX), -f (previously known as Cas14), -g, -i, and -j (previously known as CasΦ) orthologs.[14b, 44, <sup>48, 69]</sup> The properties of different Cas12 orthologs used in nucleic acid detection, along with those of Cas9 and Cas13 effectors, are summarized in Table 1. This distinctive trans-cleavage property

enables the expansion of Cas12 applications from genome editing to biosensing.

# 2.2.2. Nonspecific Trans-Cleavage for CRISPR-Cas12-Based Biosensing

The nonspecific trans-cleavage activities of Cas12 proteins have been extensively studied and applied in nucleic acid detection. To understand the mechanism, the crystal structure analysis of Francisella novicida U112 Cas12a (FnCas12a) shows that multiple steps are involved in the target DNA and nonspecific ssDNA cleavage.[40a] Upon the recognition of target DNA, the FnCas12a-crRNA-dsDNA complex undergoes a conformational change, where the non-complementary strand fits into the catalytic cleft on the RuvC domain, leading to the cis-cleavage of the non-complementary strand. Then, the catalytic cleft becomes available for a gradual, promiscuous trans-cleavage of ssDNA in the vicinity. Even after the complementary strand is cleaved, the trans-cleavage could sustain. This mechanism has also been suggested in other Cas12 ortholog structures. Cas12b,[41] Cas12i1, [52] and Cas12i2[53] all demonstrate the activation of transcleavage activities upon RNP complex formation. Cas12i1 and Cas12i2 crystal structures reveal that conformational changes induced by target binding unblock the RuvC domain and initiate nonspecific ssDNA cleavage. These recent structural data confirm findings about Cas12 cleavage patterns and could provide insights into possible engineering.

Benefiting from the nonspecific cleavage property, researchers have been designing all sorts of biosensing platforms by combining Cas12, isothermal amplification, and labeled ssDNAs. Typically, LAMP and RPA are applied to amplify target DNA at body temperature. [70] and fluorophore-guencher (FQ)labeled ssDNAs are often utilized as reporters. When target ssDNA or dsDNA binds to a Cas12 RNP complex, Cas12 ciscleaves the target DNA and in the meantime, trans-cleaves the FQ-ssDNA reporters. The guencher and the fluorophore are then separated apart, and the free fluorophore starts to generate fluorescence signals (Figure 3A).[15b] Though the trans-cleavage is nonspecific, it indeed has some bias towards certain sequences. For example, Alicyclobacillus acidiphilus Cas12b (AaCas12b) can hardly cleave homopolymer G sequences but can work efficiently on a poly(T), (A), or (C) sequence. [43] Additionally, the length[71] and the concentration<sup>[71a, 72]</sup> of the reporters may also affect the cleavage efficiency. In fact, the fluorescence recovery reaches the maximum rate when the FQ-ssDNA reporters are longer than



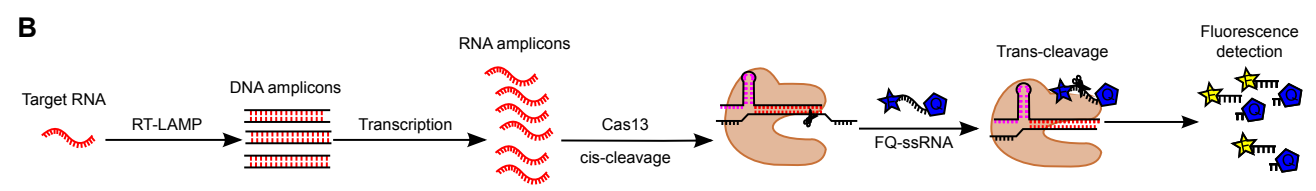


Figure 3. Mechanisms of CRISPR-Cas12/13-based biosensing. (A) CRISPR-Cas12 trans-cleavage activity. RPA: Recombinase polymerase amplification. FQ: Fluorophore-quencher. Reproduced with permission from reference. [15b] Copyright 2018 The Authors, published by American Association for the Advancement of Science. (B) CRISPR-Cas13 collateral effect. Reproduced with permission from reference. [75] Copyright 2019 Mary Ann Liebert, Inc.

### **REVIEW**

Table 2. Design Specifications of FQ Reporters for Cas12/13 Systems

| Туре    | Strain Origin                       | Homopolymer<br>Preference         | Reporter Linker Length Kinetics                                                                | Common Fluorophore                                 |
|---------|-------------------------------------|-----------------------------------|------------------------------------------------------------------------------------------------|----------------------------------------------------|
| Cas12a  | Lachnospiraceae<br>bacterium ND2006 | Poly-C or Poly-T <sup>[71a]</sup> | C <sub>20</sub> =C <sub>10</sub> >DNaseAlert>C <sub>5</sub> <sup>[71a]</sup>                   |                                                    |
| Cas13a  | Leptotrichia buccalis               |                                   | U <sub>20</sub> >U <sub>10</sub> >U <sub>5</sub> <sup>[71a]</sup>                              |                                                    |
| Cas ISa | Leptotrichia wadei                  | Poly-U <sup>[15a]</sup>           | U <sub>20</sub> >U <sub>15</sub> >U <sub>11</sub> >U <sub>5</sub> >RNaseAlert <sup>[16c]</sup> | 5'-6-FAM, <sup>[15a]</sup> 5'-HEX, 5'-Cv5, 5'-TEX, |
|         | Prevotella buccae                   | Poly-U <sup>[15a]</sup>           |                                                                                                | Alexa488, <sup>[71a]</sup> Alexa594                |
| Cas13b  | Prevotella sp.<br>MA2016            | Poly-A <sup>[15a]</sup>           |                                                                                                |                                                    |
|         | Capnocytophaga<br>canimorsus Cc5    | Poly-U <sup>[15a]</sup>           |                                                                                                |                                                    |

8 nt.<sup>[71b]</sup> Considering that the quenching effect works only when the fluorophore is in close proximity to the quencher and that a 4-nt increase in length could lead to as high as 60% increase in background fluorescence, [71c] the FQ reporters are often designed to be short. Generally, an increase in reporter concentration results in increased fluorescence intensity. [71a, 72a] However, there is a tradeoff between measured fluorescence and backgorund signals. [72b] A list of design specifications for FQ reporters is summarized in Table 2.

### 2.2.3. Engineering of Cas12 for Sensing Applications

Unlike Cas9, Cas12 proteins have limited modifications to date. Bacillus hisashii Cas12b (BhCas12b) can be engineered from a thermophilic to a moderately mesophilic variant for human genome editing.[74] Directed mutagenesis expands the PAM recognition range of Acidaminococcus sp. Cas12a (AsCas12a), and this enhanced AsCas12a (enAsCas12a) has an extensive target range and moderately improved genome editing activities.[75] More recently, AsCas12a was engineered using a bacteriostatic toxin selection marker. [76] The resulting variant, AsCas12a Ultra, has greatly improved editing capability and can target TTTT PAM. Also, the binding efficiency of Lachnospiraceae bacterium ND2006 Cas12a (LbCas12a) can be greatly enhanced by mutating DNA-proximal negatively charged residues into positively charged residues.[77] This hyperCas12a variant increases in vivo efficiency by more than 300-fold in gene activation. However, the protein engineering research has rarely focused on trans-cleavage efficiency. In a comprehensive comparison, enAsCas12a has higher trans-cleavage activities compared to wild-type AsCas12a.[78] Yet, the improvement is not significant, and its activities are heavily spacer region-dependent and sometimes lower than wild-type LbCas12a. A recent study aiming to increase genome editing activities of LbCas12a resulted in three constructs with superior cis- and trans-cleavage activities by combinations of rational mutagenesis and directed evolution.<sup>[79]</sup> On the other hand, to specifically improve nucleic acid detection, a 7-mer DNA extension on the 3' end of crRNA stabilizes the protein complex and increases the kinetics of detection. [80] The 7-mer DNA-extended crRNA and enAsCas12a were combined to generate a more robust detection platform for the SARS-CoV-2 virus. [78] Engineering of the Cas12 family could lead to higher sensitivity and potentially skip the preamplification step without compromising the readout time or requiring other sophisticated modifications. Especially with the availability of

abundant crystal structure data, rational designs could generate more efficient variants for DNA detection.

### 2.3. CRISPR-Associated Protein 13 (Cas13) System

### 2.3.1. Domain, crRNA and Target Structure

Cas13 proteins are RNA-quided ribonucleases, and their catalytic mechanism is similar to Cas9 and Cas12. However, Cas13 enzymes share few sequence similarities to Cas9 or Cas12. They all have a crRNA recognition lobe (REC) and a nuclease lobe (NUC), but the homology within the Cas13 family is also low except for one common feature, the two higher eukaryotic and prokaryotic nuclease (HEPN) domains, which exclusively exist in all Cas13 members.[81] The HEPN domain contains a wellconserved 'RΦxxxH' (R, arginine; Φ, asparagine, aspartic acid, or histidine; H, histidine) motif, which is essential for the ribonuclease activity. [14b, 62, 69, 81-82] The Cas13 crRNA structure is relatively simple, a stem-loop structured direct repeat (DR) with a 5' spacer region for Cas13a, -c and -d, or a 3' spacer region for Cas13b. The length of the spacer region ranges from 14-30 nt. Averagely 20-28 nt is optimal for RNA targeting.[83] The target ssRNA sequence needs to be flanked by a protospacer flanking sequence (PFS) for efficient interference. As opposed to Cas9 and Cas12 PAM for avoiding self-targeting of the CRISPR array dsDNA, PFS is for the identification of the target RNA.[14a] The structural diversity of Cas13 family is reminiscent of a varied requirement of PFS. For example, Leptotrichia wadei Cas13a (LwaCas13a) prefers a not-"G" P S. However, this requirement is not strict. In vivo and in vitro chemical assays using the same Cas13 can result in different PFS constraints, or no detectable PFS preferences for in vitro cleavage. [59] Most of the Cas13a PFS locates at the 3' downstream of the target. or some Cas13b orthologs, a single P S flanking at the 3' end or double PFS flanking at both 3' and 5' ends can be observed. [62]

### 2.3.2. Collateral Effect for CRISPR-Cas13-Based Biosensing

Similar to the nonspecific cleavage of ssDNA by Cas12, Cas13 also promiscuously cleaves bystander ssRNAs in trans. [20] Likewise, this collateral effect can be applied to biosensing by using FQ-ssRNAs as reporters (Figure 3B and Table 2). To understand the mechanism of Cas13-induced cleavage, extensive structure analysis has been performed on Cas13a from Leptotrichia buccalis (Lbu), [57] Leptotrichia shahii (Lsh)[59] and

### **REVIEW**

Lachnospiraceae bacterium ND2006 (Lba),[60] Cas13b from Prevotella buccae (Pbu),[61] and Cas13d from Eubacterium siraeum (Es).[64] These studies indicate that the dimerization of HEPN domains is critical for both cis-cleavage of target ssRNA and trans-cleavage of nonspecific ssRNA. The mechanism of Cas13 collateral effect is not fully understood. In vivo RNA editing in eukaryotes using Cas13 orthologs shows reduced off-target events compared to conventional short hairpin RNA (shRNA)mediated RNA knockdown or RNA interfering (RNAi) technology, [12c, 63] suggesting a possible additional machinery in preventing the trans-cleavage for in vivo settings. Particularly, Ruminococcus flavefaciens Cas13d (RfxCas13d) demonstrates high RNA targeting efficiency compared to LwaCas13a or Prevotella sp. P5-125 Cas13b (PspCas13b), and minimal offtarget effect.[63] However, recent studies have shown that the collateral activity is not negligible for in vivo RNA editing purposes.[84] The complicated mechanisms of the cis- and transcleavage of Cas13 imply that researchers should be more cautious when developing Cas13-based in vivo applications.

In vitro Cas13 assays for molecular biosensing require maximization of the collateral cleavage. Key mutations and crRNA designs can alter the binding and cleavage activities of Cas13. [576, 85] Mismatches in the seed region, the central position of the crRNA spacer region, lead to unstable or diminished RNA binding, while mismatches at the distal end of the spacer region are relatively less effective on binding specificity. [86] However, upon binding, mismatches at other positions of the spacer region may positively or negligibly affect the collateral cutting. [57b] The spacer region length also contributes to the effect of mismatch position, and the length of the spacer region-target duplex has a significant conformational impact on the HEPN domain RNase activity. [14a] From the above knowledge, we can defer that the RNA binding and cutting activity can be modified and decoupled.

### 2.3.3. Engineering of Cas13 for Sensing Applications

As of now, for more sensitive and specific Cas13-based biosensing, researchers have mostly been focusing on optimizing the spacer region length, mismatch positions, and reaction conditions. Recently, two studies showed potential to greatly alter the trans-cleavage efficiency of Cas13 proteins through different approaches. [16c, 87] Yang et al. tethered RNA binding domains onto loops that are proximal to the active site of LwaCas13a and successfully enhanced its sensitivity from 300 fM to about 10 fM after optimization. [16c] Another study by Tong et al. successfully reduced Cas13d and Cas13X trans-cleavage efficiency in vivo to reduce their cell toxicity.[87] Their work demonstrates possibilities to modulate the Cas13 trans-cleavage activities by protein engineering and elucidates key residues involved in Cas13d and Cas13X trans-cleavage activities. Engineering of Cas13 with improved trans-cleavage kinetics is challenging as higher activities lead to higher cell toxicities in vivo, and in vitro engineering would require laborious purification and testing of each individual protein. Nevertheless, these results are encouraging and shed lights on pathways for protein engineering.

# 2.4. Controversies in Cas12 and Cas13 Trans-Cleavage Kinetics

Previously, the kinetics of both Cas12 and Cas13 was measured to be diffusion limited, which makes protein engineering

unnecessary. However, two pioneering works had kinetic data revision,[15b, 61] and recent studies extensively examined the transcleavage kinetics of Cas12 and Cas13.[71a, 71b, 88] They revealed a slower kinetics than previously reported values. The  $k_{\text{cat}}/K_{\text{M}}$ values range from 10<sup>5</sup> to 10<sup>8</sup> M<sup>-1</sup>s<sup>-1</sup> depending on the enzyme, crRNA, and the reporter substrate. There are also discrepancies among all the measured data between the three studies. This contradiction in experimental data also calls for standardization to ensure reliable data. Lv et al. proposed a protocol for testing with fluorescence plate readers to minimize differences caused by equipment.[71b] Besides different standardization, measurement in cis-cleavage kinetics can be interfered by unexpected trans-cleavage events, especially for Cas13. Gel analysis shows that Cas13a cis-cleaved ssRNA target can produce more bands than expected, and the fragments are the same even with different crRNAs. [14a] This suggests that the target ssRNA is cleaved in-trans after the initial RNA binding and ciscleavage. Because the trans-cleavage kinetics is faster than ciscleavage, when using fluorophore-attached ssRNA target to measure Cas13a cis-cleavage kinetics, the fluorophores can also be trans-cleaved by activated Cas13 proteins.[71a] Hence, without excluding the effects of trans-cleavage activities, the final data analysis could overestimate the cis-cleavage kinetics of Cas13 proteins. On the contrary, Cas12 cis-cleavage activity measurement is less concerning because its trans-cleavage activities are much slower towards dsDNA targets compared to its cis-cleavage activities.[71a] Native gel separation of target DNA cleavage also shows almost identical and unique cleavage position, which indicates absence of non-specific cleavage activities.[14b]

### 2.5. Class 1-Based Biosensing

Unlike Class 2 CRISPR-Cas systems discussed thus far, Class 1 systems demand a complex of multiple subunit effectors to identify and degrade target sequences, therefore making them less ideal for biosensing applications due to the complexity. Recent studies, however, reported two Class 1-based biosensing methods. Type III-A Csm6 RNase can be employed together with Class 2 systems to further boost the detection sensitivity. [15a, 89] Csm6 protein can be activated by the cleavage products of CRISPR-Cas13 collateral activity to enable additional collateral RNA degradation and further lower the limit of detection (LOD) (Figure 4A). [15a] Else, Type III-A CRISPR-Cas systems can directly carry out target detection.[90] In 2021, following the discovery of critical roles of 5' crRNA tag and 3' target RNA antitag in RNA-guided DNA and RNA nuclease activity of Type III Cas10-Csm complex,[91] two groups of researchers developed truly Class 1-based biosensing systems. [90] For instance, upon the binding of Cas10-Csm RNP complex with the target RNA containing non-complementary 3' anti-tag, Cas10 can be allosterically activated to convert adenosine triphosphate (ATP) into cyclic oligoadenylate (cOAs). Csm6 is then activated by cOAs for collateral ssRNA reporter cleavage (Figure 4B).[90a] Such strategy benefits from a two-step signal amplification, where the collateral activity of Csm6 is coupled with the multi-turnover generation of cOAs. Moreover, on top of this approach, the collateral DNase activities of Csm1 from the Cas10 family can be further harnessed to cleave additional ssDNA reporters for enhanced signal generation.[90b] These developments further diversify the toolkits for CRISPR-based nucleic acid detection and

### REVIEW

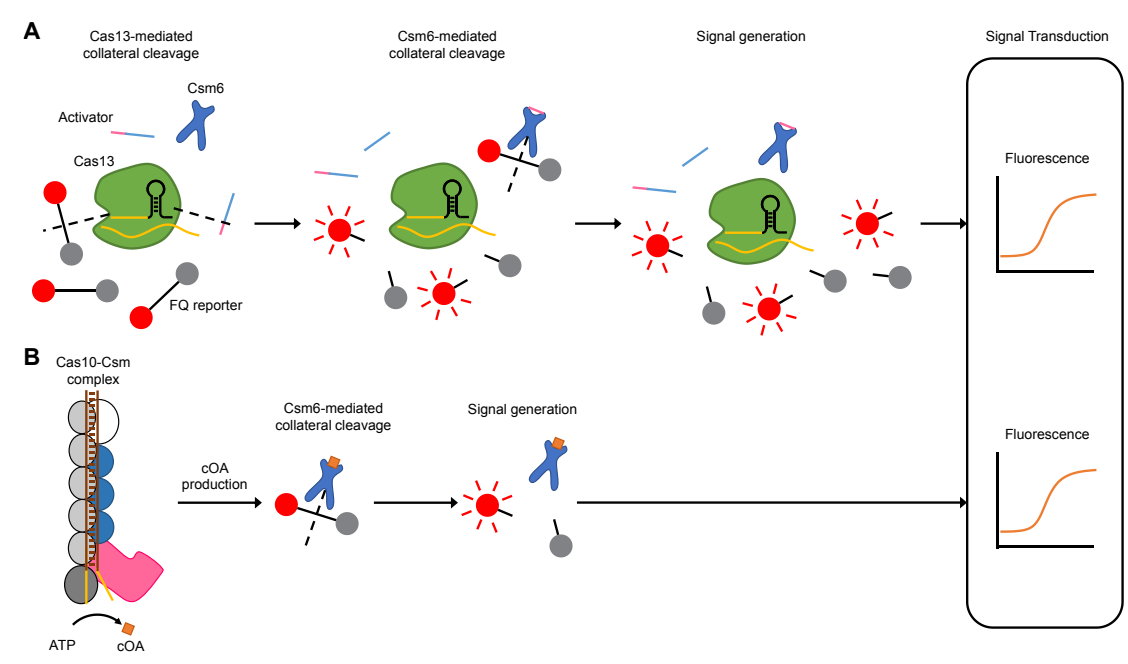


Figure 4. Mechanisms of Class 1-based biosensing. (A) Cas13-Csm6 cascade reaction. Activated Cas13 cleaves both FQ reporters and activators. The cleaved products of the activators trigger the trans-cleavage activity of Csm6, further cleaving fluorescent reporters. This tandem cleavage strategy enhances the detection sensitivity. Reproduced with permission from reference. [15a] Copyright 2018 The Authors, published by American Association for the Advancement of Science. (B) Type III CRISPR-Cas-mediated detection. Target recognition by type III CRISPR-Cas complex triggers the polymerase activity of Cas10 subunit, forming cyclic oligoadenylates and initiating Csm6 trans-cleavage of fluorescent reporters. ATP: Adenosine triphosphate. cOA: Cyclic oligoadenylate. Reproduced with permission from reference. [90a] Copyright 2021 The Authors, published by Elsevier.

allow for designs of more complex but efficient detection systems. More specifically, by combining different CRISPR systems together into a cascade, the reaction series can possibly amplify readouts from a low level of targets through multiple layers of target detection and signal generation.

### 3. CRISPR-Based Nucleic Acid Detection Systems Integrated with Diverse Signal Transduction Techniques

Signal-transducing modalities stand for a critical element in biosensing systems, in a way that caters to applications in diverse settings. For instance, field-effect transistors (FETs) are able to detect molecules down to single-molecule level, [92] thus satisfying the need for ultrasensitive detection. On the other hand, rapid and convenient POC diagnostics can be achieved by colorimetric detection. [93] In this section, we discuss recent endeavors in the integration of CRISPR technologies with numerous signal transduction techniques for nucleic acid detection. A summary of advantages and drawbacks of different transduction techniques is provided in Table 3.

# 3.1. CRISPR-Based Biosensing Systems with Optical Readouts

Optical detection, as a simple and cost-effective transduction method with high sensitivity and great stability, represents one of the most widely reported analytical strategies in the area of biosensing. [94] The non-contact nature of optical biosensing allows minimal perturbation to the biological complexes and therefore generates highly reliable and reproducible signals. Due to these advantages, the integration of CRISPR technologies with optical readouts, including fluorescence, [15b, 20, 68, 95] colorimetry, [67, 96]

surface-enhanced Raman spectroscopy (SERS), [97] and other common optical techniques, [98] has thus far been most extensively investigated. Moreover, optical biosensing allows for simple device setup with compact size and high-throughput screening, [94b] thereby holding great promises for CRISPR-based optical biosensors in the field of POC diagnostics.

### 3.1.1. Fluorescence

Fluorescence is one of the most broadly applied readouts among all optical detection techniques. Fluorescence-based biosensing employs methods such as Förster resonance energy transfer, fluorescence lifetime imaging, fluorescence correlation spectroscopy, and changes in fluorescence intensity to generate signals in response to biorecognition events. Currently, quantitative fluorescence intensity measurement remains the predominant approach for CRISPR-mediated fluorescence detection systems, mainly due to its long history for analyte detection and simplicity of application.

### 3.1.1.1. CRISPR-Cas9-Based Fluorescence Detection

Inspired by CRISPR-dCas9 mediated fluorescence in situ hybridization (FISH) for imaging of genomic loci in live human cells, [102] Guk et al. made an early attempt to employ dCas9 for fluorescence detection of *mecA* gene in methicillin-resistant *Staphylococcus aureus*. [103] As sequence-specific probes, dCas9-sgRNA RNP complexes act in a similar way to conventional antibodies and can selectively bind to the targe gene. Staining of bound genes by SYBR Green I thereby enables both simple visual readouts and quantitative fluorescence intensity measurements. Without any preamplification, this approach reached an LOD of 10 CFU/mL, higher than other non-PCR-based screening methods.

### REVIEW

Table 3. Advantages and Limitations of Different Transduction Methods for CRISPR-Based Detection

| Transduction                                                                                           | Advantages                                                                                | Limitations                                                         |
|--------------------------------------------------------------------------------------------------------|-------------------------------------------------------------------------------------------|---------------------------------------------------------------------|
| Fluorescence                                                                                           | - High sensitivity - High throughput - Real-time monitoring                               | - High background fluorescence - Photobleaching                     |
| Colorimetry                                                                                            | - Rapid deployment  - Low cost  - Direct visual readout  - Minimal instrument requirement | - Low sensitivity - High rate of false positives/negatives          |
| Bioluminescence/ Chemiluminescence  - High signal-to-noise ratio - High sensitivity - High specificity |                                                                                           | - Extra set of reagents with potential interference to CRISPR assay |
| Gel Electrophoresis                                                                                    | - Direct visual readout - Low cost                                                        | - Limited to lab settings                                           |
| Surface-Enhanced Raman<br>Spectroscopy                                                                 | - Ultrahigh sensitivity - High specificity                                                | - Poor reproducibility - High instrument requirement                |
| Refractive Index                                                                                       | - Label-free detection - Real-time monitoring                                             | - High instrument requirement                                       |
| Electrochemical Sensor                                                                                 | - Mature technique - High sensitivity                                                     | - Certain instrument requirement - High background noise            |
| Graphene Field-Effect<br>Transistor                                                                    | - Ultrahigh sensitivity - Real-time monitoring                                            | - Complicated fabrication process - High background noise           |
| Nanopore Sensor                                                                                        | - High sensitivity - Real-time monitoring                                                 | - High background noise - Low throughput                            |
| Conductivity                                                                                           | - Low instrument requirement                                                              | - Low sensitivity                                                   |

Continuing development focuses on improving the sensitivity of CRISPR-Cas9 detection systems; however, most Cas9 orthologs are considered single-turnover enzymes, indicating that they degrade DNA targets in a stoichiometric manner.[104] Although S. aureus Cas9 (SauCas9) demonstrates multi-turnover behavior, [104] the enhancement in assay activity is still constrained by the low turnover number. As a result, Cas9based detection is often accompanied by a NAA step. CRISPR-Cas9 triggered exponential amplification reaction (CAS-EXPAR) introduces PAMmers into detection assays and therefore activates site-specific ssDNA target cleavage by Cas9 to generate primers. [68] These primers initiate EXPAR for a predesigned amplification template, allowing quantification of the target ssDNA by real-time fluorescence monitoring. CAS-EXPAR achieved an LOD of 0.82 amol Listeria monocytogenes hemolysin (hly) gene fragment. In addition, CAS-EXPAR has also been demonstrated to detect hly messenger RNA (mRNA) from pathogen extracts when integrated with reverse transcription (RT) and to recognize DNA methylation after bisulfite conversion.

Another notable attempt to couple Cas9 system with NAA, CRISDA, uses nCas9 to initiate a two-step SDA reaction; however, a complex set of reagents is involved in this system, [26] including nCas9, a second nicking endonuclease Nb.BbvCl, ssDNA binding protein TP32, Klenow Fragment exo-polymerase, a pair of SDA primers, and biotin- and Cy5-tagged PNA probes. To reduce the

use of bioreagents, Wang et al. developed Cas9 nickase-based amplification reaction (Cas9nAR). In Cas9nAR, nCas9 creates two nicks on the complementary strand, allowing Klenow exopolymerase to displace the nicked strand. The nicked strand then undergoes SDA cycles in the presence of two primers, and the amplicons are monitored by real-time fluorescence measurement. This technique reported zeptomolar sensitivity within 60 min for the detection of *invA* gene in *Salmonella typhimurium* genomic DNA samples. More importantly, Cas9nAR was also validated for the detection of other bacterial genes, such as the *uidA* gene of *Escherichia coli*, *katG* gene of *Mycobacterium smegmatis*, and *indA* gene of *Saccharopolyspora erythraea*, indicating the universality of Cas9nAR in genomic DNA detection.

A shortcoming of CRISDA and Cas9nAR is the introduction of exogenous primers, which requires a high level of expertise in primer sequence design and potentially causes target-independent amplification. Furthermore, the majority of Cas9-based nucleic acid detection methods discussed so far rely on SYBR Green I staining to monitor fluorescence intensity. SYBR Green I preferentially binds to GC-rich dsDNA sequences and thus may underperform given AT-rich sequences. Consequently, Sun et al. proposed a nCas9-based MOF platform to address these issues. [27a] The complementary strand of the target dsDNA is amplified through a cycle of linear SDA, involving nicking by nCas9 and strand-displacement polymerization by Klenow exo-

### **REVIEW**

polymerase. The amplicons serve as primers for subsequent RCA of pre-designed circular probes, therefore forming a two-step amplification for augmented sensitivity. FQ reporters, originally quenched by UiO66 MOF platform, hybridize with RCA amplicons, leading to fluorescence recovery. This technique exhibited an LOD of  $4.0\times10^1$  CFU/mL with a wide linear range from  $1.3\times10^2$  CFU/mL to  $6.5\times10^4$  CFU/mL for *E. coli* O157:H7 detection, which is significantly more sensitive than the real-time PCR assay with an LOD of  $2.6\times10^4$  CFU/mL.

The development of diverse Cas9-mediated fluorescence assays has propelled the emergence of biomedical devices employing these working principles. For example, Lee et al. coupled dCas9 selective sequence binding with ion concentration polarization phenomenon on a nanoelectrokinetic detection platform. This device leverages the difference in electrophoretic mobility between dCas9-DNA complex and unbound DNA, leading to distinct concentrating patterns under a carefully tuned electric field. The stacking of dCas9-DNA

complexes can be visualized by fluorescence. This platform has been used to detect C-C chemokine receptor type 5 gene related to human immunodeficiency virus (HIV), representing a powerful liquid biopsy tool for disease diagnostics.

### 3.1.1.2. CRISPR-Cas12/13-Based Fluorescence Detection

A critical disadvantage of Cas9-mediated nucleic acid detection is the stringent requirement of assay development with respect to detection sensitivity and specificity. In addition to CRISPR gRNA, probes and amplification primers need to be carefully designed to avoid poor sensitivity or nonspecific amplification. When adapting existing assays for a wider range of applications, researchers have to put a large amount of time and effort into redesigning probes and primers. This drawback may especially impair the development of diagnostic tools for newly identified diseases, considering bacterial and viral pathogens are rapidly emerging and evolving. Alternatively, Cas12/13-based biosensing has

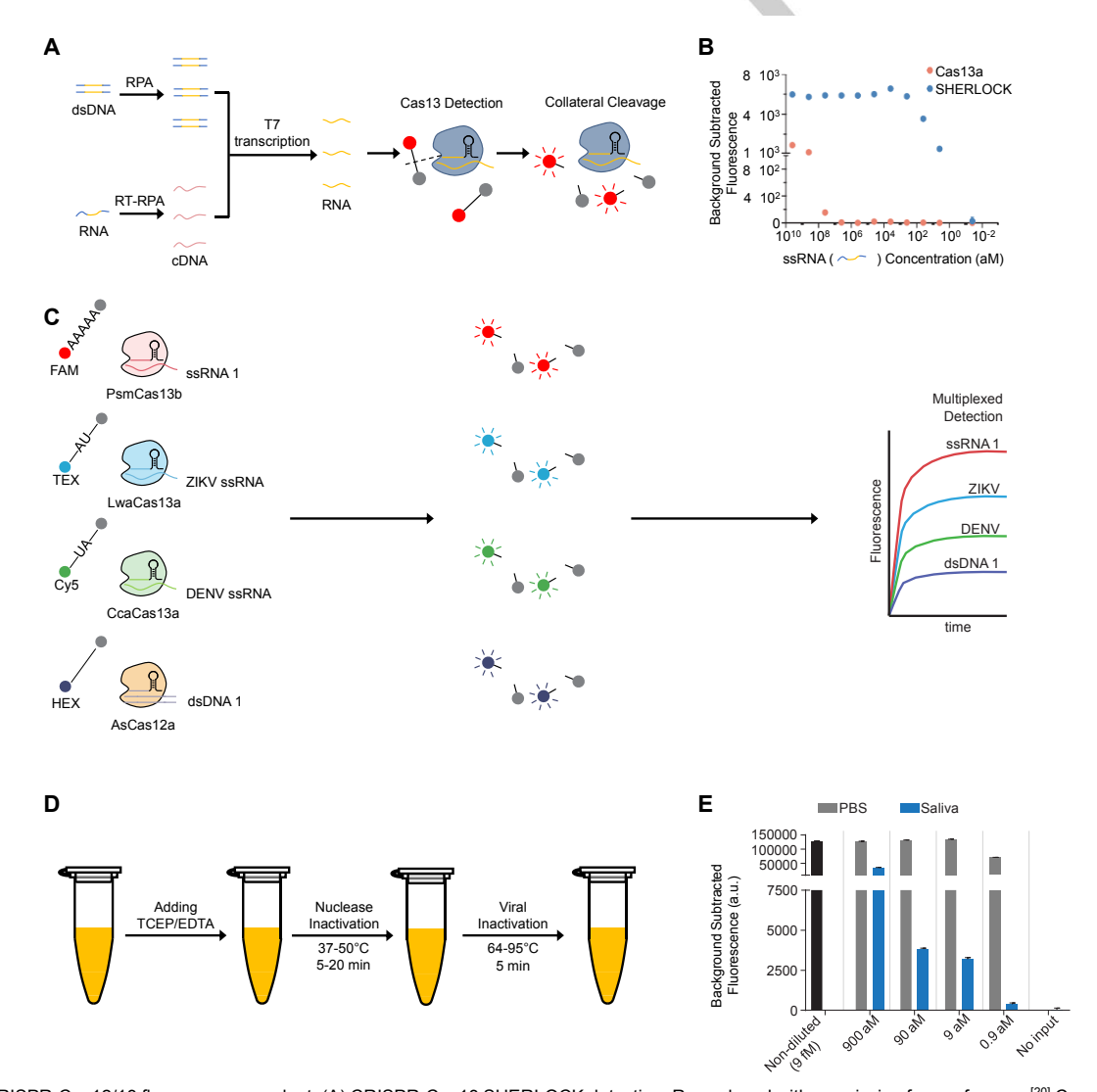


Figure 5. CRISPR-Cas12/13 fluorescence readout. (A) CRISPR-Cas13 SHERLOCK detection. Reproduced with permission from reference. [20] Copyright 2017 The Authors, published by American Association for the Advancement of Science. (B) Limit of detection for SHERLOCK is ~2 aM, as compared to ~50 fM for Cas13a alone. Reproduced with permission from reference. [20] Copyright 2017 The Authors, published by American Association for the Advancement of Science. (C) Multiplexed SHERLOCK detection. ZIKV: Zika virus. DENV: Dengue virus. Reproduced with permission from reference. [15a] Copyright 2018 The Authors, published by American Association for the Advancement of Science. (D) HUDSON procedure to extract viral RNA. Reproduced with permission from reference. [107] Copyright 2018 The Authors, published by American Association for the Advancement of Science. (E) SHERLOCK detection of Zika virus extracted from the saliva by HUDSON achieved 0.9 aM (~1 copy/μL) sensitivity. Reproduced with permission from reference. [107-108] Copyright 2018 The Authors, published by American Association for the Advancement of Science.

### **REVIEW**

provided a new choice for ultrasensitive nucleic acid detection without complicated design. The collateral activity allows activated Cas12/13 to cleave bystander probes in a sequence-independent manner. Hence, simply by changing the crRNA sequence, the assay can be adapted to detect a variety of nucleic acid targets. More importantly, the multi-turnover nature of the collateral activity converts one target recognition event into multiple probe cleavage events, resulting in intrinsic signal amplification. Although this signal amplification is still insufficient to satisfy the sensitivity requirement of amplification-free detection at the clinical level, Cas12/13-based biosensing can be integrated with a variety of strategies to further boost the sensitivity, therefore offering great potential for eliminating the need for primer design. We refer the readers to Section 4.1 for various amplification-free strategies.

Since the discovery of collateral activity, nucleic acid detection based on collateral cleavage of FQ reporters has been widely investigated. For example, often regarded as the first comprehensive and applicable CRISPR-based biosensing system,[109] specific high-sensitivity enzymatic reporter unlocking (SHERLOCK) technology (Figure 5A and B) realized detection of Zika and Dengue virus down to 2 aM by integrating 1) target preamplification via RPA or RT-RPA, 2) T7 RNA polymerase transcription of amplified DNA to RNA, and 3) Cas13a collateral cleavage of FQ reporters activated upon detection of target RNA.[20, 110] Notably, SHERLOCK is capable of discriminating single-base mismatch between target and off-target viral strains. Later, Gootenberg et al. developed SHERLOCKv2 that uses four different Cas effectors, including three Cas13 endonucleases and one Cas12 endonuclease, to achieve multiplexed nucleic acid detection with attomolar sensitivity (Figure 5C).[15a] These effectors have different dinucleotide cleavage motif preferences and therefore can trans-cleave specific reporters. By scaling up the RPA preamplification step, the sensitivity of SHERLOCKv2 can be boosted to the zeptomolar level. Moreover, SHERLOCKv2 incorporates the activation of Type III CRISPR-Cas effector Csm6 for further signal amplification. Activated LwaCas13a not only cleaves FQ reporters, but also degrades a specifically designed RNA activator containing poly(A) stretch followed by poly(U) protective stretch. The cleavage at the preferred AU dinucleotide site generates linear polyadenylates with 2'-3' cyclic phosphate ends and thus triggers the collateral activity of Csm6. This technique resulted in an enhancement of sensitivity by 3.5 times. In a follow-up study, heating unextracted diagnostic samples to obliterate nucleases (HUDSON) sample treatment method, coupled with SHERLOCK, completes a pipeline for direct virus detection from bodily fluids.[107] HUDSON uses chemical and heating treatment to inactivate RNase and lyse viral particles (Figure 5D). The entire detection process takes less than 2 hours and can detect as low as 1 copy of Zika or Dengue virus per microliter of the patient sample (Figure 5E).

Similar to SHERLOCK, for Cas12-based nucleic acid detection, a combination of target DNA amplification by RPA and DNA detection by Cas12a-mediated collateral cleavage of FQ reporters, known as DNA endonuclease-targeted CRISPR trans reporter (DETECTR), was developed for the detection of human papillomavirus 16 and 18 (HPV-16 and -18) with attomolar sensitivity. [15b] At the same time, a similar method integrating PCR with Cas12 collateral cleavage, termed one-hour low-cost multipurpose highly efficient system (HOLMES), was also reported. [95] HOLMES achieved the same attomolar level of

sensitivity as DETECTR. By including an extra RT step, HOLMES demonstrated the potential for RNA detection. Building upon this method, HOLMESv2 adopted an isothermal amplification technique, LAMP, and used Cas12b to detect various RNA targets, such as viral RNA, human cell mRNA, and circular RNA.<sup>[111]</sup> Additionally, single-nucleotide polymorphism in target DNA was successfully discriminated, and DNA methylation degree could be quantified by HOLMESv2 as well.

### 3.1.1.3. One-Pot Assay

By far, the majority of ultrasensitive CRISPR-mediated biosensing platforms have been relying on NAA, thus increasing the complexity of the detection protocols and potentially introducing human artifacts and cross-contaminations especially during sample treatment and transfer processes. Such concerns can be dealt with without compromising detection sensitivity by implementing a one-pot assay for both NAA and CRISPR reactions.

For one-pot assays, NAA proceeds in parallel with CRISPR reaction by directly mixing reagents together. [72a, 111-112] However, issues such as the stability of simultaneous reactions and compromised sensitivity due to difficulty in optimizing experimental conditions may lead to unreliable quantitative results.[113] Alternatively, several studies proposed to separate CRISPR assay from NAA reagents before the amplification step, by storing the detection assay on the tube wall, [114] at the lid, [115] or in an inner tube vessel,[113] and then allow follow-up mixing of amplicons and CRISPR reagents by either centrifugation or shaking. Interestingly, Yin et al. established a novel one-pot detection platform called dynamic aqueous multiphase reaction (DAMR) system.[116] The DAMR system consists of two phases containing different concentrations of sucrose, therefore forming a low-density top phase and a high-density bottom phase. RPA amplicons dynamically diffuse to the top phase, where the CRISPR detection reaction occurs.

### 3.1.1.4. Multiplexed Detection

Multiplexed nucleic acid detection has always been a hotspot in the field of molecular diagnostics. However, Cas12/13-mediated detection suffers from nonspecific collateral cleavage, hampering the identification of true targets among numerous candidates, whereas Cas9-based assays may not possess sufficient sensitivity due to the single-turnover nature. SHERLOCKv2 has presented a multiplexing solution as mentioned in Section 3.1.1.2, yet using multiple Cas orthologs is far from ideal, as currently there is only a limited selection of Cas enzymes developed as diagnostic tools, and they have an overlapping profile of dinucleotide motif cleavage preference. Thus, it is extremely challenging to design Cas enzyme-reporter pairs and to realize multiplexed detection with large capacity. Recently, an innovative platform called combinatorial arrayed reactions for multiplexed evaluation of nucleic acids (CARMEN) has provided opportunities for large-scale, multiplexed pathogen detection (Figure 6A and B).[117] Emulsion droplets of either target amplicons or Cas13 detection reagents are color-coded with different sets of fluorescent dyes. These droplets are pooled and then loaded onto a microwell array, thus creating pairwise combinations of input droplets. Under the exposure to an external electric field, paired droplets merge and, if a detection reaction is triggered, start to

### REVIEW

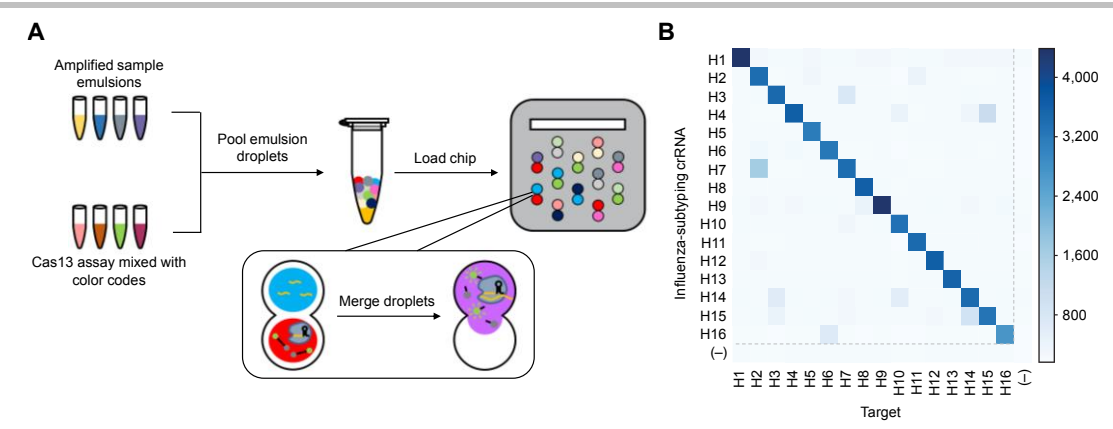


Figure 6. Combinatorial arrayed reactions for multiplexed evaluation of nucleic acids (CARMEN). (A) Workflow of CARMEN. Emulsified sample solutions and Cas13 reagents color-coded with unique fluorescent dyes are pooled and loaded onto a chip, forming all possible pairwise combinations of droplets. These droplet pairs then merge together, enabling Cas13 collateral cleavage of fluorescent reporters and emitting fluorescence with color codes specific to the droplet pairs. Reproduced with permission from reference.<sup>[117]</sup> Copyright 2020 The Authors, published by Springer Nature. (B) Identification of H1-H16 subtypes of influenza A virus. Reproduced with permission from reference.<sup>[117]</sup> Copyright 2020 The Authors, published by Springer Nature.

emit fluorescence unique to the assigned pair of color codes. CARMEN could simultaneously differentiate all 169 human-associated viruses as well as detect Zika virus with attomolar sensitivity.

### 3.1.1.5. Cas-Mediated Cascades and Nucleic Acid Circuits

Target preamplification is often considered less favorable, largely due to instrument requirements and complicated operations. More importantly, amplification-free detection methods mark a critical milestone in transitioning lab-based assays toward truly POC techniques. Yet, significantly reduced sensitivity poses a substantial challenge to amplification-free CRISPR-based diagnostics. To achieve similar level of sensitivity, common solutions include engineering Cas proteins as discussed in sections of CRISPR biochemistry, and integrating CRISPR biochemistry with ultrasensitive transduction techniques such as SERS<sup>[97]</sup> and graphene field-effect transistors (gFETs), [16b, 34] which will be discussed later in Section 3.1.5 and 3.2.2, respectively. An alternative approach involves signal amplification by implementing a Cas-mediated cascade reaction or an artificial biochemical circuit. For example, target RNA recognition by Type III Cas10-Csm complex initiates multi-turnover conversion of ATP into cOAs by Cas10, which subsequently activates multi-turnover collateral cleavage of FQ-ssRNA reporters by Csm6. [90a] However. this multiplexing signal amplification cascade reached only a sensitivity of 106 copies/µL for amplification-free SARS-CoV-2 detection. Building upon this idea, multipronged, one-pot, target RNA-induced, augmentable, rapid test system (MORIARTY) pushed the LOD of SARS-CoV-2 assay to femtomolar level (~2,000 copies/µL). This method further leverages the collateral DNase activity of Csm1 subunit to cleave FQ-ssDNA reporters in the first step of the cascade for enhanced fluorescence signals.<sup>[90b]</sup> The idea of signaling cascade has also been translated to Cas13-mediated detection, as validated in SHERLOCKv2 with a 3.5-fold sensitivity improvement. [15a] Deriving from this method, fast integrated nuclease detection in tandem (FIND-IT) further optimized the SARS-CoV-2 detection assay using chemically modified activators, resulting in an increase in sensitivity by 100 times over unmodified activators. [89] By employing a multiplexing strategy with eight different crRNAs, FIND-IT detected SARS-CoV-2 genomic sequences concentrations as low as 31 copies/µL within 20 min.

In addition to cascade reactions, an artificial catalytic nucleic acid circuit for signal amplification, known as CRISPR-Cas-only amplification network (CONAN) offers a novel solution to ultrasensitive DNA detection free of target preamplification.[118] Upon target recognition, Cas12a cleaves a specifically designed probe, generating fluorescence and releasing a second crRNA for a positive feedback circuit. This circuit triggers additional collateral activities on the probes and causes exponentially amplified signals. Compared with conventional Cas12a diagnostic tools, CONAN demonstrated an enhancement of sensitivity by six orders of magnitude to attomolar level and improves single-base specificity by 7.2- to 10.4-fold. Unlike the cascade system, this technique only uses only one Cas enzyme, avoids multiplexed targeting of different genomic regions, and therefore facilitates assay adaptation for various targets, simply by changing the initial target-recognition crRNA. As a result, CONAN is considered the most minimalistic CRISPR-mediated signal amplification detection platform thus far.[119]

### 3.1.1.6. Digital Assay

Digital assays have recently attracted much attention due to the absolute quantification of targets and increased detection accuracy.[120] In digital assays, a sample is partitioned into thousands<sup>[121]</sup> or even millions<sup>[122]</sup> of compartments containing single entities of interest.[123] As opposed to conventional analog assays that measure bulk concentration, digital assays quantify the total number of targets by calculating a Poisson distribution of the number of compartments with positive and negative detection results.[124] This absolute quantification is especially favorable to nucleic acid detection, considering the limitation of relative quantification in gPCR that may cause biases from samplespecific and sequence-dependent PCR inhibition.[125] The digitization of PCR has been widely adopted in nucleic acid testing, [126] which spurs the development of digital CRISPR-based techniques. It is intuitive to accommodate CRISPR diagnostics to formats The solution-based assavs compartmentalized into droplets of ultralow volumes (usually in the range of nanoliter to femtoliter) by microfluidics. [58b, 127] NAAbased CRISPR fluorescence assays have been directly digitized for nucleic acid detection. [127a-d] Further engineering of the reagent use in the isothermal amplification process results in warm-start assays that prevent premature amplification at room temperature,

### REVIEW

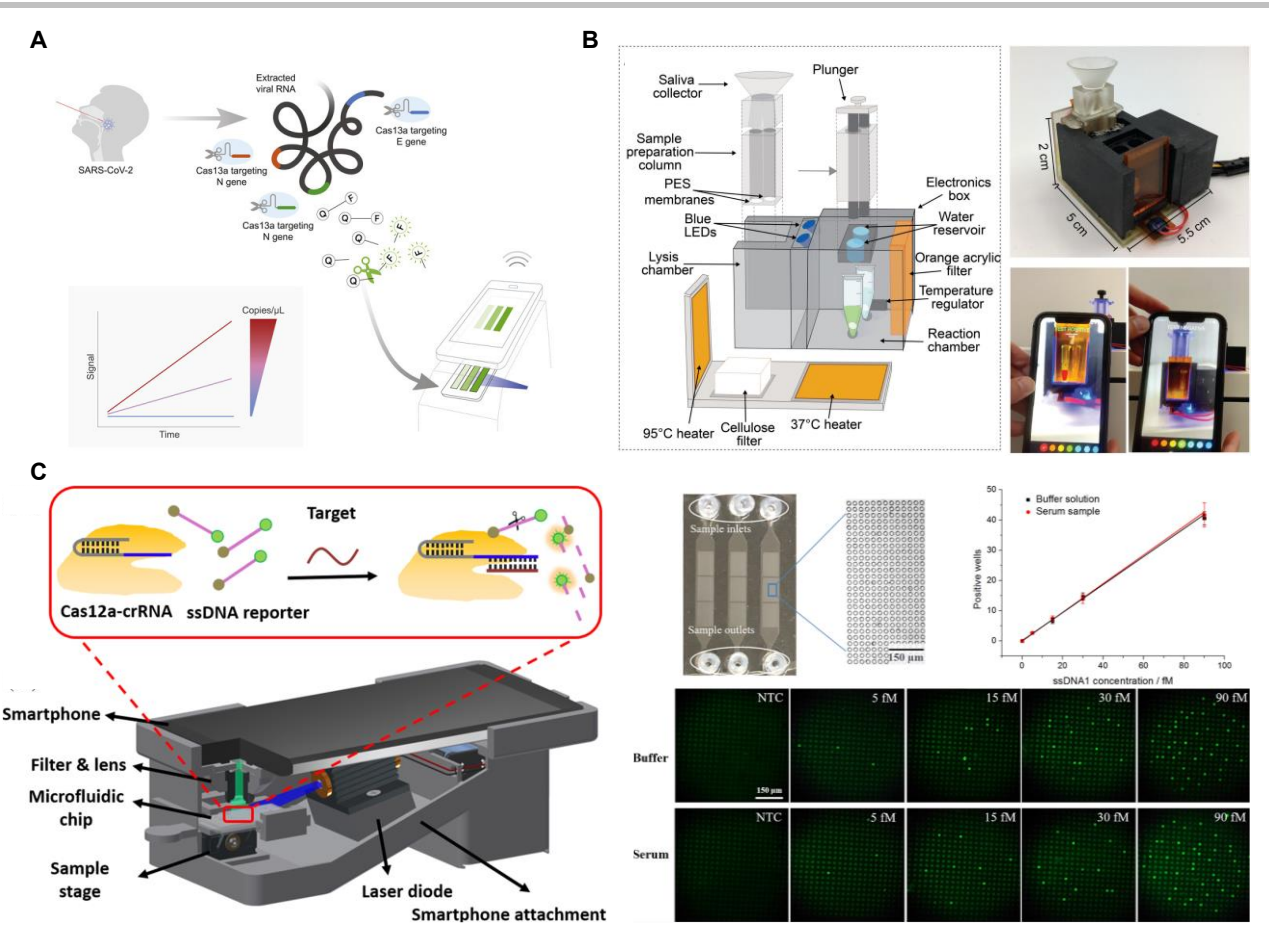


Figure 7. Smartphone-based POC CRISPR diagnostics. (A) Amplification-free SARS-CoV-2 detection with CRISPR-Cas13a and mobile phone microscopy. Reproduced with permission from reference. [18] Copyright 2020 Elsevier. (B) Minimally instrumented SHERLOCK platform for POC SARS-CoV-2 detection. Reproduced with permission from reference. [128] Copyright 2021 The Authors, published by American Association for the Advancement of Science. (C) Smartphone-based digital CRISPR for sensitive detection. Left: Schematic illustration of smartphone-based digital CRISPR platform. Right: Photo of the digital chip and images of digital CRISPR assays with a calibration curve between the number of positive wells and target DNA concentration. NTC: No-target control. Reproduced with permission from reference. [129] Copyright 2021 American Institute of Chemical Engineers.

thus generating more reliable quantitative results. [127e-g] Alternatively, the engineering of microfluidics can also avoid premature amplification in a way such that a key RPA reagent, magnesium acetate, is added through a picoinjector after droplet formation to achieve controlled initiation of target amplification. [127h] Digital NAA-based CRISPR assays often perform simultaneous amplification and detection reaction and therefore may suffer from similar drawbacks of one-pot assays. This limitation can be alleviated by employing a microfluidic device to load and partition amplification and CRISPR reagents in a sequential manner. [127i]

Compared to analog CRISPR-based assays, digital assays improve the sensitivity as a result of the confinement effect that causes an increase in local target concentration in the droplets. [58b, 127a] Leveraging this sensitivity enhancement principle, amplification-free assays have been developed, [58b, 127], 127k] and the LOD can be as low as 6 copies/µL for Cas13a-based SARS-CoV-2 detection [58b] and 17.5 copies/µL for Cas12a-based African swine fever virus (ASFV) detection. [127]]

# 3.1.1.7. Smartphone-Based Point-of-Care Fluorometric Biosensors

Smartphone-based POC CRISPR diagnostics is evolving rapidly because of the pervasive nature of smartphone users. Apart from

plate reader or real-time PCR, smartphones can easily be integrated for fluorescence signal acquisition, thus making the CRISPR diagnostic tools better suited for POC biosensing. [130] Numerous smartphone-coupled CRISPR diagnostic techniques have been reported in recent years. [18-19, 112a, 115b, 128-129, 131] For instance, Fozouni et al. designed a CRISPR-Cas13a assay to quantitatively detect SARS-CoV-2 in patient samples by smartphone imaging (Figure 7A). [18] Their sensing platform demonstrated 100 copies/µL sensitivity within 30 min without preamplification. By incorporating machine-learning algorithms, smartphone applications can be equipped with an additional capability to interpret results, in addition to data collection. [112a, 131a]

Smartphone-based detection can also be combined with devices for integrated platforms. Ning et al. built a Cas12a-based detection platform to diagnose COVID-19.<sup>[19]</sup> They fabricated a compact assay chip that can be inserted into a smartphone reader for imaging. This device exhibited an LOD of 0.38 copies/µL for the detection of SARS-CoV-2 spiked in saliva samples. Chen et al. reported a single-step CRISPR-Cas12a-assisted assay utilizing a droplet magnetofluidic device to enrich nucleic acid targets in the sample.<sup>[131b]</sup> They also designed a compact thermoplastic cartridge for fully integrated and automated operation. The entire automated device enriches targets on magnetic beads, releases them in a nearby chamber, and finally performs the RT-RPA and CRISPR-Cas12a reaction in another

### **REVIEW**

chamber. This miniaturized platform is able to detect 1 SARS-CoV-2 genome/ $\mu$ L of sample in less than 30 min. In addition, Tian et al. developed a highly efficient dual-gene diagnostic tool based on the orthogonal collateral cleavage mechanism of the Cas12a and Cas13a system on ssDNA and ssRNA, respectively. <sup>[131c]</sup> This platform performs multiplex recombinase polymerase amplification and Cas12a and Cas13a reaction in one pot and employs a two-channel smartphone fluorescence readout. The portable device demonstrated 100% sensitivity and 100% specificity for diagnosing 32 suspected SARS-CoV-2 swab samples and 35 ASFV suspected swine blood samples.

Combining all sorts of significant features mentioned above, de Puig et al. constructed a minimally instrumented SHERLOCK (miSHERLOCK) platform that incorporates a built-in sample preparation chamber with battery-powered incubation, signal readout with a smartphone camera, and result interpretation by a smartphone application (Figure 7B). The miSHERLOCK platform successfully detected SARS-CoV-2 virus from saliva samples with an LOD of 1,240 copies/mL.

Smartphones can also be used for data collection in digital CRISPR-assisted assays. Yu et al. have demonstrated a digital CRISPR-Cas12a assay based on imaging with a smartphone fluorescence reader and counting the number of positive and negative wells in a microfluidic chip (Figure 7C). [129] Using this platform, they detected hepatitis B virus (HBV) at femtomolar sensitivity without any preamplification step. The digital CRISPR assay also performed robustly in human serum samples with a recovery rate of >96%, suggesting high potential for clinical applications.

### 3.1.2. Bioluminescence and Electrochemiluminescence

The prosperity in the field of CRISPR-mediated fluorescence diagnostic platforms has stimulated the development of CRISPR biosensing based on other luminescence methods. Among a variety of luminescence biosensing techniques, bioluminescence (BL) and chemiluminescence (CL) have been successfully integrated with CRISPR technology for diagnostic applications.<sup>[24,98a]</sup> Compared with fluorescence, BL and CL rely on specific chemical reactions to generate light, leading to lower nonspecific signals and a higher signal-to-noise ratio. <sup>[132]</sup> They do not require incident light and therefore are promising optical techniques for the development of fully integrated, miniaturized CRISPR-based diagnostic tools.

Based on BL, Zhang et al. designed a paired dCas9 reporter system for *Mycobacterium tuberculosis* DNA detection.<sup>[24]</sup> In this method, split fragments of firefly luciferase are linked to a pair of dCas9 proteins and brought into close proximity for conjugation when the dCas9 pair binds to the target dsDNA. The integral luciferase enzyme then catalyzes BL reactions for signal generation. This system achieved an amplification-free sensitivity of 50 pM, and by incorporating 35 cycles of PCR, could detect as low as one genomic copy in a 500 µL pre-PCR sample.

Alternatively, electrochemiluminescence (ECL) transduction has been incorporated into a portable Cas13-driven platform for RNA detection (Figure 8). [98a] Following target recognition, LbuCas13a mediates collateral degradation of a preprimer at the preferred UU dinucleotide motif and produces a mature primer for subsequent EXPAR. ECL luminophores, [Ru(phen)<sub>2</sub>dppz]<sup>2+</sup>, ligate with the amplicons and undergo ECL reactions in the presence of coreactants on a portable ECL chip, thus generating quantifiable luminescence. This platform demonstrated the detection of miR-17 with femtomolar sensitivity and high specificity against other similar miRNAs. The paper-based ECL chip allows for simple, low-cost detection ideal for

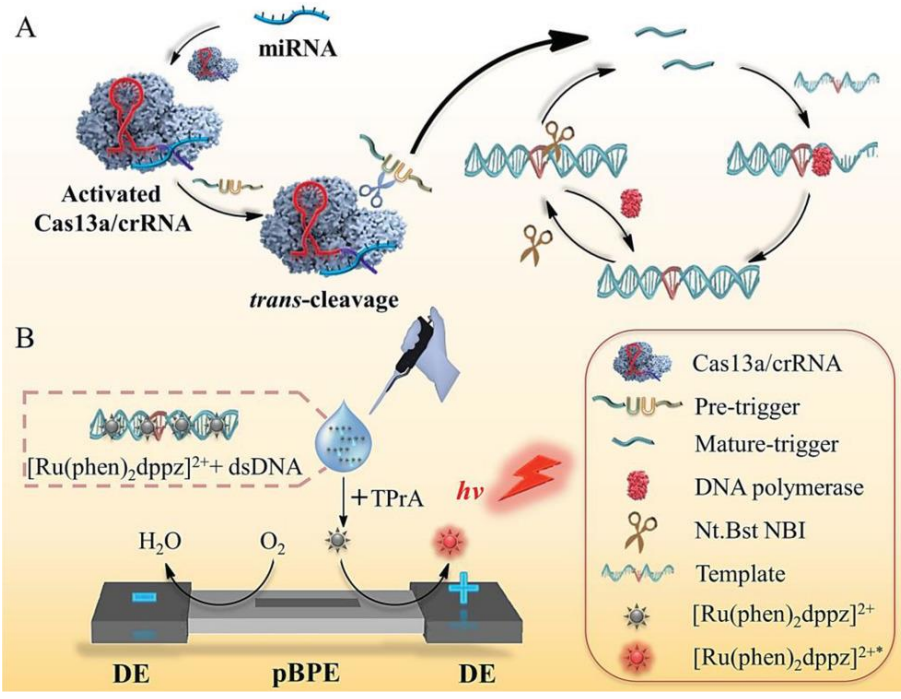


Figure 8. CRISPR-Cas13a-powered ECL chip. (A) Target miRNA detected by LwaCas13a cleaves a preprimer into a mature primer at UU motif because of its dinucleotide preference. The mature trigger serves as the primer for EXPAR amplification. (B) An ECL light switch, [Ru(phen)<sub>2</sub>dppz]<sup>2+</sup>, ligates with the amplicons, thereby initiating a reaction that generates luminescence. Reproduced with permission from reference. [98a] Copyright 2020 The Authors, published by Wiley-VCH Verlag GmbH & Co. KGaA, Weinheim.

### **REVIEW**

POC diagnostics. More importantly, the ECL reaction eliminates the need for traditional surface functionalization on biosensors, hence greatly simplifying experimental procedures.

### 3.1.3. Colorimetry

Colorimetric detection is one of the most widely used techniques for diagnostic purposes, mainly due to its rapid deployment, cost effectiveness, and minimal instrument requirements.[133] A straightforward design for CRISPR-based assays is to induce a color change as a result of colorimetric reactions following target recognition by Cas proteins. For example, Pardee et al. developed a paper-based toehold switch sensor for colorimetric discrimination between Zika and Dengue virus, and further incorporation of Cas9-driven cleavage improved specificity to differentiate variants of Zika virus (Figure 9A).[67] The biosensor uses a riboregulator called toehold switch that activates the translation of LacZ enzyme upon binding to a trigger RNA, in this case, the target RNA. Then, LacZ catalyzes the conversion of chlorophenol red-β-D-galactopyranoside into chlorophenol red, leading to a color change from yellow to purple. Coupled with nucleic acid sequence-based amplification (NASBA) and T7 transcription, this paper assay exhibited femtomolar sensitivity for detecting Zika virus. However, this method cannot distinguish between African and American strains of Zika virus, considering they have the same primer binding site and are therefore indiscriminately amplified. To address this problem, a toehold trigger is instead appended to the NASBA-amplified target RNA via reverse transcription. When a strain-specific PAM is present, Cas9-directed cleavage causes subsequent T7 transcription to generate a truncated RNA without the trigger sequence, and therefore, the paper assay remains yellow. In contrast, in the absence of the PAM sequence, Cas9 is not activated, and a fulllength RNA is transcribed, initiating the toehold reaction for a color change. The high specificity of Cas9 system allows single-base differentiation between American and African strains of Zika virus. In addition to a simple naked-eye readout, this assay can be used along with a portable electronic reader to measure light transmission through the paper substrate, providing fielddeployable, quantitative analysis of viral infections. In fact, CRISPR-mediated detection is compatible with a variety of colorimetric reactions, including the oxidation of 3,3'-5,5'tetramethylbenzidine (TMB) by horseradish peroxidase (HRP), [25, <sup>134]</sup> G-quadruplex DNAzyme, [135] or Ag<sup>+</sup>; [136] the oxidative coupling of 4-aminoantipyrine (4-AAP) and N-ethyl-N-(2-hydroxy-3sulfopropyl)-3-methylaniline (TOOS) following alucose oxidation;[137] and G-quadruplex DNAzyme-catalyzed oxidation of 2,2'-azino-bis (3-ethylbenzothiazoline-6-sulfonic acid) (ABTS)[138] or its diammonium salt ABTS2-.[139]

Lateral flow assay (LFA) is another popular format of colorimetric detection for fast and inexpensive POC diagnostics. SHERLOCK was integrated with commercial LFAs consisting of a sample pad loaded with anti-FAM antibody-conjugated gold nanoparticles (AuNPs), a control band with streptavidin, and a sample band with protein A (Figure 9B).[155a] In a typical operation, the SHERLOCK reaction mix containing FAM-biotin ssRNA reporters is added to the sample pad and carries the AuNPs through the control and sample band. Upon target detection, Cas13a trans-cleaves the reporters, reducing accumulation of AuNPs on the control band and allowing their binding on the sample band. Hence, dark purple appears on the sample band.

This LFA can detect 2 aM Zika and Dengue virus within an hour. In combination with HUDSON process for virus inactivation, SHERLOCK demonstrated streamlined LFA detection of virus from bodily fluids. [107] For diagnosis of asymptomatic malaria carriers, Lee et al. used a different sample preparation protocol termed SHERLOCK parasite rapid extraction protocol (S-PREP) to access intracellular parasites, and designed a one-pot, lyophilized SHERLOCK assay for ultrasensitive and highly specific LFA-based detection of two pathogenic species of malaria, Plasmodium falciparum and Plasmodium vivax, demonstrating CRISPR-based POC diagnostics suitable for resource-limited settings. [112b] SHERLOCK-based LFA has enabled convenient detection of various nucleic acid targets, such as CP4 EPSPS gene encoding glyphosate resistance in soybeans<sup>[73]</sup> and white spot syndrome virus in shrimp.<sup>[140]</sup> The similar collateral activity of CRISPR-Cas12 has encouraged the development of DETECTR-based or DETECTR-like LFA targeting bacteria such as Pseudomonas aeruginosa[141] and Shigella dysenteriae, [142] and viruses such as HPV-16 and HPV-18,[143] Epstein-Barr virus,[144] and ASFV.[145]

In some cases, the collateral activity may be disturbed by target-independent factors, leading to undesired inhibition or nonspecific activation.[57b, 146] Additionally, compared with the Cas12 system, Cas9 relies on the more commonly observed NGG PAM sequences, representing a more versatile tool for dsDNA detection.[146] Hence, Wang et al. developed a CRISPR-Cas9mediated lateral flow nucleic acid assay (CASLFA).[146] In CASLFA, biotinylated RPA amplicons of DNA targets bind to Cas9-sgRNA complexes. The assembled RNP complexes then flows through the LFA sample pad loaded with DNA probefunctionalized AuNPs. The Cas9 sgRNA is designed with an extended stem-loop structure that can hybridize with the DNA probes on the AuNPs. As a result, the RNP complexes pick up the AuNP-DNA probes and are captured at the LFA test line coated with streptavidin. Meanwhile, excess AuNP-DNA probes flow past the test line and accumulate at the control line. CASLFA was validated for the detection of L. monocytogenes, 35S promotor sequence in transgenic rice, and ASFV, and achieved an LOD of several hundred copies of genomic DNA, comparable to PCR-based diagnostics.

Plasmonic nanoparticles have also been extensively studied as a fundamental component for in vitro colorimetric assays.[147] The interparticle distance can be controlled by CRISPR-mediated target recognition, causing localized surface plasmon resonance shifts within the ultraviolet-visible wavelength range and associated color changes of the colloidal solution. [148] Based on this principle, Li et al. developed a Cas12a plasmonic colorimetric assay for the detection of grapevine red-blotch virus infection.[149] Cas12a-mediated collateral cleavage of ssDNA linkers prevents the crosslinking of AuNPs, and therefore, the AuNPs remain dispersed in the solution. In contrast, a lack of target DNA causes a discernible color change from red to blue due to AuNP aggregation via crosslinking. This colorimetric assay allows a simple naked-eye readout with an LOD of 200 pM, and by measuring absorbance, the LOD can be lowered to 40 pM. Combining this method with PCR can further boost the sensitivity to 10 aM of spiked targets. A follow-up study forms an orthogonal assay to reduce the possibility of false positives or negatives by adding an additional cross-validation test. [150] This extra test uses the ssDNA linker as a stabilizer to prevent aggregation of bare AuNPs at high salt concentrations. Consequently, a true positive

### **REVIEW**

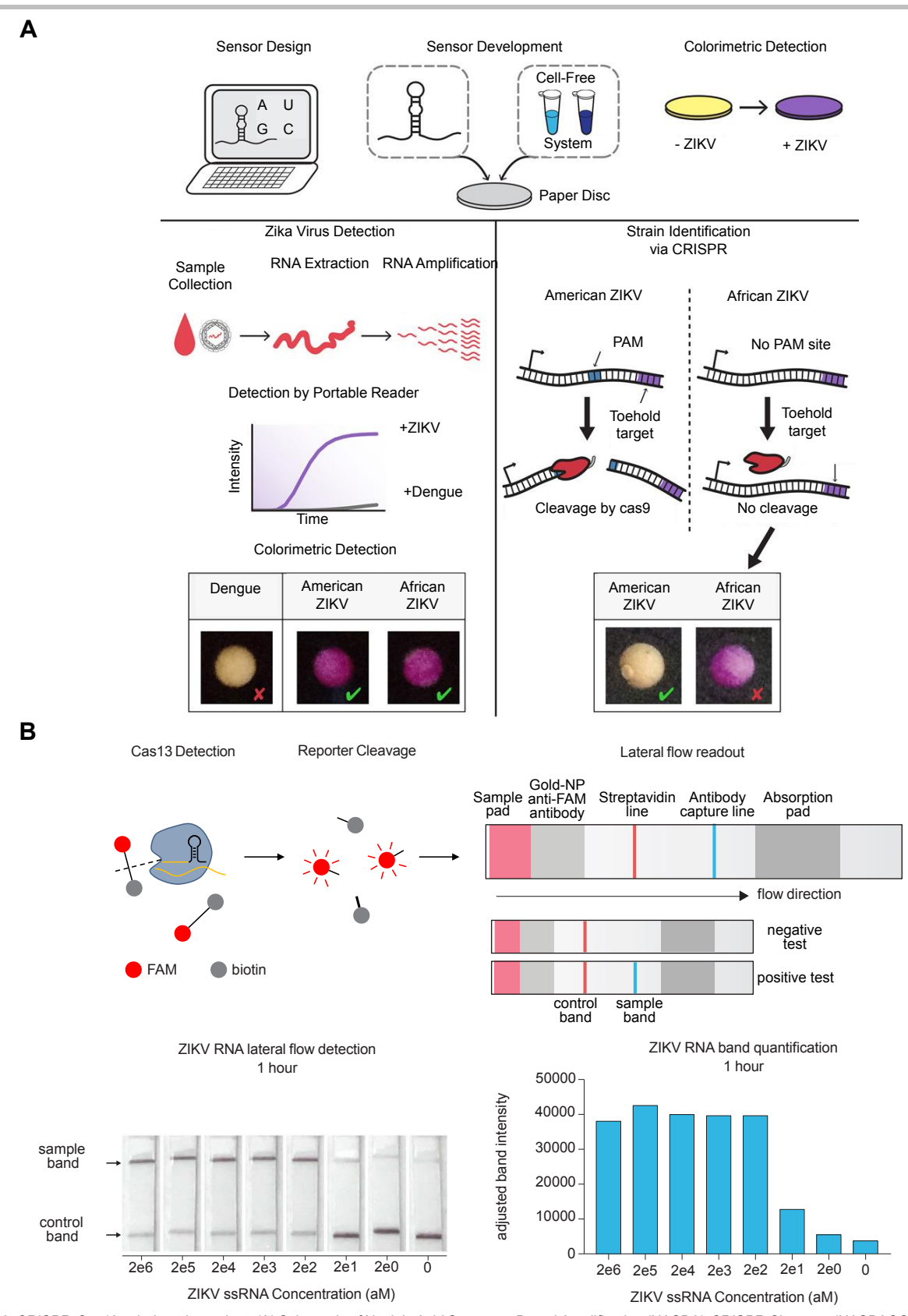


Figure 9. CRISPR-Cas13 colorimetric readout. (A) Schematic of Nucleic Acid Sequence Based Amplification (NASBA)-CRISPR Cleavage (NASBACC). NASBA amplicons undergo Cas9 cleavage and generate product sequences that trigger translation of LacZ enzyme, which is colorimetrically reported by a toehold switch reaction. Reproduced with permission from reference.<sup>[67]</sup> Copyright 2016 Elsevier. (B) Lateral flow assay for SHERLOCK detection. Reproduced with permission from reference.<sup>[15a]</sup>. Copyright 2018 The Authors, published by American Association for the Advancement of Science.

causing degradation of the ssDNA linkers should induce AuNP aggregation in the crosslinking test while maintaining the

dispersion state of AuNPs in the cross-validation test. Yuan et al. expanded the Cas12a-based colorimetric detection to Cas13

### **REVIEW**

system using ssRNA as the crosslinker, thus completing a universal Cas12/13-based AuNP colorimetric assay for nucleic acid detection. [96] The mechanism of crosslinking aggregation of plasmonic nanoparticles mediated by collateral cleavage has been extensively investigated for SARS-CoV-2[151] and Salmonella [152] detection. Further engineering attempts to control nanoparticle aggregation include 1) eliminating the use of additional crosslinkers by hybridizing ssDNAs of different lengths on the AuNPs, which leaves a ssDNA end vulnerable to Cas12a collateral cleavage; [153] 2) directly trans-cleaving ssDNAs on the AuNPs; [154] and 3) enriching AuNPs by magnetic separation for enhanced colorimetry. [155] In addition to Cas12/13-based methods, Cas9-mediated target cleavage can initiate isothermal amplification, generating amplicons that hybridize with AuNP probes to induce aggregation. [33a]

### 3.1.4. Gel Electrophoresis

So far, luminescence and colorimetry have demonstrated the potential for simple visual readout. As an extensively used technique in molecular biology for the separation of nucleic acid fragments, gel electrophoresis can also serve as a visual detection technique by inspecting nucleic acid bands on a gel image. Yet, gel electrophoresis for detection applications has been rarely investigated and almost entirely limited to lab settings, owing to the requirement of gel electrophoresis systems to induce nucleic acid separation as well as specialized personnel to prepare tests and analyze results. Nevertheless, taking a look at evolving gel electrophoresis CRISPR assays may spark the design of other platforms employing similar working principles but different transduction techniques and facilitate the development of POC diagnostics.

Gel electrophoresis plays an important role in the validation of hybridization chain reaction (HCR).[156] For detection purposes. target sequence serves as an initiator to trigger a cascade of alternating hybridization between two DNA hairpins probes, forming large chunks of hybridized strands that can be easily identified on a gel image. HCR benefits from enzyme-free signal amplification, but on the other hand, target candidates are generally limited to single-stranded sequences. CRISPR-Cas12a has equipped HCR with additional capabilities to include dsDNAs as targets and improve programmability and sensitivity. [157] In the presence of DNA targets, Cas12a mediates collateral cleavage of initiators, thus inhibiting HCR and displaying a single, sharp band on the gel image. On the contrary, HCR proceeds in the absence of DNA targes, generating broad bands. Unlike conventional HCR-based detection, where the hairpin probes have to be redesigned and validated for different targets, Cas12a-mediated HCR detection allows for easy adaptation for diverse applications by only varying crRNAs. This high programmability was verified with selective detection of tobacco curly shoot virus fragments and HBV genomes. Taking advantage of Cas12a multi-turnover trans-cleavage, this method enabled amplification-free detection of targets down to 1.5 fmol.

The size-based nucleic acid separation by gel electrophoresis has also enabled revolutionary Cas9-based multiplexed RNA detection refered to as leveraging engineered tracrRNAs and on-target DNAs for parallel RNA detection (LEOPARD). The method is based on the discovery that cellular RNA can act as crRNAs, form noncanonical crRNAs (ncrRNAs) through hybridization with tracrRNAs and activate

sequence-specific DNA cleavage activity of Cas9. Inspired by this finding, LEOPARD uses multiple reprogrammed tracrRNAs to recruit RNAs of interest as crRNAs. The resulting ncrRNAs guide Cas9 cleavage of matching DNA targets into products of distinct length. These unique DNA cleavage products can be discriminated by gel electrophoresis and traced back to target RNAs for multiplexed detection. Remarkably, LEOPARD demonstrated single-base resolution capable of differentiating wild-type SARS-CoV-2 and D614G variants. To further construct a systematic workflow for ultrasensitive detection, RNA preamplification and Bioanalyzer readout were incorporated into LEOPARD, achieving an LOD of 1.7 aM wild-type SARS-CoV-2 fragment. Although the multiplexing capability is limited to a dozen targets because of insufficient detection capacity of gel electrophoresis or Bioanalyzer, LEOPARD has the potential for multiplexed detection of millions of targets when integrated with microarrays or next-generation sequencing.

### 3.1.5. Surface-Enhanced Raman Spectroscopy

SERS takes advantage of significant enhancement of electromagnetic field induced by incident laser near metal nanostructures, along with minor chemical contributions to signal enhancement, making it one of the most sensitive spectroscopy techniques for biosensing.<sup>[159]</sup> The reported enhancement factor can be as high as 10<sup>14</sup> to 10<sup>15</sup>, and therefore, SERS is a promising candidate for achieving single-molecule level of sensitivity.[160] In light of such high sensitivity, Kim et al. developed the first CRISPR-mediated SERS assay for amplification-free detection of multidrug-resistant bacteria. [97a] The dCas9 system functions similarly to the antibody-like dCas9-sqRNA RNP complex in the CRISPR-based FISH method discussed in Section 3.1.1.1. The RNP complexes linked to gold-coated magnetic nanoparticles selectively capture target genes, and then methylene blue (MB) intercalates into the bound dsDNA targets. After magnetic separation and concentration of the nanoparticles, the Raman intensity at the 1620 cm<sup>-1</sup> characteristic peak of MB is used to quantify target concentration. Notably, the LOD of this assay reached femtomolar level without purification and preamplification. highlighting the prospect of CRISPR-mediated SERS detection as an amplification-free ultrasensitive detection technique.

The trans-cleavage activity of the CRISPR-Cas12 system has inspired alternative designs for SERS-based detection. Often in these cases, bystander ssDNA is employed as a linker to immobilize SERS tags or Raman reporter molecules. For example, TAMRA-labeled AuNPs can be tethered to a SERSactive graphene oxide/triangle gold nanoflower array via ssDNA bridges, and Cas12a collateral cleavage of these linkers upon target detection leads to a turn-off of SERS signals (Figure 10). [97b] This amplification-free method was validated with HBV, HPV-16 and HPV-18 with a detection range of 1 aM to 100 pM. A similar design anchors 4-ATP modified silver nanoparticles to magnetic beads and successfully detected 1fM SARS-CoV-2 in clinical samples using a portable Raman spectrometer. [161] Pan et al. increased compatibility with biological matrices by using Prussian blue nanoparticles due to their unique Raman characteristic peak in a biologically silent region (1800-2800 cm<sup>-1</sup>).[162] Furthermore, engineering tethered molecules can enable controlled release of Raman-active reporters.[163] Liposomes encapsulating 4nitrothiophenol (4-NTP) are immobilized on a microplate via ssDNA linkers and freed by activated Cas12. The remaining

### REVIEW

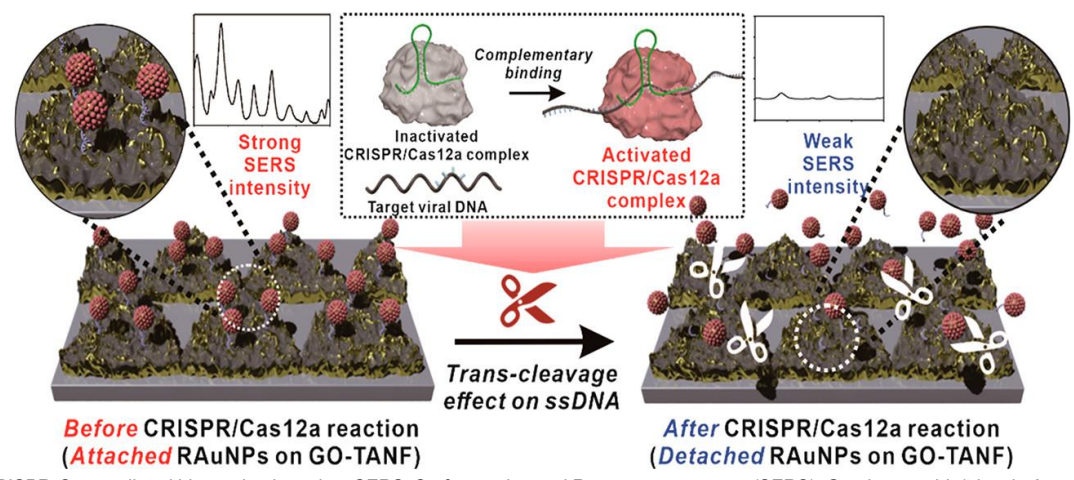


Figure 10. CRISPR-Cas mediated biosensing based on SERS. Surface-enhanced Raman spectroscopy (SERS). Graphene-oxide/triangle Au nanoflowers are functionalized with Raman probe-modified gold nanoparticles using ssDNA as the linker. Activated Cas12a cleaves the linker, resulting in a decrease in Raman intensity. Reproduced with permission from reference.<sup>[97b]</sup> Copyright 2021 American Chemical Society.

liposomes undergo breakdown in the presence of surfactants, releasing Raman-active 4-NTP for subsequent SERS measurement. This method also demonstrated versatility by enclosing cysteine in liposomes for colorimetric detection. Additionally, instead of being cut by Cas enzymes after anchoring SERS tags or reporter molecules, ssDNA can be cleaved beforehand. Degraded linkers fail to crosslink SERS tags, leaving them in dispersed form and causing weak SERS intensities. This strategy can be combined with a follow-up centrifugation step and changed into a turn-on method by measuring SERS signals in the supernatant.

As discussed in CRISPR-based colorimetric detection, AuNPs are often used in LFA to visualize detection results. Ideally, the aggregation of SERS-active nanoparticles at the LFA test line can generate sufficient SERS enhancement for quantitative and more sensitive detection. Establishing upon this idea, Pang et al. developed Cas12a-mediated SERS-LFA for the detection of HIV type 1 (HIV-1). Activated Cas12a cuts ssDNA probes, preventing SERS tags from being captured at the test line and resulting in decreased signals. This method achieved a linear detection range of 1 fM to 10 pM, with an estimated LOD of 0.3 fM. In addition, Cas12a-mediated SERS-LFA successfully discriminated 0.01% single-base drug resistance mutation from wild-type DNA background.

### 3.1.6. Refractive Index

Koo et al. have reported a dCas9-enhanced silicon microring resonator (SMR) biosensor for simultaneous NAA and nucleic acid detection in real time. [98b] In brief, RPA primers are tethered to the sensor surface and can hybridize with target DNA or complementary DNA transcribed from target RNA to initiate amplification. The amplicons on the surface of the biosensor changes the refractive index, which is monitored in terms of resonant wavelength shift. The binding of dCas9-sgRNA RNP complexes to the amplicons further increases the change in the refractive index, thus improving the sensitivity. This SMR biosensor is 100 times more sensitive than qPCR, capable of detecting tick-borne pathogens such as bacterial DNA from *Orientia tsutsugamushi* and viral RNA from *bunyavirus* with single-molecule sensitivity (~0.6 aM). Although this technique

may suffer from similar drawbacks to one-pot assays as a result of simultaneous reactions, it offers a unique label-free detection principle that may be of particular interest to optical methods encountering problems such as diminished signals due to photobleaching.

## 3.2. CRISPR-Based Biosensing Systems with Electrical Readouts

Electrical transduction modalities for biosensing rely on the measurement of biorecognition-induced changes in electrical characteristics, including impedance, voltage, and current.[167] As opposed to optical biosensors, which often require photodetectors to convert optical signals into electrical signals for processing, electrical biosensors may bypass the need for additional transducer modules as electrical signals in these platforms can be directly used for detection purposes. [167] More importantly, modern electrical devices are often equipped with additional capabilities such as sample preparation and are compatible with micro/nanofabrication contemporary techniques miniaturization, thus offering great potential for large-scale manufacturing of integrated POC platforms.[168] Additionally, electrical readouts benefit from advantages of high sensitivity, cost effectiveness, and low power requirements.[168] This section covers major efforts to incorporate CRISPR technology into electrical detection systems, including conventional threeelectrode electrochemical sensors, graphene field-effect transistors, nanopore sensors, and biomaterial-based conductivity sensors

### 3.2.1. Electrochemical Sensor

Conventional three-electrode electrochemical systems are among the first attempts to combine CRISPR with electrical transduction techniques. Dai et al. developed a Cas12a-based electrochemical biosensor, E-CRISPR, for detection of viral ssDNA, including HPV-16 and parvovirus B19 (PB-19), with picomolar sensitivity. [169] The three-electrode configuration of E-CRISPR consists of gold thin film working and counter electrodes and an Ag/AgCl reference electrode (Figure 11A). Thiolated ssDNA reporters tagged with MB are functionalized onto the gold

### REVIEW

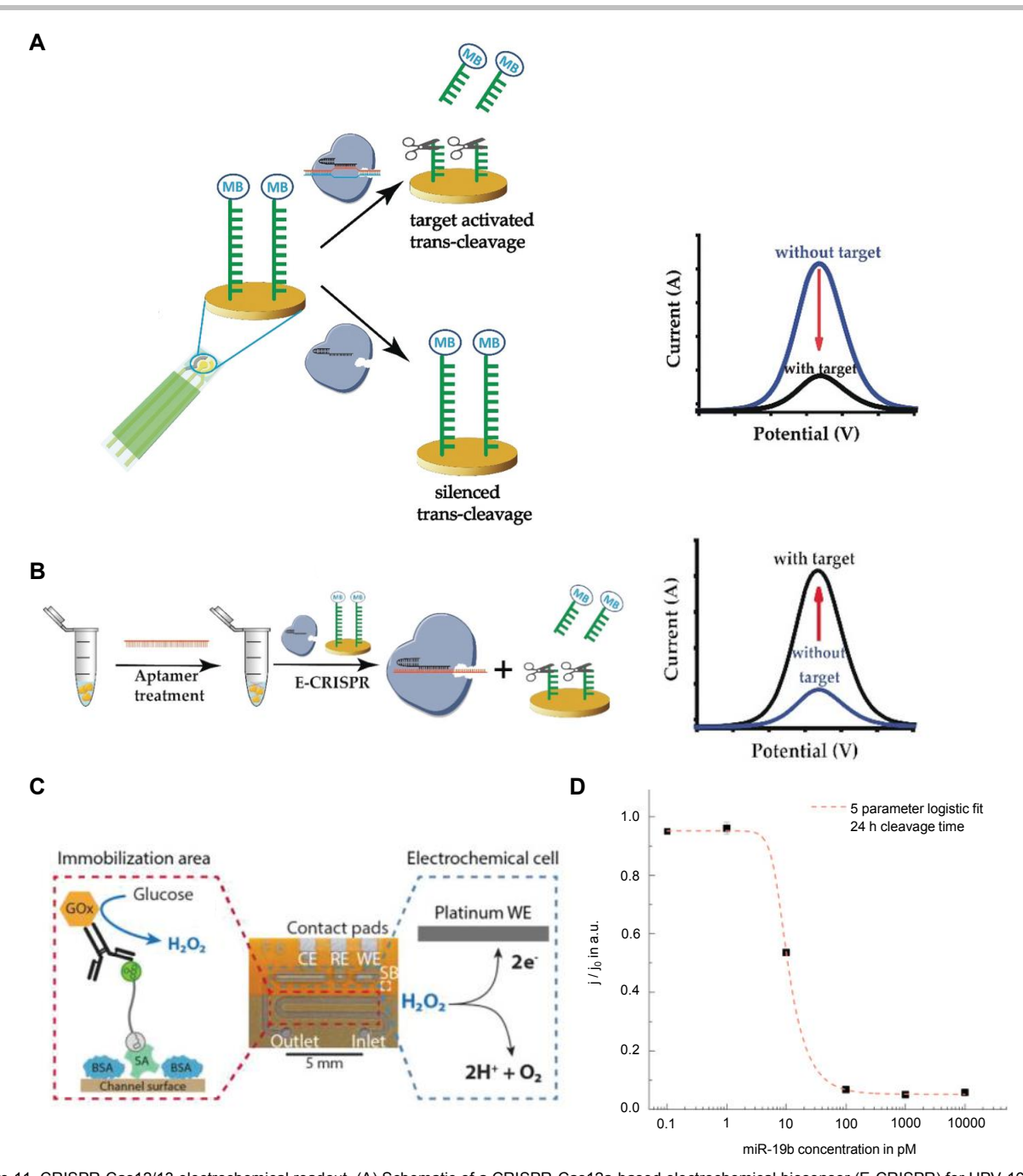


Figure 11. CRISPR-Cas12/13 electrochemical readout. (A) Schematic of a CRISPR-Cas12a-based electrochemical biosensor (E-CRISPR) for HPV-16 a PB-19 detection. Trans-cleavage of immobilized reporters on the sensor surface by activated Cas12a leads to a current decrease. Reproduced with permission from reference. [169] Copyright 2019 Wiley-VCH Verlag GmbH & Co. KGaA, Weinheim. (B) E-CRISPR cascade reaction for detection of transforming growth factor β1 (TG -β1) protein. TG -β1-specific aptamers bound to TGF-β1 proteins cannot be detected by Cas12a, resulting in an inhibition of Cas12a collateral cleavage, while in the absence of TGF-β1 proteins, collateral cleavage is unaffected. Therefore, an increase in current response is observed while TG -β1 proteins are detected. Reproduced with permission from reference. [169] Copyright 2019 Wiley-VCH Verlag GmbH & Co. KGaA, Weinheim. (C) Schematic of CRISPR-Cas13-powered electrochemical microfluidic biosensor for amplification-free detection of miRNAs. Reproduced with permission from reference. [170] Copyright 2019 The Authors, published by Wiley-VCH Verlag GmbH & Co. KGaA, Weinheim. (D) Off-chip calibration curve for miR-19b detection with 24 hours of assay incubation. The limit of detection is 2 pM. Reproduced with permission from reference. [170] Copyright 2019 The Authors, published by Wiley-VCH Verlag GmbH & Co. KGaA, Weinheim.

electrodes, and the charge transfer between the gold electrode and the redox active MB generates a measurable current signal. Upon target recognition, collateral cleavage of ssDNA reporters causes a decrease in the electrochemical current of MB, and the amount of decrease can be correlated with target concentration. Apart from nucleic acid detection, an E-CRISPR cascade reaction can be employed to enable the detection of proteins in clinical samples (Figure 11B). Aptamer probes, specifically designed to

recognize hepatocellular carcinoma-associated transforming growth factor  $\beta 1$  (TG  $-\beta 1$ ), form complexes with these protein biomarkers and become inaccessible to Cas12a target recognition. The concentration of free aptamer probes is subsequently determined by E-CRISPR. This E-CRISPR cascade represents a critical advancement of CRISPR-Cas biosensing by employing highly specific aptamer- and CRISPR-based detection

### **REVIEW**

simultaneously and expanding the range of target biomarkers beyond nucleic acids.

The electrochemical readout can also be integrated into microfluidics to prepare a miniaturized POC tool for disease diagnostics. Bruch et al. fabricated a microfluidic electrochemical sensor for the measurement of miRNAs such as miR-19b and miR-20a, of which serum levels are known to be associated with cancer.[170] The microfluidic sensor is defined with two regions, a microfluidic channel area that allows functionalization, and an electrochemical cell unit with a standard three-electrode configuration consisting of Pt working and counter electrodes and an Ag/AgCl reference electrode (Figure 11C). The microfluidic channel is pre-functionalized with streptavidin, followed by incubation with a CRISPR assay solution containing Cas13a proteins, crRNAs, ssRNA reporters dual-labeled by biotin and fluorescin 6-FAM, and sample fluid. After the incubation, glucose oxidase (GOx)-labeled anti-fluorescein antibodies are added through the inlet port. In the absence of target miRNA, ssRNA reporters can be captured by streptavidin and subsequently bind with anti-fluorescein antibodies, leading to anchoring of GOx on the channel surface. When a glucose solution is supplied to the microchannel, the immobilized GOx catalyzes glucose oxidation, and the reaction product, hydrogen peroxide, is further reduced at the working electrode, generating current signals. In contrast, the number of the immobilized GOx is decreased and less hydrogen peroxide is formed when the target sequences in the sample trigger Cas13a collateral cleavage, therefore producing lower current signals. This work managed to detect miRNAs and distinguish a single mismatch in clinical serum samples with picomolar sensitivity (Figure 11D) and represents a promising amplification-free CRISPR-based biosensor for on-site detection of disease biomarkers.

### 3.2.2. Graphene Field-Effect Transistors

The emergence of field-effect transistors (FETs) and their applications in biosensing has created additional opportunities for ultrasensitive and amplification-free nucleic acid detection. A transistor is a semiconductor device that can regulate current flow. For FET devices, an external electric field is applied to control the current passing through the semiconductor channel. In a typical three-terminal FET design, a source electrode supplies current to the semiconductor channel, and the drain electrode collects the current that flows across the channel. A third electrode called the gate electrode provides an electric field to modulate channel conductivity and thus the source-drain current. The performance of silicon-based FET devices is approaching their theoretical limit (7 nm transistor current standard vs. ~0.2 nm atomic silicon size), so researchers have been looking for alternative semiconductor materials with superior electrical properties to replace silicon.[171] Graphene, a 2D material first discovered experimentally in 2004, has very high carrier mobility (>15,000 cm<sup>2</sup>/V·s), making it a great candidate as FET channels.[172] Compared with typical FET materials such as indium oxide, the significantly higher carrier mobility of graphene has allowed it to be highly sensitive to changes in an external field. As a result, graphene field-effect transistors (gFET) are widely accepted as ultrasensitive biosensors.

Leveraging the exceptional electrical properties of graphene and high selectivity of the CRISPR-Cas system, a dCas9-mediated gFET biosensor, named CRISPR-Chip, was reported for amplification-free detection of Duchenne muscular dystrophy-associated mutations from clinical samples with an LOD of 1.7 fM within 15 min detection time (Figure 12). [34a] In CRISPR-Chip, dCas9-sgRNA complexes are covalently tethered to the graphene surface, acting as the biorecognition elements in a similar way to antibodies. The capture of negatively charged dsDNA targets alters the local electric field over the graphene channel and induced a significant change in source-drain current responses. Later, CRISPR-Chip was optimized to differentiate single-

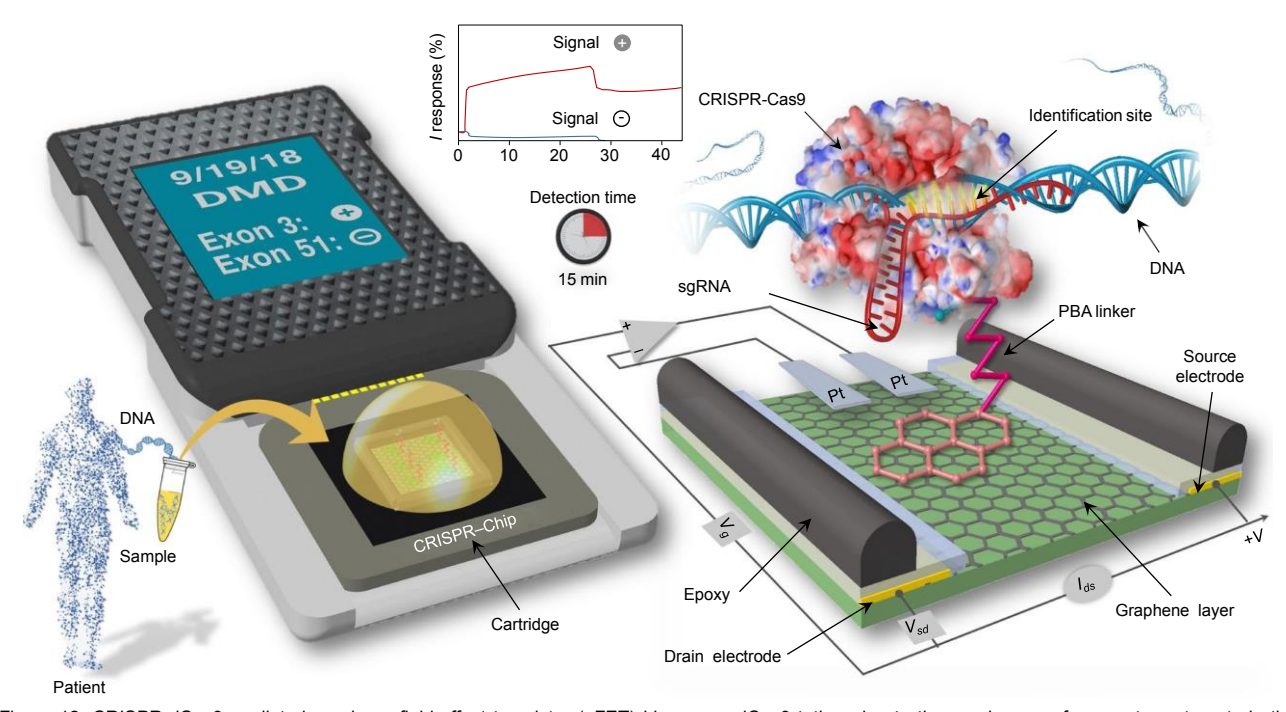


Figure 12. CRISPR-dCas9-mediated graphene field-effect transistor (gFET) biosensor. dCas9 tethered onto the graphene surface captures targets in the solution, causing a change in current. Reproduced with permission from reference. [34a] Copyright 2019 Springer Nature.

### **REVIEW**

nucleotide polymorphisms by using high-fidelity Cas9 orthologs and expanding the types of electrical measurements to record capacitance and effective gate potential in addition to sourcedrain current. [34b] As discussed earlier, Cas13-based detection is favored over Cas9-based methods because of the multi-turnover signal amplification by Cas13 collateral activities. Consequently, an amplification-free Cas13-mediated miniaturized gFET biosensor array was developed. [16b] This platform relies on Cas13 collateral cleavage of RNA probes immobilized on graphene surface and can achieve 1 aM sensitivity within 30 min for SARS-CoV-2 detection. Such detection limit is two orders of magnitude below concentrations that are generally considered relevant for diagnostic purposes.<sup>[173]</sup> More importantly, the detection reaction can be completed at room temperature as opposed to CRISPR-Chip at 37°C, marking an outstanding advance toward POC diagnostic platforms.

### 3.2.3. Nanopore-Based Resistive Pulse

Recent advances in nanofabrication processes have pushed forward resistive pulse sensing further to the development of nanopore sensors with single-molecule detection capabilities.[174] Similar to graphene field-effect transistors, nanopore resistive pulse sensors are considered candidates for preamplification-free nucleic acid detection methods. The operation of nanopore sensors relies on the Coulter Principle, whereby particles passing through a small orifice alter the electrical resistance because of the resistivity difference between the particles and the conductive media, thus creating transient changes in resistance proportional to the particle volume in the orifice, referred to as resistive pulse.[174-175] To date, a number of CRISPR-mediated nanopore sensors have been reported.[176] For example, a solid-state silicon nitride nanopore sensor generates a sharp spike in current signals as dCas9 bound onto the DNA target translocates through the nanopore, which can be clearly distinguished from current traces produced by bare DNA sequences.[176a] This platform presented single-molecule level of DNA sensing with high signal-to-noise ratio, and notably, can detect the location of dCas9 binding site based on the position of the sharp peak along the DNA signal. Furthermore, by employing multiple gRNAs targeting different

segments of a DNA target sequence, a characteristic barcode signal can be generated as several dCas9 proteins on a single sequence pass through the nanopore. [176b] Through careful design and engineering of the spacing between binding locations and the number of binding sites to create unique barcodes, this method allows multiplexed detection of lambda and T7 phage DNAs among a background *E. coli* DNA mixture.

In addition to dCas9 binding-based assay, Nouri et al. developed Cas12 collateral cleavage-based nanopore sensors for DNA detection. [176c, 176d] In brief, collateral cleavage activated by recognition of HIV-1 DNA degrades circular ssDNA reporters, reducing the event rate of reporter translocation through the nanopore. This nanopore event rate can be quantitatively related to target concentration, with an amplification-free LOD of 10 nM within a one-hour detection period. Combining with RT-PCR, an LOD of 22.5 aM for SARS-CoV-2 detection can be achieved.

### 3.2.4. Conductivity

To date, the majority of the CRISPR-based biosensing studies have been focusing on the integration of CRISPR technology with various transduction methods for different applications. In fact, engineering of biomaterials could become the next hotspot for CRISPR-based diagnostics, as the development of CRISPRresponsive smart materials was reported.[177] English et al. investigated DNA cross-linked polyacrylamide hydrogels and their responses to CRISPR-Cas12 mediated collateral cleavage. [177a] In the presence of target sequences, DNA cross-links are successfully degraded by Cas12 enzyme, resulting in disruption of polymer networks in the hydrogels and changes in mechanical properties such as permeability. Translating from this idea, a microfluidic paper-based analytical device for nucleic acid detection was designed with both optical and electrical readouts. In this platform, collateral cleavage of ssDNA cross-linker driven by CRISPR-Cas12 target recognition prevents the formation of hydrogels from polyacrylamide gel precursors in the paper channels, and therefore an unimpeded flow of a buffer solution through a color dve layer in the porous channels offers a simple visual readout. This method had an LOD of 400 pM, and when combined with RT-RPA amplification for RNA detection, the LOD

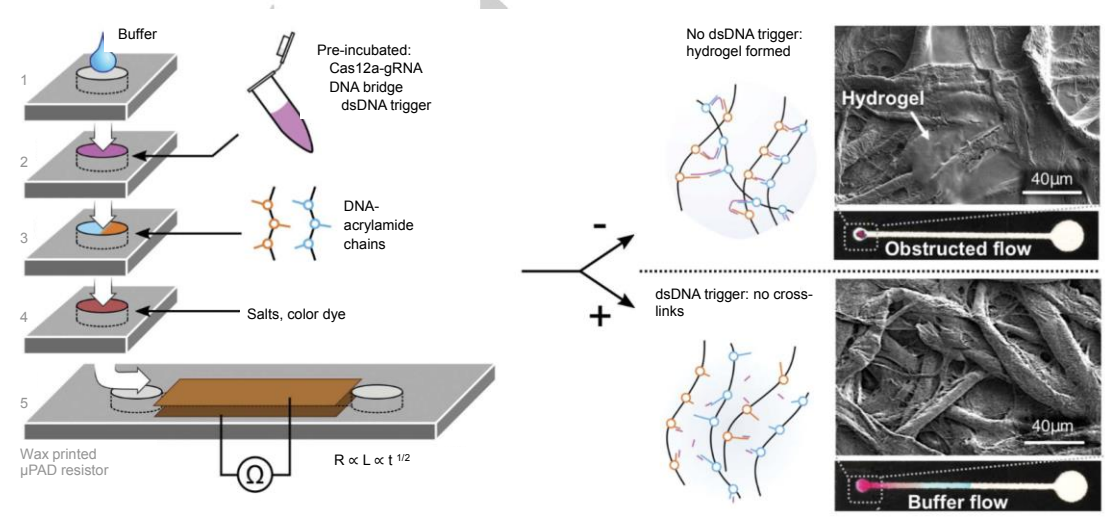


Figure 13. Paper-based fluidic device using Cas12a-controlled hydrogel. A buffer solution flows through a paper channel with a layer of hydrogel. The extent of hydrogel cross-linking is dictated by trans-cleavage of dsDNA crosslinkers by activated Cas12a and associated with buffer flow into the microfluidic channel, which is sandwiched between two electrodes. The electrical conductivity between the electrodes can be used to quantify the concentration of nucleic acids. Reproduced with permission from reference.<sup>[177a]</sup> Copyright 2019 The Authors, published by American Association for the Advancement of Science.

### **REVIEW**

was lowered to 11 aM, comparable to state-of-the-art CRISPR-based diagnostic methods. To reduce human errors and generate signals suitable for downstream data processing, electrical conductivity across the microfluidic channel was used for quantitative measurement (Figure 13). The extent of cross-linked hydrogel formation, which is inversely correlated with target concentration, governs the flow of electrolyte-containing buffer solution and hence the electrical conductivity. The electrical readout approach realized a similar sub-nanomolar sensitivity. Compared with other electrical readouts, conductivity does not rely on complicated instruments for data acquisition, as opposed to, for example, E-CRISPR, which requires high-performance potentiostat for square wave voltammetry.

# 4. Special Applications of CRISPR-Based Biosensing

By far, CRISPR-mediated biosensing has been applied to many aspects including human and animal pathogenic viral and bacterial detection, [12c, 15b, 20, 27b, 43, 67, 72a, 80, 107-108, 140, 145a, 145b, 169, 178] disease-related single-nucleotide variation (SNV) discrimination, [12c, 43, 178d, 178j] genotyping, [43] and genetically modified organism identification, [179] etc. In this section, we will

focus on four special applications in this research area besides nucleic acid detection mentioned in the above sections. The first topic is nucleic acid detection free of target preamplification. The second one discusses the detection of miRNA, most of which are shorter than 23 nt and hard to detect. Another interesting topic is to detect non-nucleic acid by CRISPR-based platform. The last topic is the ongoing development of CRISPR-mediated biosensing for the global medical crisis of COVID-19.

### 4.1. Target Amplification-Free Detection

Although CRISPR has demonstrated high sensitivity over conventional hybridization-based detection techniques, especially through the mechanism of multi-turnover collateral cleavage, the predominant strategies still rely on target preamplification in tandem with CRISPR diagnostics in order to achieve sensitivity relevant to various applications. However, traditional PCR-based nucleic acid amplification requires expensive thermocycler, limiting its applications in resource-limited settings. [180] Though isothermal amplification techniques such as RPA and LAMP are less instrument intensive, they still suffer from common drawbacks of nucleic acid amplification, including need for trained technicians and long processing time. More importantly, isothermal amplification is vulnerable to

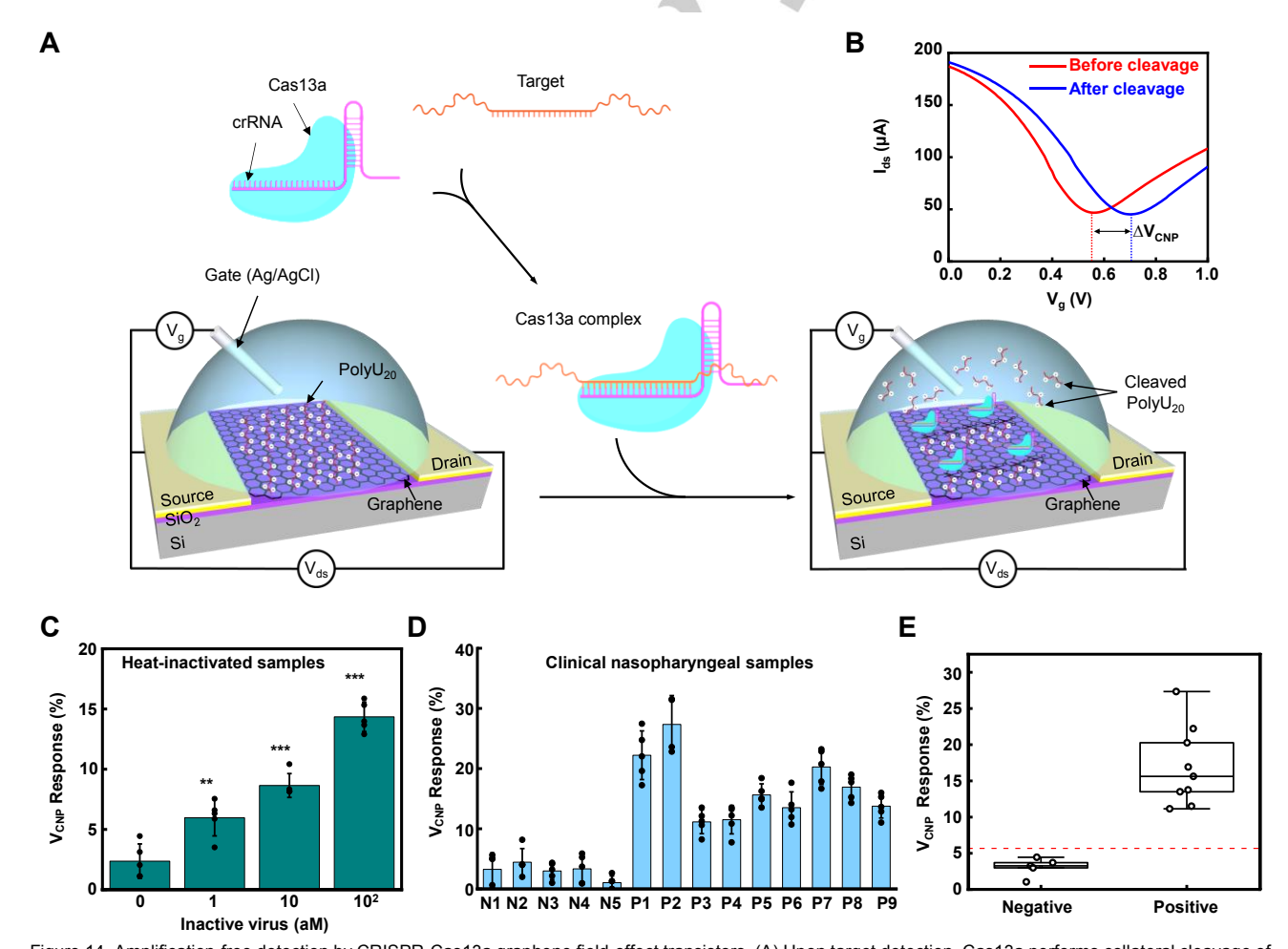


Figure 14. Amplification-free detection by CRISPR-Cas13a graphene field-effect transistors. (A) Upon target detection, Cas13a performs collateral cleavage of nonspecific reporters on the surface of graphene. (B) Reporter cleavage causes a positive shift of transfer characteristics. The change in charge neutrality voltage is used for target quantification. (C) The amplification-free CRISPR-Cas13a gFET reaches a sensitivity of 1 aM. (D-E) The CRISPR-Cas13a gFET platform is capable of differentiating five negative and nine positive clinical samples with high specificity. Reproduced with permission from reference. [16b] Copyright 2022 Wiley-VCH, GmbH.

### REVIEW

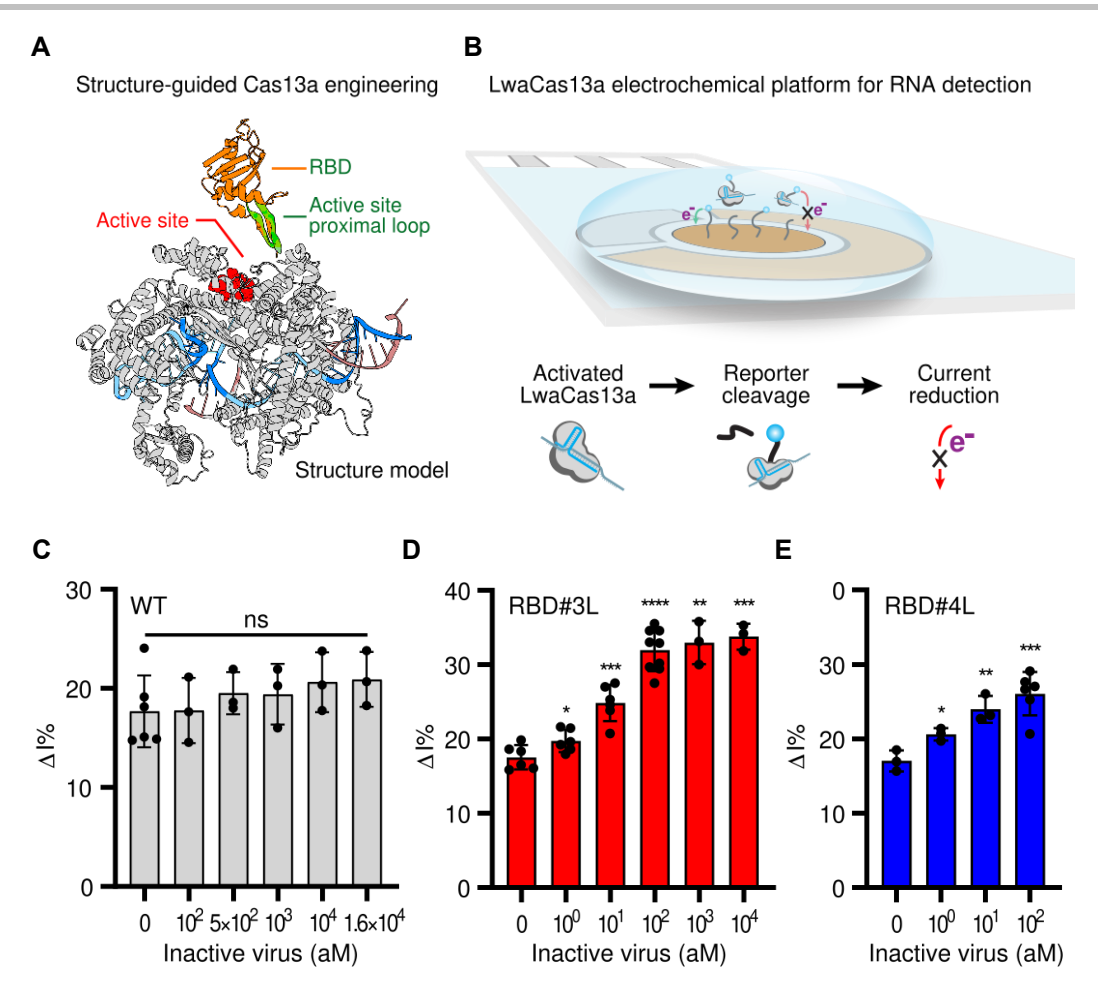


Figure 15. Engineering of LwaCas13a for enhanced collateral activity in nucleic acid detection. (A) RNA-binding domain is fused to the active-site-proximal loop of LwaCas13a for increased binding affinity to RNA target. (B) Engineered LwaCas13a performs collateral cleavage of nonspecific reporters on the surface of an electrochemical sensor, causing a decrease in current signals. (C) Wild-type LwaCas13a fails to detect 16.2 fM heat-inactivated SARS-CoV-2 using an electrochemical sensor. (D-E) RBD#3L and RBD#4L are able to achieve SARS-CoV-2 detection with 1 aM sensitivity using electrochemical sensors. Reproduced with permission from reference. [16c] Copyright 2022 The Authors, published by Springer Nature.

nonspecific amplicon formation and thus susceptible to false positive results.<sup>[16b, 16c]</sup> The nonlinear nature of the amplification process also limits its quantification capability.<sup>[16b]</sup> In addition, the introduction of target preamplification into CRISPR assay workflow requires extra sample preparation steps, increasing the risk of cross-contamination.<sup>[16b, 16c]</sup> Overall, amplification-free CRISPR diagnostics is highly desirable.

Till now, a variety of amplification-free CRISPR-based detection platforms have been reported. As mentioned earlier, the electrochemical CRISPR biosensor such as E-CRISPR<sup>[169]</sup> and CRISPR-Cas13-powered electrochemical microfluidic biosensor<sup>[170]</sup> reached picomolar sensitivity. CRISPR-Chip was able to detect 1.7 fM genomic DNA within 15 min without target preamplification. [34a] Nevertheless, the majority of amplification-free techniques do not have sufficient sensitivity in the absence of a target preamplification step. In clinical diagnostics, it is even necessary to realize attomolar-level detection for efficient medical interventions. [16c] Evidently, amid the current COVID-19 pandemic, this requirement is at the core of timely prevention of the epidemic spread, and therefore several approaches to further improve upon existing designs have been proposed.

A straightforward way to increase the sensitivity is to employ ultrasensitive sensing techniques such as gFET, [16b] SERS, [97] and digital assays. [58b, 127], 127k] For example, leveraging the collateral cleavage mechanism similar to E-CRISPR, the previously

discussed CRISPR-Cas13a gFET translated conventional electrochemical biosensing to a much more sensitive gFET technology (Figure 14A). [16b] The cleavage caused a shift of transfer characteristics, and the charge neutrality voltage could be used to quantify the shifting (Figure 14B). This sensor reported a seven-order-of-magnitude decrease in the LOD to 1 aM (Figure 14C). The clinical relevance of the sensor was proved by identifying SARS-CoV-2 in nasopharyngeal swab samples with 1 aM sensitivity (Figure 14D). The device clearly differentiated all nine positive samples from five negative samples, demonstrating excellent specificity in clinical testing (Figure 14E). The coupling of Cas12 system to SERS with attomolar detection [97b] and Cas13 to digital assays with an LOD of several copies per microliter [58b] also suggests the great potential for sensitivity boost by ultrasensitive techniques.

The revolution in CRISPR biochemistry could also further lower the LOD for current platforms. The implementation of CRISPR cascades<sup>[50]</sup> and nucleic acid circuits<sup>[118]</sup> described before could change the workflow of CRISPR reactions and achieve signal amplification from a mechanistic standpoint. Additionally, the engineering of Cas proteins could enhance the enzymatic activity as well without altering the underlying detection mechanism. For example, by fusing RNA-binding domains (RBDs) to the active-site-proximal loop of LwaCas13a (Figure 15A), the RNA target binding affinity of the fusion proteins was

### **REVIEW**

enhanced. [16c] The fusions performed collateral cleavage of reporters on an electrochemical sensor upon target RNA detection, leading to a decrease in current signals (Figure 15B). Compared with wild-type LwaCas13a that failed to detect femtomolar heat-inactivated SARS-CoV-2 (Figure 15C), both heterogeneous nuclear ribonucleoprotein (hnRNP) A1 RNA-recognition motif 2 (RRM2) and hnRNP C RRM fused with β-hairpin loop G410-G425 within the HEPN1 domain of LwaCas13a (RBD#3L and RBD#4L) resulted in SARS-CoV-2 detection with 1 aM sensitivity using electrochemical sensors (Figure 15 D and E). As opposed to previous amplification-free CRISPR-mediated electrochemical biosensing in the picomolar range using wild-type proteins, the application of engineered Cas proteins significantly improved the sensitivity and ultimately presented a novel path to ultrasensitive amplification-free detection.

### 4.2. Short Targe: Biosensing of miRNA

MicroRNA is a type of short noncoding RNAs that regulates a series of post-transcriptional modifications and perform other biological functions, [181] and can serve as biomarkers for a variety of diseases. [181b] Therefore, the detection and quantification of miRNA is critical to understand its biological and physiological functions. However, the precise measurement of miRNA has long been a challenge due to its short length (16-28 nt) and sequence similarity between different miRNA species. The conventional method to quantify miRNA is the stem-loop RT-qPCR, [182] which extends the length of miRNA by attaching a stem-loop primer and then performing RT-PCR for quantification. However, the specificity of RT-PCR is usually not high enough to discriminate miRNAs with high homology. Emerging methods based on CRISPR have been developed to address these issues. [25, 35, 50, 58, 96, 170, 183]

Initially, only Cas9 was employed for the detection of miRNA. The techniques involve using the base-complementarity of miRNA to a designed mRNA sequence to suppress or activate Cas9. Wang et al. have developed a miRNA-inducible CRISPRon (MICR-ON) system (Figure 16A). [35a] The pre-sqRNA consists of the canonical sgRNA with extra 5'- and 3'-flanking sequences. Only desired miRNA complementarity to the flanking sequences can form stable double stranded structures with the pre-sgRNAs. leading to the cleavage of the base-pairing region by endogenous cell machinery and formation of mature sqRNA. The sqRNAs activate dCas9-VPR proteins and induces the expression of RFP reporters. The corresponding miRNAs can be detected and semiquantified in proportion to the fluorescent intensity. In another strategy, Hirosawa et al. installed a miRNA complementary sequence on the mRNA 5'-UTR region of AcrllA4, a SpCas9 inhibitor (Figure 16B).[35b] The translation of AcrIIA4 is repressed by the target miRNA, leading to the activation of CRISPR-Cas9/dCas9-VPR and subsequently a fluorescence reporter. Qiu et al. utilized a dumbbell-like probe to specifically bind to the miRNA and perform RCA, resulting in a stem-loop structure DNA product (Figure 16C). [25] By using sgRNA that target the repetitive regions of this product, the dCas9 fusion with split-HRP can be recruited to the scaffold-like stem-loop structure and catalyze a colorimetric reaction to visualize and measure miRNA concentration.

Similarly, both Cas12 and Cas13 have been engineered for miRNA detection and the methods are simpler compared to Cas9 due to their collateral cleavage properties. In GOx system, as

discussed in Section 3.2.1, Bruch et al. combined LwaCas13a assays with electrochemical microfluidic chips to detect miR-19b, miR-19a, miR-20a and miR-197.[170] The miRNAs for detection are as short as 23-nt (miR-197), but the LOD is only 2 pM. To increase affinity towards miRNA, one resolution is to use Cas13a orthologs that favor shorter RNA duplex, such as LbuCas13a, which can be readily activated by a 20-bp crRNA-target binding region. Shan et al. and Tian et al. utilized LbuCas13a to detect miR-17, miR-106a, miR-20a, miR-20b, miR-10b, miR-21 and miR-155 (Figure 16D).<sup>[58]</sup> They used a syringe to create vacuum within the chip chamber to generate picoliter sized droplets from the Cas13 mix with no more than one miRNA molecule contained in each droplet. The resulting fluorescence was then measured and approached an LOD of 10 aM. On the contrary, when using the fluorescent machine for readout acquisition, an LOD of 4.5 amol was achieved. [58a] Also, nanomaterials can be integrated into the CRISPR-based miRNA detection (Figure 16E). Gold nanoparticles linking with ssRNA aggregate and transparency after low-speed centrifugation. [96] When the miRNAof-interest forming complex with crRNA and Cas13a, the linker ssDNA or ssRNA was trans-cleaved, preventing the aggregation of gold nanoparticles, resulting in a transparency-to-red visible shift from color. Sha et al. developed an amplification-free cascade CRISPR-Cas (casCRISPR) miRNA assay with a fM sensitivity (Figure 16F).[50] They designed ST-HP, a ssRNA, that acts as a bridge between LbuCas13a and Cas12f. The LbuCas13a binds target miR-17 and cleaves ST-HP, which converts it from a hairpin structure to a duplex structure. This allows ST-HP to bind and activate Cas12f and initiates transcleavage of FQ reporters, achieving fM sensitivity.

The CRISPR-Cas12a system can also be applied to miRNA detection. In the aforementioned gold nanoparticle-aided miRNA detection, using ssDNA and Cas12a to replace ssRNA linker and Cas13a can achieve similar detection results. [96] Moreover, magnetic beads can also be used for Cas12a assay. Li et al. attached magnetic beads with barcode ssDNA probes for miRNA multiplexing (Figure 16G).[183a] The probe consists of a 20mer poly(A) at the 3' terminal, a miRNA-base-complementary region in the middle, and a specific sequence barcode at the 5' terminal. The barcode is unique to each individual miRNA to facilitate multiplexing. Upon the base pairing of miRNA, DNAmiRNA hybrid is formed and then cleaved by the endogenous double stranded nuclease, releasing the 5' barcode ssDNA sequence. Then Cas12a-crRNA forms complex with different barcoding ssDNAs to discriminate and quantify multiple miRNAs. The LOD of this method is 12.6 fM. More recently, an LOD of 0.47 amol was achieved by using a more delicate design of a rolling circle transcription (RCT)-unleashed self-recruiting of crRNA by Cas12a (Cas12a-SCR) (Figure 16H).[183b] A pre-crRNA repeat is generated by using isothermal RCT and processed by Cas12a for target binding and subsequent nonspecific cleavage.

### 4.3. Beyond Nucleic Acids

CRISPR-based biosensing is intuitively related to the sensing of nucleic acids. However, with a delicate design, targets such as small molecules, [183a, 184] proteins, [183a, 185] microbes, [183a, 185] and metal ions[183a, 184a] can also be detected by the CRISPR system. The basic principle is to transduce the signal with adaptor molecules such as aptamers, [169, 184a, 186] DNAzymes, [183a, 184a] or

### **REVIEW**

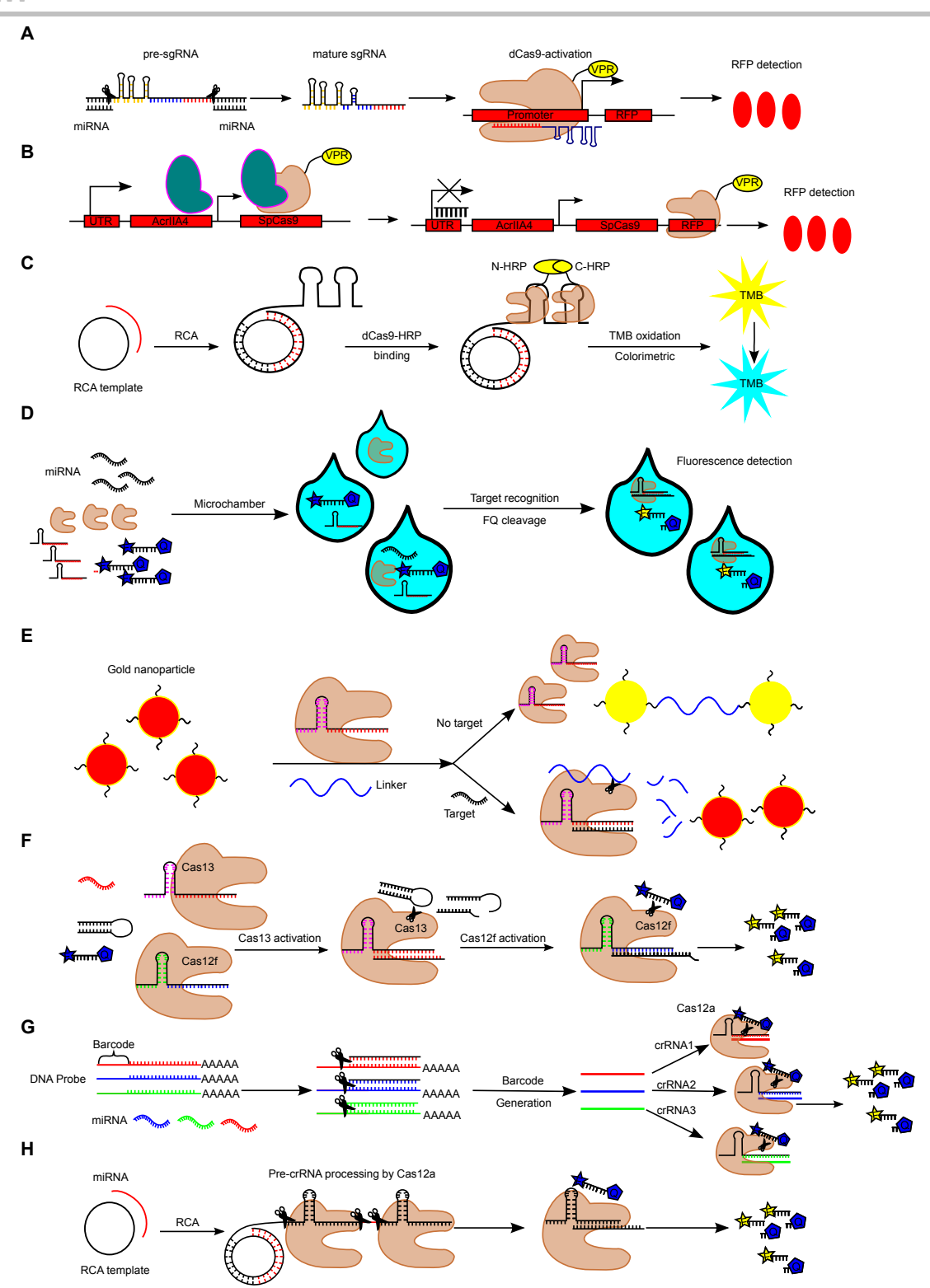


Figure 16. Mechanisms of CRISPR-based miRNA detection. (A-C) Cas9-based miRNA detection methods. (A) MICR-ON system. Reproduced with permission from reference. Copyright 2019 Springer Nature. (B) Cas9-ON system controlled by miR-AcrIIA4 switch. Reproduced with permission from reference. Copyright 2019 American Chemical Society. (C) RCA-CRISPR-split-HRP method. Reproduced with permission from reference. Copyright 2018 American Chemical Society. (D-H) Cas12/13-based miRNA detection methods. (D) Ultralocalized Cas12a/Cas13a assay by microfluidic techniques. Reproduced with permission from reference. Copyright 2021 American Chemical Society. (E) Gold-nanoparticle assisted Cas12a/Cas13a colorimetric assay. Reproduced with permission from reference. Copyright 2020 American Chemical Society. (F) Cas13a-Cas14a cascade system for miRNA detection. Reproduced with permission from reference. Copyright 2021 The Royal Society of Chemistry. (G) Multiplex miRNA detection by Cas12a. Reproduced with permission from reference. Copyright 2020 American Chemical Society. (H) Cas12a-SCR system. Reproduced with permission from reference. Copyright 2020 American Chemical Society. (H) Cas12a-SCR system. Reproduced with permission from reference.

allosteric controllers<sup>[184b, 185]</sup> that can interact with both nucleic acids and non-nucleic acid targets.

Immobilized functional DNA (fDNA) including both aptamers and DNAzymes is applied extensively to detect small molecules

### **REVIEW**

and metal ions with high specificity and fast reaction time. [183a, 184a] Xiong et al. used fDNAs such as structure-switching aptamers and DNAzymes to construct an activatable CRISPR-Cas12a system that successfully realized fast (<15 min), two-step detection of adenosine 5'-triphosphate (ATP) and sodium (Na<sup>+</sup>) ions (Figure 17A). [184a] Designed ATP aptamers have affinity to ATPs and are complementary to the activator ssDNA. These aptamer probes initially bind to the activator ssDNAs, and when encountering ATPs, undergo conformational changes to release hybridized ssDNAs. The released ssDNAs serve as target strands to activate the trans-cleavage activities of Cas12a. For Na<sup>+</sup> ion detection, a similar approach using DNAzymes was applied. Na<sup>+</sup>

Cas13a/crRNA

SSRNA

specific DNAzymes are immobilized onto a microplate. The ssDNA activators are initially locked by the DNAzymes in the absence of Na<sup>+</sup>. Upon adding Na<sup>+</sup>, DNAzymes bind to Na<sup>+</sup>, and release the ssDNA activators. The activators initiate the Cas12a trans-cleavage and subsequent generation of fluorescent signals. Li et al. also employed activatable CRISPR-Cas12 fluorometric systems by attaching the biotin-modified fDNAs onto streptavidin-coated magnetic beads.<sup>[183a]</sup> After the introduction of targets and the release of DNA activators, beads are removed by magnets, leaving these activators in the solution for subsequent activator-induced LbaCas12a collateral activities. This method was reported to be capable of detecting Pb<sup>2+</sup> down to picomolar level,

488 nm

520 nm

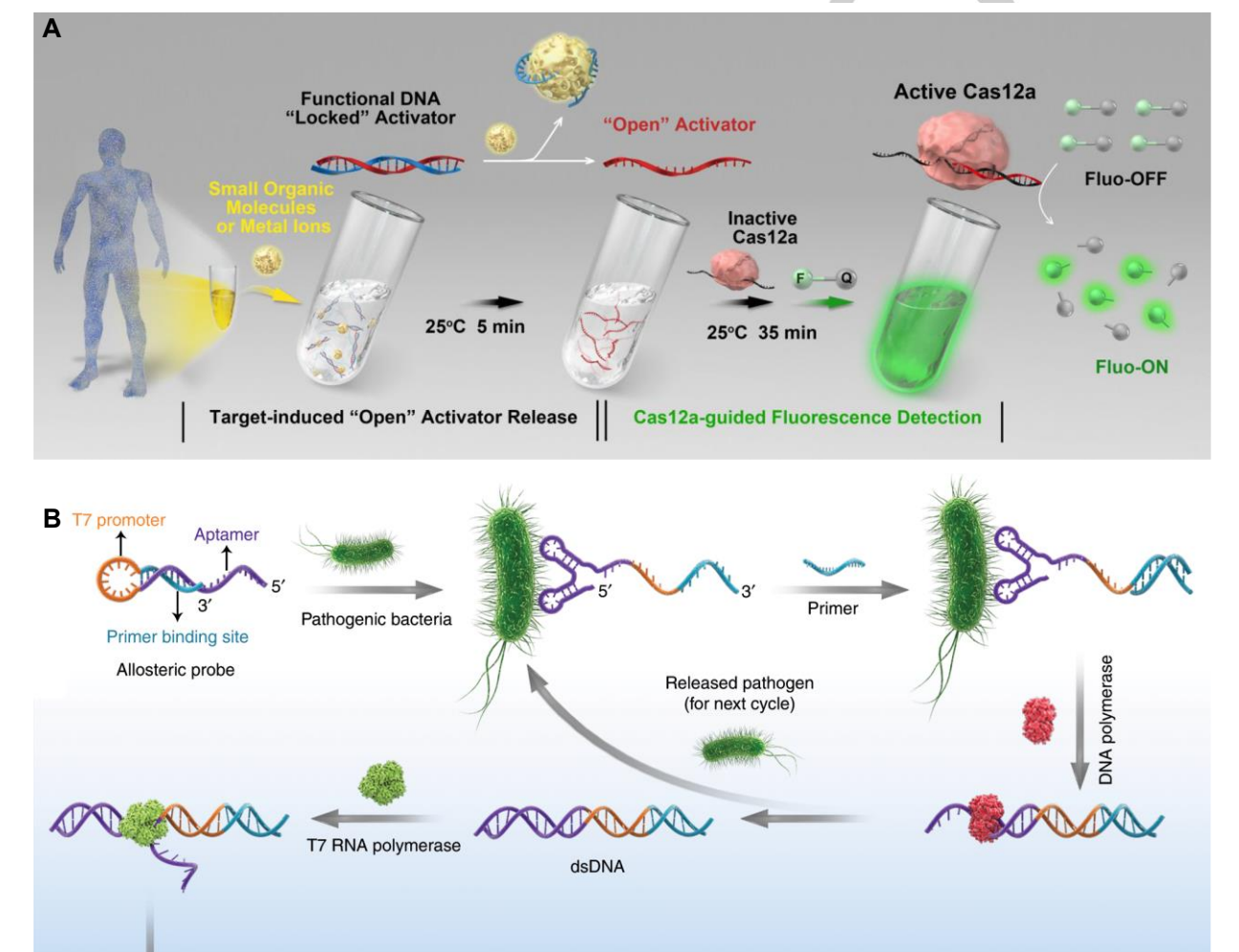


Figure 17. CRISPR-Cas-Mediated Detection of Non-Nucleic-Acid Targets. (A) Workflow of functional DNA (fDNA)-regulated CRISPR-Cas12a sensing for detection of small organic molecules and metal ions. fDNA binds to non-nucleic acid targets and releases a ssDNA activator that triggers *trans*-cleavage of fluorescent reporter by Cas12a. Reproduced with permission from reference. [184a] Copyright 2020 American Chemical Society. (B) Workflow of allosteric probe-initiated catalysis and CRISPR-Cas13a (APC-Cas) system for detection of bacterial pathogens. In the presence of target pathogen, the allosteric probe switches into an active configuration, allowing for binding with the pathogen and unlocking the primer region for DNA polymerization. DNA synthesis causes the displacement of target pathogen, and the synthesized dsDNA is transcribed into ssRNA, which activates collateral cleavage of fluorescent reporters. Reproduced with permission from reference. [185] Copyright 2020 Springer Nature.

### **REVIEW**

Acinetobacter baumannii with single-cell sensitivity, and multiplexed miRNA detection at the femtomolar level. The same concept was applied by Zhao et al. to detect exosomes by identifying transmembrane protein CD63, and a dynamic detection range of 10<sup>3</sup> to 10<sup>7</sup> particles per microliter was obtained.<sup>[186]</sup>

In addition, CRISPR-Cas12a and allosteric transcription factors (aTF) mediated small molecule detector (CaT-SMelor) was developed to detect uric acid and p-hydroxybenzoic acids and distinguish these biomolecules from structurally similar analogs. [184b] The aTFs have a substrate binding domain and a DNA binding domain. They are also fused to a cellulose-binding domain and immobilized onto microcrystalline cellulose. The functional dsDNA initially binds to the DNA binding domain. Competitive binding from target biomolecules to the substrate binding domain displaces the dsDNA and allows it to be recognized by Cas12-crRNA duplex, thus initiating collateral cleavage of FQ-ssDNA reporters. Although this method achieved nanomolar level of sensitivity, the target range this technology can detect are constrained by a limited number of target-responsive aTFs.

Not only small molecules and metal ions, but proteins and intact microbials can also be detected by CRISPR-based biosensors. As discussed in Section 3.2.1, TGF-β1 protein, an important mediator in epithelial-mesenchymal transition (EMT), can bind with and sequester its specific ssDNA aptamer.<sup>[169]</sup> The unbound free aptamers can be further detected with LbaCas12a cleavage assay coupled to an electrochemical biosensor generating a concentration-dependent electrochemical current

signal. Mentioned earlier in this Section, the pathogenic bacteria A. baumannii can be detected by CRISPR-based biosensing in a genome nucleic acid-independent manner using its specific aptamer.[183a] Shen et al. developed allosteric probe-initiated catalysis and CRISPR-Cas13a (APC-Cas) system for bacterial pathogen detection that utilizes hairpin-shaped DNA allosteric probes (AP) (Figure 17B).[185] The AP consists of three regions including the aptamer region for bacteria recognition, primer binding region for DNA extension reaction, and T7 promoter region for transcription. The AP recognizes and binds with the pathogen, causing a structural change of AP and exposing previously blocked primer binding site to primer strands. The resulting double-stranded primer domain allows DNA polymerase to initiate extension, which subsequently displaces the pathogen. T7 promoter sequence on the dsDNA produced by DNA polymerase leads to transcription of DNA template into ssRNA by T7 RNA polymerase. CRISPR-Cas13a effector hybridizes with the transcribed ssRNA, cuts FQ-ssRNA reporters, and generates measurable fluorescence signals. The three-stage process results in enhanced fluorescence intensity and ultrasensitivity. APC-Cas was found to be able to detect Salmonella enteritidis as low as 1 CFU in real food samples.

### 4.4. Coping with the COVID-19 Pandemic

With the outbreak of the COVID-19 pandemic, scientists all over the world are initiating and accelerating their COVID-19-related research to understand the basic biology of the virus, improve clinical diagnostics and develop vaccines and drugs. CRISPR

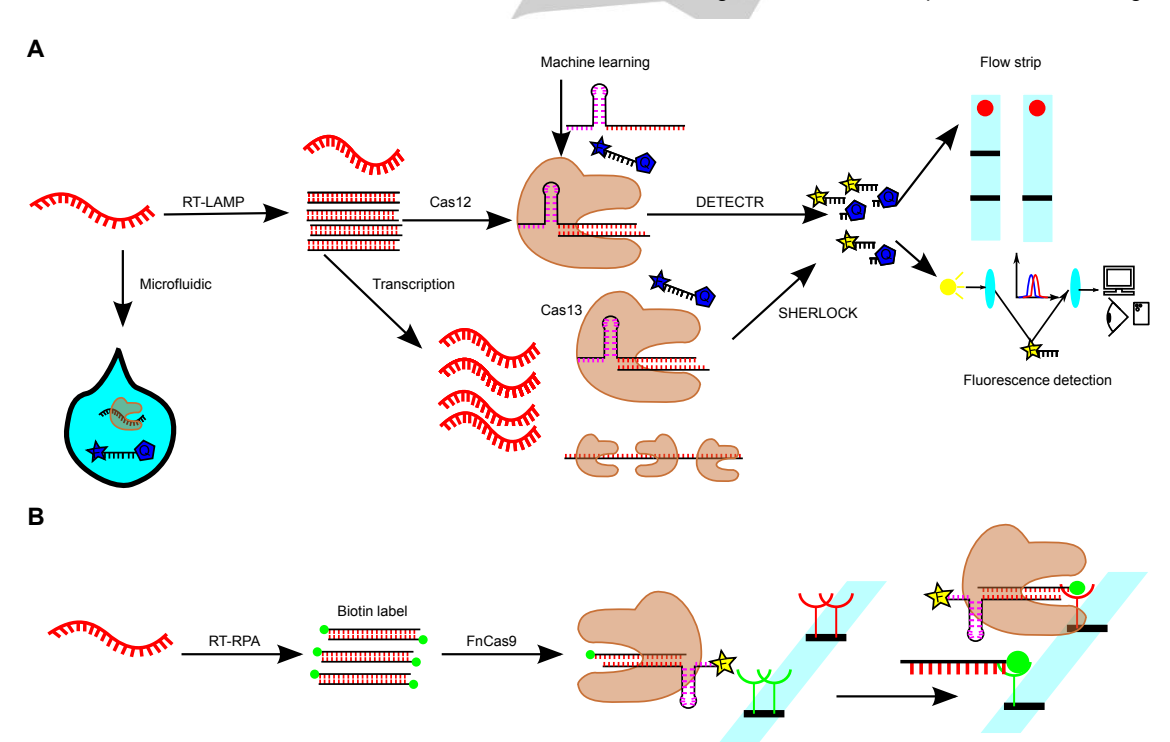


Figure 18. Schematics of CRISPR-based SARS-CoV-2 detection. (A) A summary of various methods used in SARS-CoV-2 detection. The amplification-free method utilizes microfluidic techniques to achieve highly sensitive detection. [127k] Otherwise, the viral RNA is first reverse transcribed and amplified to dsDNA. dsDNA can be detected directed by Cas12a or be transcribed into RNA and detected by Cas13a. The crRNA can be optimized by machine learning. [178h] Multiple sites can be targeted simultaneous to increase the concentration of active proteins. [18] The output signal is often produced by trans-cleavage of FQ reporters. The final detection of the reporters can be from multiple different methods including lateral flow strip. [108] computer analysis, naked eyes, [27b] and mobile phone miscroscopy. [18] Reproduced with permission from references. [177k, 178h] Copyright 2021 The Authors, published by Springer Nature. [108] Copyright 2020 Elsevier. [19] Copyright 2020 The Authors, published by Springer Nature. [108] Copyright 2021 The Authors, published by American Society for Microbiology. (B) The schematics showing the mechanism of FnCas9-based detection, FELUDA, on a lateral flow strip. Reproduced with permission from reference. [178] Copyright 2021 The Authors, published by Elsevier.

### **REVIEW**

experts are also providing candidate resolutions for testing and intervening of COVID-19. [27b, 72a, 80, 108, 178e-k, 187] This part will describe some of these studies in terms of tailoring CRISPR-based biosensing for the detection of SARS-CoV-2 viral RNA (Figure 18A). [18, 27b, 108, 127k, 178h]

As early as February 2020, Zhang et al. published a SHERLOCK-based testing protocol, targeting the S and ORF1ab gene of SARS-CoV-2.[178e] Metsky et al. designed a set of machine learning algorithms to predict amplification primers as well as maximally active Cas13 assays across virus variations for 1,933 vertebrate-infecting viral species to achieve high specificities.[178h] Rauch et al. developed Cas13-based, Rugged, Equitable, Scalable Testing (CREST) by coupling thermal cycling PCR and Cas13 assay with blue LED and orange filter readout.[27b] Broughton et al. developed a DETECTR-based method targeting both E and N gene of SARS-CoV-2.[108] They extracted the viral RNA from clinical swab samples by using a universal transport medium (UTM), then amplified the signal by using simultaneous reverse transcription and loop-mediated isothermal amplification (RT-LAMP), and finally performed Cas12a cleavage assay with lateral-flow-dipstick readout. This method, compared to CDC's RT-qPCR method, is less sensitive due to the use of colorimetric readout (10 copies vs. 1-3.2 copies per input). However, this method requires much less equipment and is time-saving (~40 min vs. 4 h). Azhar et al. developed a Cas9-based detection method, named FnCas9 editor linked uniform detection assay (FELUDA) (Figure 18B).[178j] FnCas9 is an ortholog of Cas9 from Francisella novicida, featured by a high mismatch sensitivity. Therefore, it can be used for the detection of single-nucleotide variations. Briefly, they used FAM-labeled sgRNAs and biotin-labeled amplicons for in vitro detection of target genes, including HBB gene (sickle cell anemia gene mutations), Helicobacter pylori genotype, H1N1, SARS-CoV-1 and -2. As mentioned in section 3.1.1, Ackerman et al. developed CARMEN using a massive-capacity chip (mChip).[117] Fozouni et al. demonstrated a pre-amplification free detection of SARS-CoV-2 virus using Cas13-based assays and mobile phone microscopy.[18] Similarly, Shinoda et al. developed CRISPRbased amplification-free digital RNA detection (SATORI) by combining Cas13 and microchamber technologies.[127k] The femtoliter volume of microchambers divides the target virus into single molecule droplets and increases the sensitivity to femtomolar levels and decreases the turnaround time of detection to less than five minutes. These technologies focus on designing portable and quick detection kits and demonstrate the flexibility of CRISPR-based systems. However, they also show the requirement of sensitive measurement strategies to compensate for the insufficient activities of the CRISPR-Cas proteins.

### 5. Summary and Perspectives

This review focuses on both the fundamental biochemistry of CRISPR machineries and the engineering of CRISPR-based biosensors. CRISPR has high specificity toward nucleic acids of interest, and the detection mechanism is simple and straightforward. However, CRISPR-based diagnostics is greatly constrained by inadequate sensitivity for clinical scenarios and thus often coupled with target preamplification. Consequently, such setup makes it particularly difficult to achieve truly POC detection integrating sample preparation, detection reaction, data

collection, and result interpretation. Moreover, the multiplexing capability of CRISPR-mediated detection is limited owing to compromised sensitivity from reagent mixing, potential off-target detection, and heavy dependence on labels for signal generation.

Researchers have applied engineering principles to both the enzymes and the biosensors to lower the limit of detection. From the biochemistry perspective, the binding and cleavage mechanism of Cas9, Cas12, and Cas13 is well understood due to multiple crystal structures during different stages of the reaction process. However, the promiscuous trans-cleavage mechanism of Cas12 and Cas13 proteins is still poorly demonstrated from the available data. In addition, protein engineering is not extensively applied to Cas12 and Cas13 to improve their trans-cleavage properties. Further studies in this direction could potentially simplify biosensor designs with fewer detection steps and easier manufacturing. On the other hand, from the perspective of the engineering of biosensing technologies, amplification-free detection that involves less complicated reagents is generally favorable toward the development of a truly POC platform. In this regard, ulrasensitive readout methods combined with multiturnover collateral cleavage by Cas12 or Cas13 for intrinsic signal amplification are the preferred strategy. Ongoing research continues to explore possibilities to incorporate different readouts, for example, piezoelectric sensing  $^{[188]}$  or even as simple as imaging and counting the number of bubble generation.[189] Another foreseeable trend is high-throughput, multiplexed detection assisted by machine learning.[178h] Hence, we anticipate the future of CRISPR-mediated biosensing to be an integrated POC diagnostic platform with optimized CRISPR machineries and transduction modalities for amplification-free, ultrasensitive, highly specific, multiplexed, and large-scale disease screening.

This field is developing rapidly by the contributions from multiple disciplines as researchers are racing to find more solutions to the current COVID-19 pandemic. By tackling the issues from both biochemistry and bioengineering perspectives, toolkit designs with fewer steps and simpler materials have emerged while maintaining the detection specificity. With the recent development of amplification-free assays, the prospect of this new technology becoming an alternative to the PCR-based detection methods is increasingly promising, and the properties of the enzymes and the design of the toolkits can not only expand the testing capacity of the current facilities but also provide low-cost, time-saving, and user-friendly portable devices to ordinary people as POC solutions.

### **Acknowledgements**

We acknowledge the funding support by the University of Connecticut start-up fund (to Y.Z.), NSF CBET-2103025 and ECCS-2113736 (to Y.Z.), Rice University Startup fund (to X.G.), NSF CBET-2031242 (to X.G.), Welch Foundation C-1952 (to X.G.), and NSF CBET-1944167 (to Q.W.).

**Keywords:** CRISPR-Cas Biochemistry • Biosensors • Molecular Diagnostics • SARS-CoV-2 • Amplification-Free Detection

- [1] Y. V. Suseela, N. Narayanaswamy, S. Pratihar, T. Govindaraju, Chem Soc Rev 2018, 47, 1098-1131.
- [2] a) A. Cassedy, A. Parle-McDermott, R. O'Kennedy, Front Mol Biosci 2021, 8, 637559; b) J. W. Law, N. S. Ab

### **REVIEW**

- Mutalib, K. G. Chan, L. H. Lee, Front Microbiol 2014, 5, 770.
- [3] M. de Planell-Saguer, M. C. Rodicio, *Anal Chim Acta* 2011, 699, 134-152.
- [4] M. Lisboa Bastos, G. Tavaziva, S. K. Abidi, J. R. Campbell, L. P. Haraoui, J. C. Johnston, Z. Lan, S. Law, E. MacLean, A. Trajman, D. Menzies, A. Benedetti, F. Ahmad Khan, *BMJ* 2020, 370, m2516.
- [5] S. A. Bustin, V. Benes, J. A. Garson, J. Hellemans, J. Huggett, M. Kubista, R. Mueller, T. Nolan, M. W. Pfaffl, G. L. Shipley, J. Vandesompele, C. T. Wittwer, *Clin Chem* 2009, 55, 611-622.
- [6] M. L. Wong, J. F. Medrano, *Biotechniques* **2005**, 39, 75-85.
- [7] a) F. Palaz, A. K. Kalkan, A. Tozluyurt, M. Ozsoz, Clin Biochem 2021, 89, 1-13; b) B. D. Kevadiya, J. Machhi, J. Herskovitz, M. D. Oleynikov, W. R. Blomberg, N. Bajwa, D. Soni, S. Das, M. Hasan, M. Patel, A. M. Senan, S. Gorantla, J. McMillan, B. Edagwa, R. Eisenberg, C. B. Gurumurthy, S. P. M. Reid, C. Punyadeera, L. Chang, H. E. Gendelman, Nat Mater 2021, 20, 593-605.
- [8] T. Notomi, H. Okayama, H. Masubuchi, T. Yonekawa, K. Watanabe, N. Amino, T. Hase, *Nucleic Acids Res* 2000, 28, e63.
- [9] O. Piepenburg, C. H. Williams, D. L. Stemple, N. A. Armes, PLoS Biol 2006, 4, e204.
- [10] a) A. Abi, Z. Mohammadpour, X. Zuo, A. Safavi, Biosens Bioelectron 2018, 102, 479-489; b) A. Asghari, C. Wang, K. M. Yoo, A. Rostamian, X. Xu, J. D. Shin, H. Dalir, R. T. Chen, Appl Phys Rev 2021, 8, 031313.
- [11] a) R. Barrangou, C. Fremaux, H. Deveau, M. Richards, P. Boyaval, S. Moineau, D. A. Romero, P. Horvath, *Science* 2007, 315, 1709-1712; b) E. Deltcheva, K. Chylinski, C. M. Sharma, K. Gonzales, Y. Chao, Z. A. Pirzada, M. R. Eckert, J. Vogel, E. Charpentier, *Nature* 2011, 471, 602-607; c) M. Jinek, K. Chylinski, I. Fonfara, M. Hauer, J. A. Doudna, E. Charpentier, *Science* 2012, 337, 816-821.
- Doudna, E. Charpentier, *Science* **2012**, *337*, 816-821.

  a) L. Cong, F. A. Ran, D. Cox, S. Lin, R. Barretto, N. Habib, P. D. Hsu, X. Wu, W. Jiang, L. A. Marraffini, F. Zhang, *Science* **2013**, *339*, 819-823; b) F. A. Ran, L. Cong, W. X. Yan, D. A. Scott, J. S. Gootenberg, A. J. Kriz, B. Zetsche, O. Shalem, X. Wu, K. S. Makarova, E. V. Koonin, P. A. Sharp, F. Zhang, *Nature* **2015**, *520*, 186-191; c) O. O. Abudayyeh, J. S. Gootenberg, P. Essletzbichler, S. Han, J. Joung, J. J. Belanto, V. Verdine, D. B. T. Cox, M. J. Kellner, A. Regev, E. S. Lander, D. F. Voytas, A. Y. Ting, F. Zhang, *Nature* **2017**, *550*, 280-284; d) J. Strecker, A. Ladha, Z. Gardner, J. L. Schmid-Burgk, K. S. Makarova, E. V. Koonin, F. Zhang, *Science* **2019**, *365*, 48-53.
- [13] a) Y. Wu, D. Liang, Y. Wang, M. Bai, W. Tang, S. Bao, Z. Yan, D. Li, J. Li, Cell Stem Cell 2013, 13, 659-662; b) H. Yin, W. Xue, S. Chen, R. L. Bogorad, E. Benedetti, M. Grompe, V. Koteliansky, P. A. Sharp, T. Jacks, D. G. Anderson, *Nat Biotechnol* **2014**, *32*, 551-553; c) C. Long, J. R. McAnally, J. M. Shelton, A. A. Mireault, R. Bassel-Duby, E. N. Olson, *Science* **2014**, *345*, 1184-1188; d) C. E. Nelson, C. H. Hakim, D. G. Ousterout, P. I. Thakore, E. A. Moreb, R. M. Castellanos Rivera, S. Madhavan, X. Pan, F. A. Ran, W. X. Yan, A. Asokan, F. Zhang, D. Duan, C. A. Gersbach, Science 2016, 351, 403-407; e) H. Ma, N. Marti-Gutierrez, S. W. Park, J. Wu, Y. Lee, K. Suzuki, A. Koski, D. Ji, T. Hayama, R. Ahmed, H. Darby, C. Van Dyken, Y. Li, E. Kang, A. R. Park, D. Kim, S. T. Kim, J. Gong, Y. Gu, X. Xu, D. Battaglia, S. A. Krieg, D. M. Lee, D. H. Wu, D. P. Wolf, S. B. Heitner, J. C. I. Belmonte, P. Amato, J. S. Kim, S. Kaul, S. Mitalipov, Nature 2017, 548, 413-419; f) E. A. Stadtmauer, J. A. Fraietta, M. M. Davis, A. D. Cohen, K. L. Weber, E. Lancaster, P. A. Mangan, I. Kulikovskaya, M. Gupta, F. Chen, L. Tian, V. E. Gonzalez, J. Xu, I. Y. Jung, J. J. Melenhorst, G. Plesa, J. Shea, T. Matlawski, A. Cervini, A. L. Gaymon, S. Desjardins, A. Lamontagne, J. Salas-Mckee, A. Fesnak, D. L. Siegel, B. L. Levine, J. K. Jadlowsky, R. M. Young, A. Chew, W. T. Hwang, E. O. Hexner, B. M. Carreno, C. L. Nobles, F. D.

- Bushman, K. R. Parker, Y. Qi, A. T. Satpathy, H. Y. Chang, Y. Zhao, S. F. Lacey, C. H. June, *Science* **2020**, *367*, eaba7365; g) H. Frangoul, D. Altshuler, M. D. Cappellini, Y. S. Chen, J. Domm, B. K. Eustace, J. Foell, J. de la Fuente, S. Grupp, R. Handgretinger, T. W. Ho, A. Kattamis, A. Kernytsky, J. Lekstrom-Himes, A. M. Li, F. Locatelli, M. Y. Mapara, M. de Montalembert, D. Rondelli, A. Sharma, S. Sheth, S. Soni, M. H. Steinberg, D. Wall, A. Yen, S. Corbacioglu, *N Engl J Med* **2021**, *384*, 252-260; h) J. D. Gillmore, E. Gane, J. Taubel, J. Kao, M. Fontana, M. L. Maitland, J. Seitzer, D. O'Connell, K. R. Walsh, K. Wood, J. Phillips, Y. Xu, A. Amaral, A. P. Boyd, J. E. Cehelsky, M. D. McKee, A. Schiermeier, O. Harari, A. Murphy, C. A. Kyratsous, B. Zambrowicz, R. Soltys, D. E. Gutstein, J. Leonard, L. Sepp-Lorenzino, D. Lebwohl, *N Engl J Med* **2021**, *385*, 493-502.
- [14] a) O. O. Abudayyeh, J. S. Gootenberg, S. Konermann, J. Joung, I. M. Slaymaker, D. B. Cox, S. Shmakov, K. S. Makarova, E. Semenova, L. Minakhin, K. Severinov, A. Regev, E. S. Lander, E. V. Koonin, F. Zhang, *Science* 2016, 353, aaf5573; b) B. Zetsche, J. S. Gootenberg, O. O. Abudayyeh, I. M. Slaymaker, K. S. Makarova, P. Essletzbichler, S. E. Volz, J. Joung, J. van der Oost, A. Regev, E. V. Koonin, F. Zhang, *Cell* 2015, 163, 759-771.
  [15] a) J. S. Gootenberg, O. O. Abudayyeh, M. J. Kellner, J. Joung, J. J. Collins, F. Zhang, *Science* 2018, 360, 439-444; b) J. S. Chen, E. Ma, L. B. Harrington, M. Da Costa, X. Tian, J. M. Palefsky, J. A. Doudna, *Science* 2018, 360,
- 436-439.

  a) Y. Wu, S. X. Liu, F. Wang, M. S. Zeng, *Clin Chem* **2019**, *65*, 591-592; b) H. Li, J. Yang, G. Wu, Z. Weng, Y. Song, Y. Zhang, J. A. Vanegas, L. Avery, Z. Gao, H. Sun, Y. Chen, K. D. Dieckhaus, X. Gao, Y. Zhang, *Angew Chem Int Ed* **2022**, *61*, e202203826; *Angew Chem* **2022**, *134*, e202203826; c) J. Yang, Y. Song, X. Deng, J. A. Vanegas, Z. You, Y. Zhang, Z. Weng, L. Avery, K. D. Dieckhaus, A. Peddi, Y. Gao, Y. Zhang, X. Gao, *Nat*
- Chem Biol 2023, 19, 45-54.
  J. E. van Dongen, J. T. W. Berendsen, R. D. M. Steenbergen, R. M. F. Wolthuis, J. C. T. Eijkel, L. I. Segerink, Biosens Bioelectron 2020, 166, 112445.
  P. Fozouni, S. Son, M. Diaz de Leon Derby, G. J. Knott, C. N. Gray, M. V. D'Ambrosio, C. Zhao, N. A. Switz, G. R. Kumar, S. I. Stephens, D. Boehm, C. L. Tsou, J. Shu, A. Bhuiya, M. Armstrong, A. R. Harris, P. Y. Chen, J. M. Osterloh, A. Meyer-Franke, B. Joehnk, K. Walcott, A. Sil, C. Langelier, K. S. Pollard, E. D. Crawford, A. S. Puschnik, M. Phelps, A. Kistler, J. L. DeRisi, J. A. Doudna, D. A. Fletcher, M. Ott, Cell 2021, 184, 323-333.
- [19] B. Ning, T. Yu, S. Zhang, Z. Huang, D. Tian, Z. Lin, A. Niu, N. Golden, K. Hensley, B. Threeton, C. J. Lyon, X. M. Yin, C. J. Roy, N. S. Saba, J. Rappaport, Q. Wei, T. Y. Hu, Sci Adv 2021, 7, eabe3703.
- [20] J. S. Gootenberg, O. O. Abudayyeh, J. W. Lee, P. Essletzbichler, A. J. Dy, J. Joung, V. Verdine, N. Donghia, N. M. Daringer, C. A. Freije, C. Myhrvold, R. P. Bhattacharyya, J. Livny, A. Regev, E. V. Koonin, D. T. Hung, P. C. Sabeti, J. J. Collins, F. Zhang, Science 2017, 356, 438-442.
- [21] J. Y. Wang, P. Pausch, J. A. Doudna, *Nat Rev Microbiol* 2022, 20, 641-656.
- [22] a) F. Jiang, J. A. Doudna, Annu Rev Biophys 2017, 46, 505-529; b) F. Zhang, Quarterly Reviews of Biophysics 2019, 52, e6; c) M. Adli, Nat Commun 2018, 9, 1911; d) P. D. Hsu, E. S. Lander, F. Zhang, Cell 2014, 157, 1262-1278.
- [23] J. E. Garneau, M. E. Dupuis, M. Villion, D. A. Romero, R. Barrangou, P. Boyaval, C. Fremaux, P. Horvath, A. H. Magadan, S. Moineau, *Nature* **2010**, *468*, 67-71.
- [24] Y. Zhang, L. Qian, W. Wei, Y. Wang, B. Wang, P. Lin, W. Liu, L. Xu, X. Li, D. Liu, S. Cheng, J. Li, Y. Ye, H. Li, X. Zhang, Y. Dong, X. Zhao, C. Liu, H. M. Zhang, Q. Ouyang, C. Lou, ACS Synth Biol 2017, 6, 211-216.

|      | VIEW                                                                                                                                                                                                                                              |      |                                                                                                                                                                                                                                                |
|------|---------------------------------------------------------------------------------------------------------------------------------------------------------------------------------------------------------------------------------------------------|------|------------------------------------------------------------------------------------------------------------------------------------------------------------------------------------------------------------------------------------------------|
| [25] | X. Y. Qiu, L. Y. Zhu, C. S. Zhu, J. X. Ma, T. Hou, X. M. Wu, S. S. Xie, L. Min, D. A. Tan, D. Y. Zhang, L. Zhu, <i>ACS Synth Biol</i> <b>2018</b> , <i>7</i> , 807-813.                                                                           | [40] | <ul> <li>a) D. C. Swarts, M. Jinek, Mol Cell 2019, 73, 589-600</li> <li>e584; b) D. C. Swarts, J. van der Oost, M. Jinek, Mol Cell 2017, 66, 221-233 e224.</li> </ul>                                                                          |
| [26] | W. Zhou, L. Hu, L. Ying, Z. Zhao, P. K. Chu, X. F. Yu, <i>Nat Commun</i> <b>2018</b> , 9, 5012.                                                                                                                                                   | [41] | H. Yang, P. Gao, K. R. Rajashankar, D. J. Patel, <i>Cell</i> <b>2016</b> , <i>167</i> , 1814-1828.                                                                                                                                             |
| [27] | a) X. Sun, Y. Wang, L. Zhang, S. Liu, M. Zhang, J. Wang, B. Ning, Y. Peng, J. He, Y. Hu, Z. Gao, <i>Anal Chem</i> <b>2020</b> ,                                                                                                                   | [42] | F. Teng, T. Cui, G. Feng, L. Guo, K. Xu, Q. Gao, T. Li, J. Li, Q. Zhou, W. Li, <i>Cell Discov</i> <b>2018</b> , <i>4</i> , 63.                                                                                                                 |
|      | 92, 3032-3041; b) J. N. Rauch, E. Valois, S. C. Solley, F. Braig, R. S. Lach, M. Audouard, J. C. Ponce-Rojas, M. S.                                                                                                                               | [43] | F. Teng, L. Guo, T. Cui, X. G. Wang, K. Xu, Q. Gao, Q. Zhou, W. Li, <i>Genome Biol</i> <b>2019</b> , <i>20</i> , 132.                                                                                                                          |
|      | Costello, N. J. Baxter, K. S. Kosik, C. Arias, D. Acosta-Alvear, M. Z. Wilson, <i>J Clin Microbiol</i> <b>2021</b> , <i>59</i> , e02402-20.                                                                                                       | [44] | W. X. Yan, P. Hunnewell, L. E. Alfonse, J. M. Carte, E. Keston-Smith, S. Sothiselvam, A. J. Garrity, S. Chong, K. S. Makarova, E. V. Koonin, D. R. Cheng, D. A. Scott,                                                                         |
| 28]  | F. A. Ran, P. D. Hsu, C. Y. Lin, J. S. Gootenberg, S. Konermann, A. E. Trevino, D. A. Scott, A. Inoue, S. Matoba, Y. Zhang, F. Zhang, <i>Cell</i> <b>2013</b> , <i>154</i> , 1380-1389.                                                           | [45] | Science <b>2019</b> , 363, 88-91.<br>Z. Wang, C. Zhong, <i>Int J Biol Macromol</i> <b>2021</b> , 193, 441-449.                                                                                                                                 |
| 29]  | L. S. Qi, M. H. Larson, L. A. Gilbert, J. A. Doudna, J. S. Weissman, A. P. Arkin, W. A. Lim, <i>Cell</i> <b>2013</b> , <i>152</i> , 1173-                                                                                                         | [46] | B. Zhang, J. Lin, V. Perculija, Y. Li, Q. Lu, J. Chen, S. Ouyang, <i>Nucleic Acids Res</i> <b>2022</b> , <i>50</i> , 11820-11833.                                                                                                              |
|      | 1183.                                                                                                                                                                                                                                             | [47] | J. J. Liu, N. Orlova, B. L. Oakes, E. Ma, H. B. Spinner, K.                                                                                                                                                                                    |
| 30]  | a) A. C. Komor, Y. B. Kim, M. S. Packer, J. A. Zuris, D. R. Liu, <i>Nature</i> 2016, 533, 420-424; b) K. Nishida, T. Arazoe, N. Yachie, S. Banno, M. Kakimoto, M. Tabata, M. Mochizuki, A. Miyabe, M. Araki, K. Y. Hara, Z. Shimatani,            |      | L. M. Baney, J. Chuck, D. Tan, G. J. Knott, L. B. Harrington, B. Al-Shayeb, A. Wagner, J. Brotzmann, B. T. Staahl, K. L. Taylor, J. Desmarais, E. Nogales, J. A. Doudna, <i>Nature</i> <b>2019</b> , <i>566</i> , 218-223.                     |
|      | A. Kondo, <i>Science</i> <b>2016</b> , <i>353</i> , aaf8729; c) N. M. Gaudelli, A. C. Komor, H. A. Rees, M. S. Packer, A. H. Badran, D. I. Bryson, D. R. Liu, <i>Nature</i> <b>2017</b> , <i>551</i> , 464-471.                                   | [48] | L. B. Harrington, D. Burstein, J. S. Chen, D. Paez-Espino, E. Ma, I. P. Witte, J. C. Cofsky, N. C. Kyrpides, J. F. Banfield, J. A. Doudna, <i>Science</i> <b>2018</b> , <i>362</i> , 839-842.                                                  |
| 31]  | a) A. V. Anzalone, P. B. Randolph, J. R. Davis, A. A. Sousa, L. W. Koblan, J. M. Levy, P. J. Chen, C. Wilson, G.                                                                                                                                  | [49] | S. N. Takeda, R. Nakagawa, S. Okazaki, H. Hirano, K.<br>Kobayashi, T. Kusakizako, T. Nishizawa, K. Yamashita, H                                                                                                                                |
|      | A. Newby, A. Raguram, D. R. Liu, <i>Nature</i> <b>2019</b> , <i>576</i> , 149-157; b) Q. Lin, Y. Zong, C. Xue, S. Wang, S. Jin, Z. Zhu,                                                                                                           | [50] | Nishimasu, O. Nureki, <i>Mol Cell</i> <b>2021</b> , <i>81</i> , 558-570.<br>Y. Sha, R. Huang, M. Huang, H. Yue, Y. Shan, J. Hu, D.                                                                                                             |
| 201  | Y. Wang, A. V. Anzalone, A. Raguram, J. L. Doman, D. R. Liu, C. Gao, <i>Nat Biotechnol</i> <b>2020</b> , <i>38</i> , 582-585.                                                                                                                     | [51] | Xing, Chem Commun (Camb) <b>2021</b> , 57, 247-250.<br>Z. Li, H. Zhang, R. Xiao, R. Han, L. Chang, <i>Nat Chem Bio</i>                                                                                                                         |
| 32]  | A. Chavez, J. Scheiman, S. Vora, B. W. Pruitt, M. Tuttle, P. R. I. E, S. Lin, S. Kiani, C. D. Guzman, D. J. Wiegand, D. T. Changan, D. J. Braff, M. Davidscha, B. F.                                                                              | [52] | <b>2021</b> , <i>17</i> , 387-393. B. Zhang, D. Luo, Y. Li, V. Perculija, J. Chen, J. Lin, Y. Ye                                                                                                                                               |
|      | D. Ter-Ovanesyan, J. L. Braff, N. Davidsohn, B. E. Housden, N. Perrimon, R. Weiss, J. Aach, J. J. Collins, G. M. Church, Net Mathada 2015, 13, 236, 238                                                                                           | [53] | S. Ouyang, <i>Nat Commun</i> <b>2021</b> , <i>12</i> , 3476.  X. Huang, W. Sun, Z. Cheng, M. Chen, X. Li, J. Wang, G.                                                                                                                          |
| 33]  | <ul> <li>M. Church, <i>Nat Methods</i> <b>2015</b>, <i>12</i>, 326-328.</li> <li>a) W. Chang, W. Liu, Y. Liu, F. Zhan, H. Chen, H. Lei, Y. Liu, <i>Microchim Acta</i> <b>2019</b>, <i>186</i>, 243; b) R. Wang, X. Zhao,</li> </ul>               | [54] | <ul> <li>Sheng, W. Gong, Y. Wang, Nat Commun 2020, 11, 5241.</li> <li>P. Pausch, B. Al-Shayeb, E. Bisom-Rapp, C. A. Tsuchida,</li> <li>Z. Li, B. F. Cress, G. J. Knott, S. E. Jacobsen, J. F.</li> </ul>                                       |
|      | X. Chen, X. Qiu, G. Qing, H. Zhang, L. Zhang, X. Hu, Z.<br>He, D. Zhong, Y. Wang, Y. Luo, <i>Anal Chem</i> <b>2020</b> , <i>92</i> ,                                                                                                              | [55] | Banfield, J. A. Doudna, <i>Science</i> <b>2020</b> , <i>369</i> , 333-337.<br>A. Carabias, A. Fuglsang, P. Temperini, T. Pape, N.                                                                                                              |
| 34]  | 2176-2185. a) R. Hajian, S. Balderston, T. Tran, T. deBoer, J. Etienne,                                                                                                                                                                           | 150) | Sofos, S. Stella, S. Erlendsson, G. Montoya, <i>Nat Commun</i> <b>2021</b> , <i>12</i> , 4476.                                                                                                                                                 |
|      | M. Sandhu, N. A. Wauford, J. Y. Chung, J. Nokes, M. Athaiya, J. Paredes, R. Peytavi, B. Goldsmith, N. Murthy, I. M. Conboy, K. Aran, <i>Nat Biomed Eng</i> <b>2019</b> , <i>3</i> , 427-437;                                                      | [56] | A. East-Seletsky, M. R. O'Connell, S. C. Knight, D. Burstein, J. H. Cate, R. Tjian, J. A. Doudna, <i>Nature</i> <b>2016</b> , 538, 270-273.                                                                                                    |
|      | b) S. Balderston, J. J. Taulbee, E. Celaya, K. Fung, A.<br>Jiao, K. Smith, R. Hajian, G. Gasiunas, S. Kutanovas, D.                                                                                                                               | [57] | a) L. Liu, X. Li, J. Ma, Z. Li, L. You, J. Wang, M. Wang, X. Zhang, Y. Wang, <i>Cell</i> <b>2017</b> , <i>170</i> , 714-726; b) A. Tambe,                                                                                                      |
|      | Kim, J. Parkinson, K. Dickerson, J. J. Ripoll, R. Peytavi, H. W. Lu, F. Barron, B. R. Goldsmith, P. G. Collins, I. M. Conboy, V. Siksnys, K. Aran, <i>Nat Biomed Eng</i> <b>2021</b> , <i>5</i> ,                                                 | [58] | A. East-Seletsky, G. J. Knott, J. A. Doudna, M. R. O'Connell, <i>Cell Rep</i> <b>2018</b> , <i>24</i> , 1025-1036. a) Y. Shan, X. Zhou, R. Huang, D. Xing, <i>Anal Chem</i> <b>2019</b>                                                        |
| 35]  | 713-725. a) X. W. Wang, L. F. Hu, J. Hao, L. Q. Liao, Y. T. Chiu, M.                                                                                                                                                                              |      | 91, 5278-5285; b) T. Tian, B. Shu, Y. Jiang, M. Ye, L. Liu, Z. Guo, Z. Han, Z. Wang, X. Zhou, <i>ACS Nano</i> <b>2021</b> , <i>15</i> ,                                                                                                        |
|      | Shi, Y. Wang, <i>Nat Cell Biol</i> <b>2019</b> , <i>21</i> , 522-530; b) M.<br>Hirozawa, Y. Fujita, H. Saito, <i>ACS Synth Biol</i> <b>2019</b> , <i>8</i> ,                                                                                      | [59] | 1167-1178.<br>L. Liu, X. Li, J. Wang, M. Wang, P. Chen, M. Yin, J. Li, G.                                                                                                                                                                      |
| 36]  | 1575-1582. a) P. Horvath, R. Barrangou, <i>Science</i> <b>2010</b> , 327, 167-170; b) B. Wiedenheft, S. H. Sternberg, J. A. Doudna, <i>Nature</i>                                                                                                 | [60] | Sheng, Y. Wang, <i>Cell</i> <b>2017</b> , <i>168</i> , 121-134.<br>G. J. Knott, A. East-Seletsky, J. C. Cofsky, J. M. Holton, E Charles, M. R. O'Connell, J. A. Doudna, <i>Nat Struct Mol</i>                                                  |
|      | <b>2012</b> , <i>482</i> , 331-338; c) G. Gasiunas, R. Barrangou, P. Horvath, V. Siksnys, <i>Proc Natl Acad Sci USA</i> <b>2012</b> , <i>109</i> , E2579-E2586; d) S. H. Sternberg, S. Redding, M. Jinek,                                         | [61] | Biol <b>2017</b> , <i>24</i> , 825-833.  I. M. Slaymaker, P. Mesa, M. J. Kellner, S. Kannan, E. Brignole, J. Koob, P. R. Feliciano, S. Stella, O. O.                                                                                           |
| 37]  | E. C. Greene, J. A. Doudna, <i>Nature</i> <b>2014</b> , <i>50</i> 7, 62-67.<br>a) J. P. K. Bravo, M. S. Liu, G. N. Hibshman, T. L.                                                                                                                |      | Abudayyeh, J. S. Gootenberg, J. Strecker, G. Montoya, F Zhang, <i>Cell Rep</i> <b>2019</b> , <i>26</i> , 3741-3751.                                                                                                                            |
|      | Dangerfield, K. Jung, R. S. McCool, K. A. Johnson, D. W. Taylor, <i>Nature</i> <b>2022</b> , <i>603</i> , 343-347; b) M. Pacesa, L. Loeff, I. Querques, L. M. Muckenfuss, M. Sawicka, M. Jinek, <i>Nature</i> <b>2022</b> , <i>609</i> , 191-196. | [62] | A. A. Smargon, D. B. T. Cox, N. K. Pyzocha, K. Zheng, I.<br>M. Slaymaker, J. S. Gootenberg, O. A. Abudayyeh, P.<br>Essletzbichler, S. Shmakov, K. S. Makarova, E. V. Koonir<br>F. Zhang, Mol Cell 2017, 65, 618-630.                           |
| 38]  | T. Yamano, B. Zetsche, R. Ishitani, F. Zhang, H. Nishimasu, O. Nureki, <i>Mol Cell</i> <b>2017</b> , <i>67</i> , 633-645 e633.                                                                                                                    | [63] | S. Konermann, P. Loffy, N. J. Brideau, J. Oki, M. N. Shokhirev, P. D. Hsu, <i>Cell</i> <b>2018</b> , <i>173</i> , 665-676 e614.                                                                                                                |
| 39]  | a) T. Yamano, H. Nishimasu, B. Zetsche, H. Hirano, I. M. Slaymaker, Y. Li, I. Fedorova, T. Nakane, K. S. Makarova, E. V. Koonin, R. Ishitani, F. Zhang, O. Nureki, <i>Cell</i> <b>2016</b> ,                                                      | [64] | C. Zhang, S. Konermann, N. J. Brideau, P. Lotfy, X. Wu, S. J. Novick, T. Strutzenberg, P. R. Griffin, P. D. Hsu, D. Lyumkis, <i>Cell</i> <b>2018</b> , <i>175</i> , 212-223.                                                                   |
|      | 165, 949-962; b) H. Nishimasu, T. Yamano, L. Gao, F. Zhang, R. Ishitani, O. Nureki, <i>Mol Cell</i> <b>2017</b> , 67, 139-147 e132.                                                                                                               | [65] | S. Li, X. Li, W. Xue, L. Zhang, L. Z. Yang, S. M. Cao, Y. N<br>Lei, C. X. Liu, S. K. Guo, L. Shan, M. Wu, X. Tao, J. L.<br>Zhang, X. Gao, J. Zhang, J. Wei, J. Li, L. Yang, L. L.<br>Chen, <i>Nat Methods</i> <b>2021</b> , <i>18</i> , 51-59. |

| REV  | IEW                                                                                                                                                                                                                                                                                                                                                                                                                                                               |              |                                                                                               |
|------|-------------------------------------------------------------------------------------------------------------------------------------------------------------------------------------------------------------------------------------------------------------------------------------------------------------------------------------------------------------------------------------------------------------------------------------------------------------------|--------------|-----------------------------------------------------------------------------------------------|
| [66] | M. R. O'Connell, B. L. Oakes, S. H. Sternberg, A. East-<br>Seletsky, M. Kaplan, J. A. Doudna, <i>Nature</i> <b>2014</b> , <i>516</i> ,<br>263-266.                                                                                                                                                                                                                                                                                                                | [86]<br>[87] | A. J. Mees<br>H. Tong, J<br>Yang, D. I                                                        |
| [67] | K. Pardee, A. A. Green, M. K. Takahashi, D. Braff, G.<br>Lambert, J. W. Lee, T. Ferrante, D. Ma, N. Donghia, M.<br>Fan, N. M. Daringer, I. Bosch, D. M. Dudley, D. H.                                                                                                                                                                                                                                                                                             |              | Wei, C. Xi<br>Li, K. Fan<br>10.1038/s                                                         |
|      | O'Connor, L. Gehrke, J. J. Collins, Cell 2016, 165, 1255-<br>1266.                                                                                                                                                                                                                                                                                                                                                                                                | [88]         | A. Ramac<br>7456-746                                                                          |
| [68] | M. Huang, X. Zhou, H. Wang, D. Xing, <i>Anal Chem</i> <b>2018</b> , <i>90</i> , 2193-2200.                                                                                                                                                                                                                                                                                                                                                                        | [89]         | T. Y. Liu,<br>Son, A. Bl                                                                      |
| [69] | S. Shmakov, O. O. Abudayyeh, K. S. Makarova, Y. I. Wolf, J. S. Gootenberg, E. Semenova, L. Minakhin, J. Joung, S. Konermann, K. Severinov, F. Zhang, E. V. Koonin, <i>Mol Cell</i> <b>2015</b> , <i>60</i> , 385-397.                                                                                                                                                                                                                                             |              | Diaz de Le<br>Harris, E.<br>S. I. Steph<br>lavarone,                                          |
| [70] | Y. Zhao, F. Chen, Q. Li, L. Wang, C. Fan, <i>Chemical Reviews</i> <b>2015</b> , <i>115</i> , 12491-12545.                                                                                                                                                                                                                                                                                                                                                         |              | Dugan, I.<br>Ott, D. A.                                                                       |
| [71] | a) E. A. Nalefski, N. Patel, P. J. Y. Leung, Z. Islam, R. M. Kooistra, I. Parikh, E. Marion, G. J. Knott, J. A. Doudna, A. M. Le Ny, D. Madan, <i>iScience</i> <b>2021</b> , <i>24</i> , 102996; b) H. Lv, J. Wang, J. Zhang, Y. Chen, L. Yin, D. Jin, D. Gu, H. Zhao, Y. Xu, J. Wang, <i>Front Microbiol</i> <b>2021</b> , <i>12</i> , 766464; c) C. W. Smith, M. J. Kachwala, N. Nandu, M. V. Yigit, <i>ACS Synth Biol</i> <b>2021</b> , <i>10</i> , 1785-1791. | [90]         | J. A. Doud<br>a) A. Sant<br>Nemudryi,<br>Snyder, J.<br>A. Jutila, N<br>2, 100319<br>H. Dennis |
| [72] | a) X. Ding, K. Yin, Z. Li, R. V. Lalla, E. Ballesteros, M. M. Sfeir, C. Liu, <i>Nat Commun</i> <b>2020</b> , <i>11</i> , 4711; b) S. Xie, D. Tao, Y. Fu, B. Xu, Y. Tang, L. Steinaa, J. D. Hemmink, W. Pan, X. Huang, X. Nie, C. Zhao, J. Ruan, Y. Zhang, J. Han, L. Fu, Y. Ma, X. Li, X. Liu, S. Zhao, <i>ACS Synth Biol</i>                                                                                                                                     | [91]         | a) P. Sam<br>Hatoum-A<br>1174; b) L<br>Wang, L. I<br>Cell <b>2019</b> ,                       |
| [73] | <b>2022</b> , <i>11</i> , 383-396. O. O. Abudayyeh, J. S. Gootenberg, M. J. Kellner, F. Zhang, <i>CRISPR J</i> <b>2019</b> , <i>2</i> , 165-171.                                                                                                                                                                                                                                                                                                                  | [92]         | E. Macchi<br>Ghittorelli,<br>Palazzo, (                                                       |
| [74] | J. Strecker, S. Jones, B. Koopal, J. Schmid-Burgk, B. Zetsche, L. Gao, K. S. Makarova, E. V. Koonin, F. Zhang, <i>Nat Commun</i> <b>2019</b> , <i>10</i> , 212.                                                                                                                                                                                                                                                                                                   | [93]         | 3223.<br>Y. Liu, L. 2<br>Nano <b>202</b>                                                      |
| [75] | B. P. Kleinstiver, A. A. Sousa, R. T. Walton, Y. E. Tak, J. Y. Hsu, K. Clement, M. M. Welch, J. E. Horng, J. Malagon-                                                                                                                                                                                                                                                                                                                                             | [94]         | a) C. Chei<br>Damborsk                                                                        |
| [76] | Lopez, I. Scarfo, M. V. Maus, L. Pinello, M. J. Aryee, J. K. Joung, <i>Nat Biotechnol</i> <b>2019</b> , 37, 276-282. L. Zhang, J. A. Zuris, R. Viswanathan, J. N. Edelstein, R. Turk, B. Thommandru, H. T. Rube, S. E. Glenn, M. A.                                                                                                                                                                                                                               | [95]         | 91-100.<br>S. Y. Li, Q<br>Gao, R. B<br>20.                                                    |
|      | Collingwood, N. M. Bode, S. F. Beaudoin, S. Lele, S. N.                                                                                                                                                                                                                                                                                                                                                                                                           | [96]         | C. Yuan,                                                                                      |

- Joung, *Nat Biotechnol* **2019**, *37*, 276-282.
  L. Zhang, J. A. Zuris, R. Viswanathan, J. N. Edelstein, R. Turk, B. Thommandru, H. T. Rube, S. E. Glenn, M. A. Collingwood, N. M. Bode, S. F. Beaudoin, S. Lele, S. N. Scott, K. M. Wasko, S. Sexton, C. M. Borges, M. S. Schubert, G. L. Kurgan, M. S. McNeill, C. A. Fernandez, V. E. Myer, R. A. Morgan, M. A. Behlke, C. A. Vakulskas, *Nat Commun* **2021**, *12*, 3908.
- [77] L. Y. Guo, J. Bian, A. E. Davis, P. Liu, H. R. Kempton, X. Zhang, A. Chemparathy, B. Gu, X. Lin, D. A. Rane, X. Xu, R. M. Jamiolkowski, Y. Hu, S. Wang, L. S. Qi, *Nat Cell Biol* **2022**, *24*, 590-600.
- [78] K. H. Ooi, M. M. Liu, J. W. D. Tay, S. Y. Teo, P. Kaewsapsak, S. Jin, C. K. Lee, J. Hou, S. Maurer-Stroh, W. Lin, B. Yan, G. Yan, Y. G. Gao, M. H. Tan, *Nat Commun* **2021**, *12*, 1739.
- [79] E. Ma, K. Chen, H. Shi, E. C. Stahl, B. Adler, M. Trinidad, J. Liu, K. Zhou, J. Ye, J. A. Doudna, *Nucleic Acids Res* 2022, 50, 12689-12701.
- [80] L. T. Nguyen, B. M. Smith, P. K. Jain, *Nat Commun* 2020, 11, 4906.
- [81] M. C. Pillon, K. H. Goslen, J. Gordon, M. L. Wells, J. G. Williams, R. E. Stanley, *J Biol Chem* **2020**, 295, 5857-5870
- [82] W. X. Yan, S. Chong, H. Zhang, K. S. Makarova, E. V. Koonin, D. R. Cheng, D. A. Scott, *Mol Cell* 2018, 70, 327-339.
- [83] M. R. O'Connell, J Mol Biol 2019, 431, 66-87.
- [84] a) P. Shi, M. R. Murphy, A. O. Aparicio, J. S. Kesner, Z. Fang, Z. Chen, A. Trehan, X. Wu, bioRxiv 2021, doi: 10.1101/2021.11.30.470032; b) Y. Ai, D. Liang, J. E. Wilusz, Nucleic Acids Res 2022, 50, e65.
- [85] a) B. Wang, T. Zhang, J. Yin, Y. Yu, W. Xu, J. Ding, D. J. Patel, H. Yang, Mol Cell 2021, 81, 1100-1115; b) A. East-Seletsky, M. R. O'Connell, D. Burstein, G. J. Knott, J. A. Doudna, Mol Cell 2017, 66, 373-383; c) E. J. Charles, S. E. Kim, G. J. Knott, D. Smock, J. Doudna, D. F. Savage, bioRxiv 2021, doi: 10.1101/2021.05.26.445687.

- [86] A. J. Meeske, L. A. Marraffini, Mol Cell 2018, 71, 791-801.
  [87] H. Tong, J. Huang, Q. Xiao, B. He, X. Dong, Y. Liu, X. Yang, D. Han, Z. Wang, X. Wang, W. Ying, R. Zhang, Y. Wei, C. Xu, Y. Zhou, Y. Li, M. Cai, Q. Wang, M. Xue, G. Li, K. Fang, H. Zhang, H. Yang, Nat Biotechnol 2022, doi: 10.1038/s41587-022-01419-7.
- [88] A. Ramachandran, J. G. Santiago, Anal Chem 2021, 93, 7456-7464.
- [89] T. Y. Liu, G. J. Knott, D. C. J. Smock, J. J. Desmarais, S. Son, A. Bhuiya, S. Jakhanwal, N. Prywes, S. Agrawal, M. Diaz de Leon Derby, N. A. Switz, M. Armstrong, A. R. Harris, E. J. Charles, B. W. Thornton, P. Fozouni, J. Shu, S. I. Stephens, G. R. Kumar, C. Zhao, A. Mok, A. T. lavarone, A. M. Escajeda, R. McIntosh, S. Kim, E. J. Dugan, I. G. I. T. Consortium, K. S. Pollard, M. X. Tan, M. Ott, D. A. Fletcher, L. F. Lareau, P. D. Hsu, D. F. Savage, J. A. Doudna, Nat Chem Biol 2021, 17, 982-988.
- [90] a) A. Santiago-Frangos, L. N. Hall, A. Nemudraia, A. Nemudryi, P. Krishna, T. Wiegand, R. A. Wilkinson, D. T. Snyder, J. F. Hedges, C. Cicha, H. H. Lee, A. Graham, M. A. Jutila, M. P. Taylor, B. Wiedenheft, Cell Rep Med 2021, 2, 100319; b) S. Sridhara, H. N. Goswami, C. Whyms, J. H. Dennis, H. Li, Nat Commun 2021, 12, 5653.
- [91] a) P. Samai, N. Pyenson, W. Jiang, G. W. Goldberg, A. Hatoum-Aslan, L. A. Marraffini, Cell 2015, 161, 1164-1174; b) L. You, J. Ma, J. Wang, D. Artamonova, M. Wang, L. Liu, H. Xiang, K. Severinov, X. Zhang, Y. Wang, Cell 2019, 176, 239-253.
- [92] E. Macchia, K. Manoli, B. Holzer, C. Di Franco, M. Ghittorelli, F. Torricelli, D. Alberga, G. F. Mangiatordi, G. Palazzo, G. Scamarcio, L. Torsi, *Nat Commun* 2018, 9, 3223.
- [93] Y. Liu, L. Zhan, Z. Qin, J. Sackrison, J. C. Bischof, ACS Nano 2021, 15, 3593-3611.
- [94] a) C. Chen, J. Wang, Analyst 2020, 145, 1605-1628; b) P. Damborsky, J. Svitel, J. Katrlik, Essays Biochem 2016, 60, 91-100.
- [95] S. Y. Li, Q. X. Cheng, J. M. Wang, X. Y. Li, Z. L. Zhang, S. Gao, R. B. Cao, G. P. Zhao, J. Wang, Cell Discov 2018, 4, 20
- [96] C. Yuan, T. Tian, J. Sun, M. Hu, X. Wang, E. Xiong, M. Cheng, Y. Bao, W. Lin, J. Jiang, C. Yang, Q. Chen, H. Zhang, H. Wang, X. Wang, X. Deng, X. Liao, Y. Liu, Z. Wang, G. Zhang, X. Zhou, Anal Chem 2020, 92, 4029-4037
- [97] a) H. Kim, S. Lee, H. W. Seo, B. Kang, J. Moon, K. G. Lee, D. Yong, H. Kang, J. Jung, E. K. Lim, J. Jeong, H. G. Park, C. M. Ryu, T. Kang, ACS Nano 2020, 14, 17241-17253; b) J. H. Choi, M. Shin, L. Yang, B. Conley, J. Yoon, S. N. Lee, K. B. Lee, J. W. Choi, ACS Nano 2021, 15, 13475-13485.
- [98] a) T. Zhou, R. Huang, M. Huang, J. Shen, Y. Shan, D. Xing, Adv Sci 2020, 7, 1903661; b) B. Koo, D. E. Kim, J. Kweon, C. E. Jin, S. H. Kim, Y. Kim, Y. Shin, Sens Actuators B Chem 2018, 273, 316-321.
- [99] S. M. Borisov, O. S. Wolfbeis, Chem Rev 2008, 108, 423-461.
- [100] W. Nawrot, K. Drzozga, S. Baluta, J. Cabaj, K. Malecha, Sensors 2018, 18, 2357.
- [101] M. Staiano, P. Bazzicalupo, M. Rossi, S. D'Auria, *Mol Biosyst* 2005, 1, 354-362.
- [102] B. Chen, L. A. Gilbert, B. A. Cimini, J. Schnitzbauer, W. Zhang, G. W. Li, J. Park, E. H. Blackburn, J. S. Weissman, L. S. Qi, B. Huang, Cell 2013, 155, 1479-1491.
- [103] K. Guk, J. O. Keem, S. G. Hwang, H. Kim, T. Kang, E. K. Lim, J. Jung, *Biosens Bioelectron* **2017**, *95*, 67-71.
- [104] P. Yourik, R. T. Fuchs, M. Mabuchi, J. L. Curcuru, G. B. Robb, RNA 2019, 25, 35-44.
- [105] T. Wang, Y. Liu, H. H. Sun, B. C. Yin, B. C. Ye, Angew Chem Int Ed 2019, 58, 5382-5386; Angew Chem 2019, 131, 5436-5440.
- [106] H. Lee, J. Choi, E. Jeong, S. Baek, H. C. Kim, J. H. Chae, Y. Koh, S. W. Seo, J. S. Kim, S. J. Kim, Nano Lett 2018, 18, 7642-7650.

### REVIEW

- [107] C. Myhrvold, C. A. Freije, J. S. Gootenberg, O. O. Abudayyeh, H. C. Metsky, A. F. Durbin, M. J. Kellner, A. L. Tan, L. M. Paul, L. A. Parham, K. F. Garcia, K. G. Barnes, B. Chak, A. Mondini, M. L. Nogueira, S. Isern, S. F. Michael, I. Lorenzana, N. L. Yozwiak, B. L. MacInnis, I Bosch, L. Gehrke, F. Zhang, P. C. Sabeti, Science 2018, 360, 444-448.
- J. P. Broughton, X. Deng, G. Yu, C. L. Fasching, V. Servellita, J. Singh, X. Miao, J. A. Streithorst, A. [108] Granados, A. Sotomayor-Gonzalez, K. Zorn, A. Gopez, E. Hsu, W. Gu, S. Miller, C. Y. Pan, H. Guevara, D. A Wadford, J. S. Chen, C. Y. Chiu, Nat Biotechnol 2020, 38, 870-874.
- Y. Li, S. Li, J. Wang, G. Liu, Trends Biotechnol 2019, 37, [109]
- [110] M. J. Kellner, J. G. Koob, J. S. Gootenberg, O. O. Abudayyeh, F. Zhang, Nat Protoc 2019, 14, 2986-3012.
- [111] L. Li, S. Li, N. Wu, J. Wu, G. Wang, G. Zhao, J. Wang, ACS Synth Biol 2019, 8, 2228-2237.
- [112] a) A. Mahas, T. Marsic, M. Lopez-Portillo Masson, Q. Wang, R. Aman, C. Zheng, Z. Ali, M. Alsanea, A. Al-Qahtani, B. Ghanem, F. Alhamlan, M. Mahfouz, Proc Natl Acad Sci USA 2022, 119, e2118260119; b) R. A. Lee, H. Puig, P. Q. Nguyen, N. M. Angenent-Mari, N. M. Donghia, J. P. McGee, J. D. Dvorin, C. M. Klapperich, N. R. Pollock, J. J. Collins, Proc Natl Acad Sci USA 2020, 117, 25722-25731; c) J. Joung, A. Ladha, M. Saito, N. G. Kim, A. E. Woolley, M. Segel, R. P. J. Barretto, A. Ranu, R. K. Macrae, G. Faure, E. I. Ioannidi, R. N. Krajeski, R. Bruneau, M. W. Huang, X. G. Yu, J. Z. Li, B. D. Walker, D. T. Hung, A. L. Greninger, K. R. Jerome, J. S. Gootenberg, O. O. Abudayyeh, F. Zhang, N Engl J Med 2020, 383, 1492-1494; d) S. Li, J. Huang, L. Ren, W. Jiang, M. Wang, L. Zhuang, Q. Zheng, R. Yang, Y. Zeng, L. D. W. Luu, Y. Wang, J. Tai, Talanta 2021, 233, 122591.
- [113] F. Hu, Y. Liu, S. Zhao, Z. Zhang, X. Li, N. Peng, Z. Jiang,
- Biosens Bioelectron **2022**, 202, 113994. Z. Ali, R. Aman, A. Mahas, G. S. Rao, M. Tehseen, T. [114] Marsic, R. Salunke, A. K. Subudhi, S. M. Hala, S. M. Hamdan, A. Pain, F. S. Alofi, A. Alsomali, A. M. Hashem, A. Khogeer, N. A. M. Almontashiri, M. Abedalthagafi, N. Hassan, M. M. Mahfouz, Virus Res 2020, 288, 198129.
- [115] a) Y. Wang, Y. Ke, W. Liu, Y. Sun, X. Ding, ACS Sens 2020, 5, 1427-1435; b) Y. Chen, Y. Shi, Y. Chen, Z. Yang, H. Wu, Z. Zhou, J. Li, J. Ping, L. He, H. Shen, Z. Chen, J. Wu, Y. Yu, Y. Zhang, H. Chen, Biosens Bioelectron 2020, 169, 112642.
- [116] K. Yin, X. Ding, Z. Li, H. Zhao, K. Cooper, C. Liu, Anal Chem 2020, 92, 8561-8568.
- [117] C. M. Ackerman, C. Myhrvold, S. G. Thakku, C. A. Freije, H. C. Metsky, D. K. Yang, S. H. Ye, C. K. Boehm, T. F. Kosoko-Thoroddsen, J. Kehe, T. G. Nguyen, A. Carter, A. Kulesa, J. R. Barnes, V. G. Dugan, D. T. Hung, P. C. Blainey, P. C. Sabeti, Nature 2020, 582, 277-282.
- K. Shi, S. Xie, R. Tian, S. Wang, Q. Lu, D. Gao, C. Lei, H. [118] Zhu, Z. Nie, Sci Adv 2021, 7, eabc7802
- J. Zhang, H. Lv, L. Li, M. Chen, D. Gu, J. Wang, Y. Xu, [119] Front Microbiol 2021, 12, 751408.
- P. R. Debski, P. Garstecki, Biomol Detect Quantif 2016, [120] 10, 24-30.
- [121] D. M. Rissin, C. W. Kan, T. G. Campbell, S. C. Howes, D. R. Fournier, L. Song, T. Piech, P. P. Patel, L. Chang, A. J. Rivnak, E. P. Ferrell, J. D. Randall, G. K. Provuncher, D. R. Walt, D. C. Duffy, Nat Biotechnol 2010, 28, 595-599.
- S. H. Kim, S. Iwai, S. Araki, S. Sakakihara, R. Iino, H. Noji, [122] Lab Chip 2012, 12, 4986-4991.
- D. Witters, B. Sun, S. Begolo, J. Rodriguez-Manzano, W. [123] Robles, R. F. Ismagilov, Lab Chip 2014, 14, 3225-3232.
- R. T. Morales, J. Ko, ACS Nano 2022, 16, 11619-11645. [124]
- T. Bar, M. Kubista, A. Tichopad, Nucleic Acids Res 2012, [125] 40, 1395-1406.
- [126] K. R. Sreejith, C. H. Ooi, J. Jin, D. V. Dao, N. T. Nguyen, Lab Chip **2018**, *18*, 3717-3732.
  a) J. S. Park, K. Hsieh, L. Chen, A. Kaushik, A. Y. Trick, T.
- [127] H. Wang, Adv Sci 2021, 8, 2003564; b) X. Wu, J. K. Tay,

- C. K. Goh, C. Chan, Y. H. Lee, S. L. Springs, Y. Wang, K. S. Loh, T. K. Lu, H. Yu, *Biomaterials* **2021**, *274*, 120876; c) F. X. Liu, J. Q. Cui, H. Park, K. W. Chan, T. Leung, B. Z. Tang, S. Yao, Anal Chem 2022, 94, 5883-5892; d) C. Zhang, Z. Cai, Z. Zhou, M. Li, W. Hong, W. Zhou, D. Yu, P. Wei, J. He, Y. Wang, C. Huang, X. Wang, J. Wu, Biosens Bioelectron 2023, 222, 114956; e) X. Ding, K. Yin, Z. Li, M. M. Sfeir, C. Liu, *Biosens Bioelectron* **2021**, *184*, 113218; f) X. Luo, Y. Xue, E. Ju, Y. Tao, M. Li, L. Zhou, C. Yang, J. Zhou, J. Wang, *Anal Chim Acta* **2022**, *1192*, 339336; g) X. Wu, C. Chan, S. L. Springs, Y. H. Lee, T. K. Lu, H. Yu, *Anal Chim Acta* **2022**, *1196*, 339494; h) J. Q. Cui, F. X. Liu, H. Park, K. W. Chan, T. Leung, B. Z. Tang, S. Yao, Biosens Bioelectron 2022, 202, 114019; i) Z. Yu, L. Xu, W. Lyu, F. Shen, Lab Chip 2022, 22, 2954-2961; j) H. Yue, B. Shu, T. Tian, E. Xiong, M. Huang, D. Zhu, J. Sun, Q. Liu, S. Wang, Y. Li, X. Zhou, *Nano Lett* **2021**, *21*, 4643-4653; k) H. Shinoda, Y. Taguchi, R. Nakagawa, A. Makino, S. Okazaki, M. Nakano, Y. Muramoto, C. Takahashi, I. Takahashi, J. Ando, T. Noda, O. Nureki, H. Nishimasu, R. Watanabe, Commun Biol 2021, 4, 476. H. de Puig, R. A. Lee, D. Najjar, X. Tan, L. R. Soeknsen, N. M. Angenent-Mari, N. M. Donghia, N. E. Weckman, A. Ory, C. F. Ng, P. Q. Nguyen, A. S. Mao, T. C. Ferrante, G. Lansberry, H. Sallum, J. Niemi, J. J. Collins, Sci Adv 2021, 7, eabh2944.
- T. Yu, S. Zhang, R. Matei, W. Marx, C. L. Beisel, Q. Wei, [129] AIChE Journal 2021, 67, e17365.

[128]

- [130] N. Mohammad, S. S. Katkam, Q. Wei, CRISPR J 2022, 5, 500-516.
- a) J. Arizti-Sanz, C. A. Freije, A. C. Stanton, B. A. Petros, C. K. Boehm, S. Siddiqui, B. M. Shaw, G. Adams, T. F. [131] Kosoko-Thoroddsen, M. E. Kemball, J. N. Uwanibe, F. V. Ajogbasile, P. E. Eromon, R. Gross, L. Wronka, K. Caviness, L. E. Hensley, N. H. Bergman, B. L. MacInnis, C. T. Happi, J. E. Lemieux, P. C. Sabeti, C. Myhrvold, Nat Commun 2020, 11, 5921; b) F. E. Chen, P. W. Lee, A. Y. Trick, J. S. Park, L. Chen, K. Shah, H. Mostafa, K. C Carroll, K. Hsieh, T. H. Wang, Biosens Bioelectron 2021, 190, 113390; c) T. Tian, Z. Qiu, Y. Jiang, D. Zhu, X. Zhou, Biosens Bioelectron 2022, 196, 113701.
- a) A. Roda, M. Guardigli, P. Pasini, M. Mirasoli, *Anal Bioanal Chem* **2003**, 377, 826-833; b) A. Roda, M. Guardigli, *Anal Bioanal Chem* **2012**, *402*, 69-76. [132]
- A. Piriya V.S, P. Joseph, K. Daniel S.C.G, S. Lakshmanan, T. Kinoshita, S. Muthusamy, *Mater Sci Eng* [133] C 2017, 78, 1231-1245.
- J. Moon, H. J. Kwon, D. Yong, I. C. Lee, H. Kim, H. Kang, E. K. Lim, K. S. Lee, J. Jung, H. G. Park, T. Kang, ACS [134] Sens 2020, 5, 4017-4026.
- L. Yin, N. Duan, S. Chen, Y. Yao, J. Liu, L. Ma, Sens [135] Actuators B Chem 2021, 347, 130586.
- L. Wei, Z. Wang, J. Wang, X. Wang, Y. Chen, Anal Chim [136] Acta 2022, 1230, 340357.
- a) S. Gong, S. Zhang, X. Wang, J. Li, W. Pan, N. Li, B. [137] Tang, Anal Chem 2021, 93, 15216-15223; b) S. Gong, X. Wang, P. Zhou, W. Pan, N. Li, B. Tang, Anal Chem 2022, 94, 15839-15846.
- a) X. Wang, X. Chen, C. Chu, Y. Deng, M. Yang, D. Huo, F. Xu, C. Hou, J. Lv, *Talanta* **2021**, 233, 122554; b) J. [138] Song, B. Cha, J. Moon, H. Jang, S. Kim, J. Jang, D. Yong, H. J. Kwon, I. C. Lee, E. K. Lim, J. Jung, H. G. Park, T. Kang, *ACS Nano* **2022**, *16*, 11300-11314.
- [139] a) T. Zhou, M. Huang, J. Lin, R. Huang, D. Xing, Anal Chem 2021, 93, 2038-2044; b) X. Chen, L. Wang, F. He, G. Chen, L. Bai, K. He, F. Zhang, X. Xu, Anal Chem 2021, 93, 14300-14306; c) H. Zhou, S. Bu, Y. Xu, L. Xue, Z. Li, Z. Hao, J. Wan, F. Tang, *Anal Bioanal Chem* **2022**, *414*, 8437-8445.
- T. J. Sullivan, A. K. Dhar, R. Cruz-Flores, A. G. Bodnar, [140] Sci Rep 2019, 9, 19702.
- [141] O. Mukama, J. Wu, Z. Li, Q. Liang, Z. Yi, X. Lu, Y. Liu, Y. Liu, M. Hussain, G. G. Makafe, J. Liu, N. Xu, L. Zeng, Biosens Bioelectron 2020, 159, 112143.

### **REVIEW**

| [142] | Y. Sun, H. Liu, Y. Shen, X. Huang, F. Song, X. Ge, A.  |
|-------|--------------------------------------------------------|
|       | Wang, K. Zhang, Y. Li, C. Li, Y. Wan, J. Li, ACS Omega |
|       | <b>2020</b> . <i>5</i> . 14814-14821.                  |

- a) O. Mukama, T. Yuan, Z. He, Z. Li, J. d. D. Habimana, [143] M. Hussain, W. Li, Z. Yi, Q. Liang, L. Zeng, Sens Actuators B Chem 2020, 316, 128119; b) J. H. Tsou, Q. Leng, F. Jiang, Transl Oncol 2019, 12, 1566-1573.
- T. Yuan, O. Mukama, Z. Li, W. Chen, Y. Zhang, J. de Dieu [144] Habimana, Y. Zhang, R. Zeng, C. Nie, Z. He, L. Zeng, Analyst 2020, 145, 6388-6394.
- [145] a) J. Bai, H. Lin, H. Li, Y. Zhou, J. Liu, G. Zhong, L. Wu, W. Jiang, H. Du, J. Yang, Q. Xie, L. Huang, *Front Microbiol* **2019**, *10*, 2830; b) X. Wang, P. Ji, H. Fan, L. Dang, W. Wan, S. Liu, Y. Li, W. Yu, X. Li, X. Ma, X. Ma, Q. Zhao, X. Huang, M. Liao, Commun Biol 2020, 3, 62; c) J. Wu, O. Mukama, W. Wu, Z. Li, J. D. Habimana, Y. Zhang, R. Zeng, C. Nie, L. Zeng, Biosensors 2020, 10, 203.
- X. Wang, E. Xiong, T. Tian, M. Cheng, W. Lin, H. Wang, G. Zhang, J. Sun, X. Zhou, ACS Nano 2020, 14, 2497-[146]
- L. Tang, J. Li, ACS Sens 2017, 2, 857-875. [147]
- [148] X. Ou, Y. Liu, M. Zhang, L. Hua, S. Zhan, Microchim Acta 2021, 188, 304.
- Y. Li, H. Mansour, T. Wang, S. Poojari, F. Li, Anal Chem [149] 2019, 91, 11510-11513.
- [150] R. Zhou, Y. Li, T. Dong, Y. Tang, F. Li, Chem Commun **2020**, 56, 3536-3538.
- [151] a) Y. Zhang, M. Chen, C. Liu, J. Chen, X. Luo, Y. Xue, Q. Liang, L. Zhou, Y. Tao, M. Li, D. Wang, J. Zhou, J. Wang, Sens Actuators B Chem 2021, 345, 130411; b) L. Ma, L. Yin, X. Li, S. Chen, L. Peng, G. Liu, S. Ye, W. Zhang, S. Man, Biosens Bioelectron 2022, 195, 113646.
- L. Ma, L. Peng, L. Yin, G. Liu, S. Man, ACS Sens 2021, 6, [152]
- J. H. Choi, J. Lim, M. Shin, S. H. Paek, J. W. Choi, Nano [153] Lett 2021, 21, 693-699.
- W. S. Zhang, J. Pan, F. Li, M. Zhu, M. Xu, H. Zhu, Y. Yu, G. Su, *Anal Chem* **2021**, *93*, 4126-4133. [154]
- [155] a) M. Hu, C. Yuan, T. Tian, X. Wang, J. Sun, E. Xiong, X. Zhou, J Am Chem Soc 2020, 142, 7506-7513; b) Y. Jiang, M. Hu, A. A. Liu, Y. Lin, L. Liu, B. Yu, X. Zhou, D. W. Pang, ACS Sens 2021, 6, 1086-1093; c) S. Liu, T. Xie, X. Pei, S. Li, Y. He, Y. Tong, G. Liu, Sens Actuators B Chem 2023, 377, 133009.
- R. M. Dirks, N. A. Pierce, Proc Natl Acad Sci USA 2004, [156] 101, 15275-15278.
- M. J. Kachwala, C. W. Smith, N. Nandu, M. V. Yigit, Anal [157] Chem 2021, 93, 1934-1938.
- C. Jiao, S. Sharma, G. Dugar, N. L. Peeck, T. Bischler, F. [158] Wimmer, Y. Yu, L. Barquist, C. Schoen, O. Kurzai, C. M. Sharma, C. L. Beisel, Science 2021, 372, 941-948.
- C. Zong, M. Xu, L. J. Xu, T. Wei, X. Ma, X. S. Zheng, R. [159] Hu, B. Ren, Chem Rev 2018, 118, 4946-4980.
- [160] S. Nie, S. R. Emory, Science 1997, 275, 1102-1106.
- J. Liang, P. Teng, W. Xiao, G. He, Q. Song, Y. Zhang, B. [161] Peng, G. Li, L. Hu, D. Cao, Y. Tang, J Nanobiotechnology 2021, 19, 273.
- [162] R. Pan, J. Liu, P. Wang, D. Wu, J. Chen, Y. Wu, G. Li, J Agric Food Chem 2022, 70, 4484-4491.
- J. Liu, J. Chen, D. Wu, M. Huang, J. Chen, R. Pan, Y. Wu, [163] G. Li, Anal Chem 2021, 93, 10167-10174.
- A. Su, Y. Liu, X. Cao, W. Xu, C. Liang, S. Xu, Sens Actuators B Chem **2022**, 369, 132295. [164]
- J. Zhuang, Z. Zhao, K. Lian, L. Yin, J. Wang, S. Man, G. [165] Liu, L. Ma, Biosens Bioelectron 2022, 207, 114167.
- Y. Pang, Q. Li, C. Wang, S. zhen, Z. Sun, R. Xiao, *Chem Eng J* **2022**, 429, 132109.
  B. Reddy, E. Salm, R. Bashir, *Annu Rev Biomed Eng* [166]
- [167] 2016, 18, 329-355.
- [168] a) M. Gabig-Ciminska, Microb Cell Fact 2006, 5, 9; b) J. Wang, Anal Chim Acta 2002, 469, 63-71.
- [169] Y. Dai, R. A. Somoza, L. Wang, J. F. Welter, Y. Li, A. I. Caplan, C. C. Liu, Angew Chem Int Ed 2019, 58, 17399-17405; Angew Chem 2019, 131, 17560-17566.

- R. Bruch, J. Baaske, C. Chatelle, M. Meirich, S. Madlener, [170] W. Weber, C. Dincer, G. A. Urban, Adv Mater 2019, 31, e1905311.
- K. S. Novoselov, A. K. Geim, S. V. Morozov, D. Jiang, Y. [171] Zhang, S. V. Dubonos, I. V. Grigorieva, A. A. Firsov, Science 2004, 306, 666-669
- [172] A. K. Geim, K. S. Novoselov, Nat Mater 2007, 6, 183-191.
- D. B. Larremore, B. Wilder, E. Lester, S. Shehata, J. M. [173] Burke, J. A. Hay, M. Tambe, M. J. Mina, R. Parker, Sci Adv 2021, 7, eabd5393.
- D. Kozak, W. Anderson, R. Vogel, M. Trau, Nano Today [174] 2011, 6, 531-545.
- Y. Song, J. Zhang, D. Li, Micromachines 2017, 8, 204. [175]
- a) W. Yang, L. Restrepo-Perez, M. Bengtson, S. J. [176] Heerema, A. Birnie, J. van der Torre, C. Dekker, Nano Lett 2018, 18, 6469-6474; b) N. E. Weckman, N. Ermann, R. Gutierrez, K. Chen, J. Graham, R. Tivony, A. Heron, U. F. Keyser, ACS Sens 2019, 4, 2065-2072; c) R. Nouri, Y. Jiang, X. L. Lian, W. Guan, *ACS Sens* **2020**, *5*, 1273-1280; d) R. Nouri, Y. Jiang, Z. Tang, X. L. Lian, W. Guan, *Nano Lett* **2021**, *21*, 8393-8400.
- [177] a) M. A. English, L. R. Soenksen, R. V. Gayet, H. de Puig, N. M. Angenent-Mari, A. S. Mao, P. Q. Nguyen, J. J. Collins, *Science* **2019**, *365*, 780-785; b) R. V. Gayet, H. de Puig, M. A. English, L. R. Soenksen, P. Q. Nguyen, A. S. Mao, N. M. Angenent-Mari, J. J. Collins, Nat Protoc 2020, 15, 3030-3063.
  - a) P. Qin, M. Park, K. J. Alfson, M. Tamhankar, R. Carrion, J. L. Patterson, A. Griffiths, Q. He, A. Yildiz, R. Mathies, K. Du, ACS Sens 2019, 4, 1048-1054; b) Y. Liu, H. Xu, C. Liu, L. Peng, H. Khan, L. Cui, R. Huang, C. Wu, S. Shen, S. Wang, W. Liang, Z. Li, B. Xu, N. He, *J Biomed Nanotechnol* **2019**, *15*, 790-798; c) C. A. Freije, C. Myhrvold, C. K. Boehm, A. E. Lin, N. L. Welch, A. Carter, H. C. Metsky, C. Y. Luo, O. O. Abudayyeh, J. S. Gootenberg, N. L. Yozwiak, F. Zhang, P. C. Sabeti, Mol Cell 2019, 76, 826-837; d) M. M. Kaminski, M. A. Alcantar, I. T. Lape, R. Greensmith, A. C. Huske, J. A. Valeri, F. M. Marty, V. Klambt, J. Azzi, E. Akalin, L. V. Riella, J. J. Collins, Nat Biomed Eng 2020, 4, 601-609; e) F. Zhang, O. O. Abudayyeh, J. S. Gootenberg, 2020, A Protocol for Detection of COVID-19 Using CRISPR Diagnostics, https://www.broadinstitute.org/files/publications/special/CO VID-19%20detection%20(updated).pdf; f) L. A. Curti, I. Primost, S. Valla, D. Ibanez Alegre, C. Olguin Perglione, G. D. Repizo, J. Lara, I. Parcerisa, A. Palacios, M. E. Llases, A. Rinflerch, M. Barrios, F. Pereyra Bonnet, C. A Gimenez, D. N. Marcone, *Viruses* **2021**, *13*, 420; g) L. Guo, X. Sun, X. Wang, C. Liang, H. Jiang, Q. Gao, M. Dai, B. Qu, S. Fang, Y. Mao, Y. Chen, G. Feng, Q. Gu, R. R. Wang, Q. Zhou, W. Li, Cell Discov 2020, 6, 34; h) H. C. Metsky, N. L. Welch, P. P. Pillai, N. J. Haradhvala, L. Rumker, S. Mantena, Y. B. Zhang, D. K. Yang, C. M. Ackerman, J. Weller, P. C. Blainey, C. Myhrvold, M. Mitzenmacher, P. C. Sabeti, Nat Biotechnol 2022, 40, 1123-1131; i) T. Hou, W. Zeng, M. Yang, W. Chen, L. Ren, J. Ai, J. Wu, Y. Liao, X. Gou, Y. Li, X. Wang, H. Su, B. Gu, J. Wang, T. Xu, PLoS Pathog 2020, 16, e1008705; j) M. Azhar, R. Phutela, M. Kumar, A. H. Ansari, R. Rauthan, S. Gulati, N. Sharma, D. Sinha, S. Sharma, S. Singh, S. Acharya, S. Sarkar, D. Paul, P. Kathpalia, M. Aich, P. Sehgal, G. Ranjan, R. C. Bhoyar, V. G. Indian Co, C. Genetic Epidemiology, K. Singhal, H. Lad, P. K. Patra, G. Makharia, G. R. Chandak, B. Pesala, D. Chakraborty, S. Maiti, Biosens Bioelectron 2021, 183, 113207; k) B. Udugama, P. Kadhiresan, H. N. Kozlowski, A. Malekjahani, M. Osborne, V. Y. C. Li, H. Chen, S. Mubareka, J. B. Gubbay, W. C. W. Chan, *ACS Nano* **2020**, *14*, 3822-3835; I) H. Khan, A. Khan, Y. Liu, S. Wang, S. Bibi, H. Xu, Y. Liu, S. Durrani, L. Jin, N. He, T. Xiong, Chin Chem Lett 2019, 30, 2201-2204; m) Y. Chang, Y. Deng, T. Li, J. Wang, T. Wang, F. Tan, X. Li, K. Tian, Transbound Emerg Dis 2020, 67, 564-571; n) S. Lu, F. Li, Q. Chen, J. Wu, J. Duan, X. Lei, Y. Zhang, D. Zhao,

Z. Bu, H. Yin, Cell Discov 2020, 6, 18.

[178]

### REVIEW

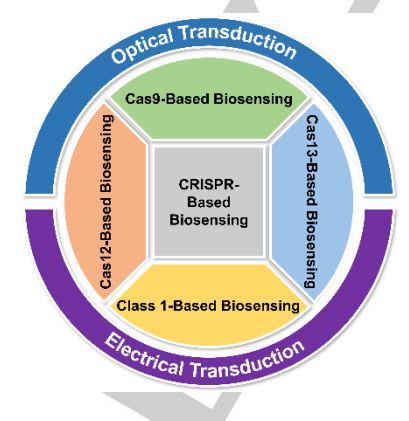
| [179] | a) H. Wu, J. S. He, F. Zhang, J. Ping, J. Wu, Anal Chim |
|-------|---------------------------------------------------------|
|       | Acta 2020, 1096, 130-137; b) Ym. Zhang, Y. Zhang, K.    |
|       | Xie, Mol Breed 2020, 40, 11.                            |

- [180] H. Xu, A. Xia, D. Wang, Y. Zhang, S. Deng, W. Lu, J. Luo, Q. Zhong, F. Zhang, L. Zhou, W. Zhang, Y. Wang, C. Yang, K. Chang, W. Fu, J. Cui, M. Gan, D. Luo, M. Chen, Sci Adv 2020, 6, eaaz7445.
- [181] a) J. O'Brien, H. Hayder, Y. Zayed, C. Peng, Front Endocrinol 2018, 9, 402; b) L. F. R. Gebert, I. J. MacRae, Nat Rev Mol Cell Biol 2019, 20, 21-37.
- [182] C. Chen, D. A. Ridzon, A. J. Broomer, Z. Zhou, D. H. Lee, J. T. Nguyen, M. Barbisin, N. L. Xu, V. R. Mahuvakar, M. R. Andersen, K. Q. Lao, K. J. Livak, K. J. Guegler, *Nucleic Acids Res* 2005, 33, e179.
- [183] a) J. Li, S. Yang, C. Zuo, L. Dai, Y. Guo, G. Xie, ACS Sens 2020, 5, 970-977; b) G. Wang, W. Tian, X. Liu, W. Ren, C. Liu, Anal Chem 2020, 92, 6702-6708.
- [184] a) Y. Xiong, J. Zhang, Z. Yang, Q. Mou, Y. Ma, Y. Xiong, Y. Lu, J Am Chem Soc 2020, 142, 207-213; b) M. Liang, Z. Li, W. Wang, J. Liu, L. Liu, G. Zhu, L. Karthik, M. Wang, K. F. Wang, Z. Wang, J. Yu, Y. Shuai, J. Yu, L. Zhang, Z. Yang, C. Li, Q. Zhang, T. Shi, L. Zhou, F. Xie, H. Dai, X.

- Liu, J. Zhang, G. Liu, Y. Zhuo, B. Zhang, C. Liu, S. Li, X. Xia, Y. Tong, Y. Liu, G. Alterovitz, G. Y. Tan, L. X. Zhang, Nat Commun **2019**, *10*, 3672.
- [185] J. Shen, X. Zhou, Y. Shan, H. Yue, R. Huang, J. Hu, D. Xing, Nat Commun 2020, 11, 267.
- [186] X. Zhao, W. Zhang, X. Qiu, Q. Mei, Y. Luo, W. Fu, Anal Bioanal Chem 2020, 412, 601-609.
- [187] T. R. Abbott, G. Dhamdhere, Y. Liu, X. Lin, L. Goudy, L. Zeng, A. Chemparathy, S. Chmura, N. S. Heaton, R. Debs, T. Pande, D. Endy, M. F. La Russa, D. B. Lewis, L. S. Qi, Cell 2020, 181, 865-876.
- [188] J. Huang, Z. Liang, Y. Liu, J. Zhou, F. He, *Anal Chem* **2022**, *94*, 11409-11415.
- [189] F. S. R. Silva, E. Erdogmus, A. Shokr, H. Kandula, P. Thirumalaraju, M. K. Kanakasabapathy, J. M. Hardie, L. G. C. Pacheco, J. Z. Li, D. R. Kuritzkes, H. Shafiee, Adv Mater Technol 2021, 6, 2100602.

### **Entry for the Table of Contents**

This review focuses on recent developments in both fundamental CRISPR biochemistry and CRISPR-based molecular diagnostic technologies. Four emerging research topics on target preamplification-free detection, microRNA (miRNA) detection, non-nucleic-acid detection, and SARS-CoV-2 detection are also covered.



Institute and/or researcher Twitter usernames: Yi Zhang at the University of Connecticut, Storrs: @YiZhang87459624; Xue (Sherry) Gao at Rice University: @XueSherryGao